



**NTNU – Trondheim**  
Norwegian University of  
Science and Technology

# Study of the role of engine control in the value chain for biofuels in modern "ultra clean" engines

**Line Bjugstad**

Master of Science in Mechanical Engineering

Submission date: March 2014

Supervisor: Terese Løvås, EPT

Norwegian University of Science and Technology  
Department of Energy and Process Engineering



EPT-M-2013-151

**MASTER THESIS**

for

Stud.techn. Line Bjugstad

Autumn 2013

***Study of the role of engine control in the value chain for biofuels in modern «ultra clean» engines****Studie av motorrelaterte kontrollparametere sin rolle i verdikjeden for biodrivstoff i moderne "ultra-rene" motorer***Background and objective**

Increased use of biofuels for transportation is one of the most realistic actions in the short run in order to reduce dependency on fossil fuels, especially for heavy duty systems (land and marine systems). However, there are still many uncertainties related to the increased use of biofuels related both to operation and to sustainability throughout the value chain from production to distribution to end use (emissions/fuel consumption etc.).

The master project involves studying how different biofuels and blends thereof behave during typical combustion conditions in modern state-of-the art engines. The focus fuels will be comparisons between conventional fuels and 2<sup>nd</sup> generation biofuel such as Fischer Tropsch fuels. This will be carried out using available simulation software. The results will possibly be compared to experimental data from DTU (Denmark) through the collaborative project *BioEng*.

*The master is a continuation of the project work. However, more emphasise will be on engine control parameters and fuel blend effects.*

**The following tasks are to be considered:**

1. Using the stochastic reactor model investigate combustion of fuel blends (diesel surrogate (PRF) and 30% bio Fischer Tropsch (FT) fuel) for a set of given operating conditions taken from experimental values. Varying operating conditions can be
  - I. speed,
  - II. load and
  - III. exhaust gas recirculation (EGR).
2. Validation of chemical models used: PRF from Livermore Laboratories or Loge AB, as well as in-house reduced model for the FT-fuel for 30% blend.

Within 14 days of receiving the written text on the master thesis, the candidate shall submit a research plan for his project to the department.

When the thesis is evaluated, emphasis is put on processing of the results, and that they are presented in tabular and/or graphic form in a clear manner, and that they are analyzed carefully.

The thesis should be formulated as a research report with summary both in English and Norwegian, conclusion, literature references, table of contents etc. During the preparation of the text, the candidate should make an effort to produce a well-structured and easily readable report. In order to ease the evaluation of the thesis, it is important that the cross-references are correct. In the making of the report, strong emphasis should be placed on both a thorough discussion of the results and an orderly presentation.

The candidate is requested to initiate and keep close contact with his/her academic supervisor(s) throughout the working period. The candidate must follow the rules and regulations of NTNU as well as passive directions given by the Department of Energy and Process Engineering.

Risk assessment of the candidate's work shall be carried out according to the department's procedures. The risk assessment must be documented and included as part of the final report. Events related to the candidate's work adversely affecting the health, safety or security, must be documented and included as part of the final report. If the documentation on risk assessment represents a large number of pages, the full version is to be submitted electronically to the supervisor and an excerpt is included in the report.


Pursuant to "Regulations concerning the supplementary provisions to the technology study program/Master of Science" at NTNU §20, the Department reserves the permission to utilize all the results and data for teaching and research purposes as well as in future publications.

The final report is to be submitted digitally in DAIM. An executive summary of the thesis including title, student's name, supervisor's name, year, department name, and NTNU's logo and name, shall be submitted to the department as a separate pdf file. Based on an agreement with the supervisor, the final report and other material and documents may be given to the supervisor in digital format.

- Work to be done in lab (Water power lab, Fluids engineering lab, Thermal engineering lab)  
 Field work

Department of Energy and Process Engineering, 21. October 2013

  
\_\_\_\_\_  
Olav Bolland  
Department Head

  
\_\_\_\_\_  
Terese Løvås  
Academic Supervisor

Research Advisors: Azhar Malik, NTNU.



## SUMMARY

The climate changes caused by the combustion of fossil fuels in the transportation sector have, along with a decrease in fossil fuel reserves, resulted in an increased interest in developing alternative fuels. Biofuels are one of the most prominent options and with an expansion in the use of these fuels, it is important to understand all aspects of the environmental effect they impose.

First generation biofuels are the commercial available biofuels today. Since their feedstock origins from food and oil-seed crops there is a great skepticism around their sustainability, creating a focus on research and development of second generation and advanced biofuels. These fuels are more environmental beneficial, however expensive to produce due to a more complex structure of the feedstocks. This requires a more advanced conversion technology, and additionally research is needed to make these fuels economically competitive. Fischer Tropsch Diesel (FTD) is one of the most promising second generation biofuels, yielding great reduction in greenhouse gas (GHG) emissions and fossil fuel consumption when looking at its whole life cycle.

There are uncertainties around the combustion characteristics and the end use emissions of the different biofuels. This especially applies to the use of biofuels in blend with diesel, which is the most common form of utilizing biofuels today. In order to increase the use of these fuels the uncertainties need to be fully explored to ensure their sustainability. This research has traditionally been performed experimentally, but later years computational simulation has arisen as a powerful tool. It saves time and cost, and can also reveal information not possible to obtain by experiments in real engines. In order to obtain reliable results from the simulations, both high quality physical and chemical models are required. In this thesis a Stochastic Reactor Model (SRM) is used, where the volume in the cylinder is divided into a number of smaller volumes. These are known as particles and have their own chemical composition, temperature and mass. Since the SRM is a 0-dimensional model no characteristics regarding the position in space are given, but a Probability Density Function (PDF) gives a distribution of the properties of the particles and enables them to mix and exchange heat with the cylinder walls. By doing so the model takes into account in-homogeneities and turbulence. The engine type used is a direct injection compression ignition (DICI) engine where fuel is directly injected, hence good models are required for both the mixing process as well as the chemical kinetics.

The chemical models used for simulations should withhold the same characteristics as the original fuels, however due to time limitations for the computational calculations less important species and reaction paths should be eliminated. This is done through a reduction process, where there always exists a trade-off between the quality of the model, and the time consumption. The chemical models applied in this thesis are substitutions and simplifications of the original fuels, namely diesel and FTD. N-heptane ( $nC_7H_{16}$ ) has been used as a surrogate fuel for diesel, while the fuel composition representing FTD is 0.772  $nC_{14}H_{30}$ , 0.047  $C_{14}H_{30-2}$  and 0.181  $C_{14}H_{28-1}$ .

The simulations have been run for the engine speeds 900rpm, 1500rpm and 2500rpm, with altered fuel injections to approximate real engine conditions. To save computational time most of the

cycles have been run from -20CAD to 60CAD, with inlet gas temperature and pressure of  $T_i=700\text{K}$  and  $P_i=2.33\text{E}06\text{N/m}^2$ .

The combustion characteristics of the different fuels and engine settings have been compared with regard to parameters such as pressure and temperature profiles, heat release, converted fuel and the production of the criteria pollutants CO, CO<sub>2</sub> and NO<sub>x</sub>. Only small alterations in the combustion cycle is seen for the FTD surrogate with regard to n-heptane, which is most likely an effect of the substantial simplifications applied in the models. These simplifications were also evident in the last part of the thesis, where the emission profiles from the simulations were compared to experimental values. Here some of the cases showed deviating results, however others had correlating trends and could be qualitatively validated. The injection profiles were tuned with regard to the point of injection, where advanced injections obtain higher temperature and pressure peaks. Accordingly more work is produced, however also elevated levels of NO<sub>x</sub>. The effect of Exhaust Gas Recirculation (EGR) has been tested, where the NO<sub>x</sub> emissions are expected to diminish due to reduced concentration of oxygen. Here huge NO<sub>x</sub> reductions are observed, but also a trade-off with regard to elevated levels of CO and reduced levels of CO<sub>2</sub>. This reflects the main problem to be resolved when applying EGR, namely to what extent EGR should be applied before the negative effects related to a more incomplete combustion surpasses the NO<sub>x</sub> savings.

## SAMMENDRAG

Klimaforandringene forårsaket av forbrenningen av fossilt drivstoff i transportsektoren har, i tillegg til minkende reserver, økt interessen for utviklingen av alternative drivstoff fra fornybare ressurser. Biodrivstoff er et av de mest lovende alternativene til å erstatte fossilt drivstoff, og med en økende bruk er det viktig å avdekke hvilken effekt dette har på miljøet.

Førstegenerasjons biodrivstoff er kommersielt tilgjengelige i dag, og bruker mat og olje fra korn som råmateriale. Dette har reist spørsmål rundt hvor bærekraftige de er, noe som har bidratt til et større fokus på forskning og utvikling av andregenerasjons og avanserte biodrivstoff. Disse stammer fra mer fordelaktige råmaterialer med hensyn til miljøet, men er dyre å produsere på grunn av råmaterialenes komplekse struktur. Råmaterialene krever en mer avansert teknologi for å kunne omdannes til drivstoff, og mer forskning må til for å gjøre biodrivstoffene konkurransedyktige. Fischer Tropsch Diesel (FTD) er et av de mest lovende andre generasjons biodrivstoff. Når FTD erstatter fossil diesel vil det gi store reduksjoner i utslippene av klimagasser og minke forbruket av fossilt drivstoff betraktelig.

Man vet at ulike biodrivstoff vil påvirke motorens kjøreegenskaper og utslipp, men effekten er per i dag ikke fullstendig utforsket. Det er spesielt høy usikkerhet når de brukes i kombinasjon med fossile drivstoff, som er den vanligste bruksformen av biodrivstoff. For å kunne øke bruken av biodrivstoffene og sikre deres bærekraftighet, må deres fulle effekt avdekkes. Dette er forskning som tradisjonelt har blitt utført eksperimentelt, men i de senere årene har databaserte beregningsverktøy blitt benyttet for å spare tid og kostnader knyttet til arbeidet. Her kan man også trekke ut nyttig informasjon som ikke er mulig å avdekke ved forsøk i en ekte motor. For å kunne oppnå pålitelige resultater fra simuleringene må både fysiske og kjemiske modeller av høy kvalitet benyttes. I dette arbeidet brukes en Stokastisk Reaktor Modell (SRM) for å simulere motoren. Volumet i sylindren er delt i et antall mindre volumer kalt partikler, med sin egen kjemiske sammensetning, temperatur og masse. Siden SRM er en 0-dimensjonal modell vil ingen posisjon i rommet være gitt, men en sannsynlighetstetthetsfunksjon (PDF) gir en fordeling av egenskapene til partiklene. Dette muliggjør at partiklene blandes og utveksler varme med sylinderveggene. Slik tar modellen hensyn til inhomogene forhold og turbulens. Motortypen som brukes operer med en direkte innsprøyting av drivstoff, før miksen av luft og drivstoff selvantennes som følge av en kompresjonsprosess (DICI-motor). Siden drivstoffet sprøytes direkte inn i sylindren må man ha gode modeller for både blandeprosessen, så vel som den kjemiske kinetikken.

De kjemiske modellene som benyttes for simulering bør inneha de samme egenskapene som det originale drivstoffet, men på grunn av tidsbegrensninger for beregningene bør mindre viktige atomer, molekyler og reaksjonsveier elimineres. Dette gjøres gjennom en reduksjonsprosess. Det vil alltid være en avveining mellom kvaliteten på modellen og tidsforbruket ved simuleringene, med tanke på hvor stor del av modellen som elimineres. De kjemiske modellene som brukes i denne avhandlingen er erstatninger og forenklinger av de opprinnelige drivstoffene diesel og FTD. N-heptan ( $nC_7H_{16}$ ) har blitt brukt som et surrogatdrivstoff for diesel, mens surrogatdrivstoffet som representerer FTD består av 0,772  $nC_{14}H_{30}$ , 0,047  $C_{14}H_{30-2}$  og 0,181  $C_{14}H_{28-1}$ .



Simuleringene har blitt kjørt med motorhastighetene 900rpm, 1500rpm og 2500rpm, og med forskjellige innsprøytningsprofiler for å tilnærme forholdene i en ekte motor. For å spare beregningstid har syklusene blitt kjørt fra -20CAD til 60CAD, hvor forholdene ved innsugningstakten er  $T_i = 700\text{k}$  og  $P_i = 2.33\text{E}6\text{N/m}^2$ .

I denne avhandlingen har forbrenningsegenskapene knyttet til de to surrogatdrivstoffene ved ulike motorinnstillinger og innsprøytningsprofiler blitt sammenlignet ved parametere som trykk- og temperaturprofiler, varmeavgivelse, andel omdannet drivstoff og utslippene av de viktige forurensningskomponentene CO, CO<sub>2</sub> og NO<sub>x</sub>. Forbrenningsegenskapene til surrogatdrivstoffene viste kun mindre forskjeller, noe som antagelig skyldes de mange forenklingene i modellene. Disse forenklingene var også fremtredende i siste del av arbeidet, hvor utslippsprofilene fra simuleringene ble sammenlignet med eksperimentell data. Her viste noen av tilfellene sprikende tendenser, men viktige trender kunne likevel observeres og kvalitativt valideres. Innsprøytningsprofilene ble endret i forhold til hvor drivstoffet først blir sprøytet inn. Fremskyndet innsprøytning har vist seg å gi høyere temperatur- og trykktopper, noe som indikerer en større produksjon av arbeid, men også høyere utslipp av NO<sub>x</sub>. Effekten av eksosgassresirkulering (EGR) har blitt testet, hvor NO<sub>x</sub> utslippene er forventet å synke på grunn av mindre tilgang til oksygen. Her ble store NO<sub>x</sub>-reduksjoner observert, men også forhøyede nivåer av CO og reduserte nivåer av CO<sub>2</sub>. Dette gjenspeiler hovedproblemet knyttet til EGR, nemlig i hvilken grad EGR kan benyttes før de negative effektene knyttet til en mer ufullstendig forbrenning overgår besparelsene av NO<sub>x</sub>.

## **ACKNOWLEDGEMENT**

The work presented in this thesis has been performed at the Department of Energy of Process engineering, NTNU. It is the last part of my master degree, and with this my time at NTNU has come to an end.

I would like to thank my supervisor Terese Løvås who has guided throughout this work, even though she is still partially in maternity leave. I would also like to thank post doc Azhar Malik who helped provide the chemical model for FTD, and has supported me in performing the simulations. When I lost the license to DARS he performed the remaining simulations, and made it possible for me to finish. Without these people the thesis would not have been possible.

# TABLE OF CONTENT

1. INTRODUCTION .....	1
1.1 Background.....	1
1.2 Objective.....	5
1.3 Extent and limitations .....	5
1.4 Report composition.....	6
2. BIOFUELS – AN OVERVIEW .....	7
2.1 First generation biofuels .....	8
2.1.1 Biodiesel.....	8
2.1.2 Conventional Bioethanol.....	8
2.1.3 Biogas (biomethane) .....	9
2.2 Second generation biofuels.....	9
2.2.1 Bio-chemical route .....	10
2.2.2 Thermo-chemical processing .....	11
2.3 Advanced biofuels .....	13
2.3.1 Algae.....	13
2.3.2 Bio-SNG – Bio-synthetic natural gas .....	14
2.3.3 Pyrolysis diesel.....	14
2.3.4 Hydrogen.....	14
2.3.5 Consolidated bioprocessing (CBP).....	15
3. ENGINE TYPE AND FUEL SIMULATED .....	16
3.1 Diesel engine .....	16
3.1.1 CI engine .....	16
3.1.2 Direct injection (DI) engine .....	17
3.1.3 Emission and exhaust gas recirculation (EGR) .....	17
3.2 Fuel .....	19
3.2.1 Sustainability of FTD .....	20
4. CHEMICAL MODELING .....	22
4.1 Reducing chemical models .....	23
4.1.1 Important factors for this paper .....	25
4.2 Diesel surrogate .....	26
4.3 FTD surrogate.....	26

5.	PHYSICAL MODELING.....	27
5.1	Model description.....	27
5.2	Calculation.....	28
5.2.1	<i>Energy and mass conservation in a closed system</i> .....	28
5.2.2	<i>PDF</i> .....	31
5.2.3	<i>Heat release</i> .....	36
6.	CASE SETUP.....	38
6.1	<i>Engine geometry</i> .....	38
6.2	<i>Engine speed</i> .....	38
6.3	<i>Load</i> .....	38
6.4	<i>Injection input file</i> .....	39
6.5	<i>Equivalence ratio, <math>\phi</math></i> .....	40
6.6	<i>Exhaust gas recirculation, EGR</i> .....	41
7.	RESULTS SIMULATING N-HEPTANE.....	42
7.1	Base injection profile.....	42
7.1.1	<i>Gas properties</i> .....	42
7.1.2	<i>Pressure profiles</i> .....	43
7.1.3	<i>Temperature profiles</i> .....	45
7.1.4	<i>Heat release per crank angel degree</i> .....	46
7.1.5	<i>Mass fraction of fuel burned (MFB), emission of carbon monoxide (CO) and carbon dioxide (CO<sub>2</sub>)</i> .....	47
7.2	Modified mechanism including NO <sub>x</sub> .....	48
7.3	Tuning n-heptane.....	49
7.3.1	<i>Fuel1</i> .....	49
7.3.2	<i>Fuel2</i> .....	54
7.3.3	<i>Fuel3</i> .....	56
7.3.1	<i>Fuel4 and 5</i> .....	57
7.4	NO <sub>x</sub> emissions.....	60
7.5	EGR.....	61
7.5.1	<i>Fuel1</i> .....	62
7.5.2	<i>Fuel2 and 3</i> .....	63
8.	RESULTS – SIMULATING FTD SURRUGATE.....	66
8.1	Base case Fuel1-3.....	66
8.2	NO <sub>x</sub> emissions.....	68

8.3	EGR .....	69
9.	QUALITATIV VALIDATION OF MODELS UTILIZED.....	72
9.1	Evaluating Fuel2.....	72
9.2	Evaluating the impact of EGR.....	73
10.	CONCLUSION .....	75
11.	REFERENCES.....	77

## LIST OF TABLES

Table 1:	European market status for technology, today and prospected [6]. .....	2
Table 2:	Classification of 2nd generation biofuels, their feedstock and production path [12]. .....	9
Table 3:	Engine geometry specifications. ....	38
Table 4:	Base fuel injection profile defining the fraction of fuel injected at each CAD.....	40
Table 5:	Overview of simulated cases with regard to engine speed, injected fuel and load representation. ....	42

## LIST OF FIGURES

Figure 1:	Emission of CO <sub>2</sub> -equivilants in million ton by sector from 1991-2006. Red line represents transport [3]. .....	1
Figure 2:	Emission of CO <sub>2</sub> -equivilants in million ton by sector from 1990-2011, isolating road traffic (blue line) [2]. .....	1
Figure 3:	Registered petrol and diesel cars in Norway [8].....	4
Figure 4:	Sale of petrol and diesel fuel in Norway (1000L) [8].....	4
Figure 5:	Biofuel conversion routes [20]. ....	7
Figure 6:	Products from thermal biomass conversion. CHP stands for combined heat and power [26].....	11
Figure 7:	Percentage change in energy use, GHG emission and emissions of criteria pollutants per mile driven of BIO-FTD, relative to diesel in a conventional DICI engine [48]. .....	21
Figure 8:	Operator splitting loop. ....	32
Figure 9:	Steps in the fuel injection model. ....	34
Figure 10:	Illustration of the base fuel injection profile, defining the fraction of fuel injected at each CAD. ....	40
Figure 11:	Temperature and pressure profiles for n-heptane running at 900rpm with equivalence ratio, $\Phi$ , set to 1 and 0 in the case settings.....	43

Figure 12: Pressure profiles for n-heptane for the cases Fuel1-5.....	44
Figure 13: Temperature profiles for n-heptane for the cases Fuel1-5.....	45
Figure 14: Heat release profiles for n-heptane for the cases Fuel1-5.....	46
Figure 15: Mass fraction of burned fuel at the end of the cycle, and mole fraction of CO and CO <sub>2</sub> in the end emissions for Fuel1-5 for n-heptane. ....	48
Figure 16: Pressure profiles for n-heptane for Fuel1 and 2 with the initial chemical model and a modified mechanism including NO <sub>x</sub> . ....	49
Figure 17: Pressure, temperature and heat release profiles for Fuel1 operating with different injection points for n-heptane. The heat release is given for a smaller CAD than the two others due to a smaller window of interest. ....	50
Figure 18: Mole fraction of CO, CO <sub>2</sub> and mass fraction of burned fuel at the end of the cycle, and the ignition delay for Fuel1 operating with different injection points for n-heptane. ....	51
Figure 19: Pressure, temperature and heat release profiles for Fuel1 operating with different injection points given for two manners of injecting fuel: one main injection and a duel injection of n-heptane. ....	53
Figure 20: Pressure, temperature and heat release profiles for Fuel2 operating with different injection points of n-heptane. ....	54
Figure 21: Mole fraction of CO and CO <sub>2</sub> in the end emissions and the ignition delay for Fuel2 operating with different injection points for n-heptane. ....	55
Figure 22: Pressure, temperature and heat release profiles for Fuel3 operating with different injection points of n-heptane. ....	56
Figure 23: Mole fraction of CO, CO <sub>2</sub> and mass fraction of burned fuel at the end of the cycle, and the ignition delay for Fuel3 operating with different injection points of n-heptane.....	57
Figure 24: Pressure and temperature profiles for Fuel4 and 5 at altered points of injection of n-heptane.....	58
Figure 25: The mass fraction of burned fuel and the mole fraction of CO and CO <sub>2</sub> in the end emissions for Fuel4 and Fuel5 at altered injection points for n-heptane. ....	59
Figure 26: Pressure and temperature profiles for an engine speed of 2500rpm with an injection at -0.2CAD and -8.8CAD when reducing the amount of n-heptane injected from case Fuel4. ....	60
Figure 27: Mole fractions of NO in the end emissions for Fuel1-3, at different injection points of n-heptane. Be aware that the values on the y-axis show different ranges. ....	61
Figure 28: Temperature, pressure and heat release profiles and mass fraction of burned fuel for Fuel1 operating with 15% EGR for n-heptane. ....	62
Figure 29: Mole fractions of NO, NO <sub>2</sub> , CO and CO <sub>2</sub> for Fuel1 running with 15% EGR at different EGR cycles for n-heptane. ....	63
Figure 30: Temperature, pressure and heat release profiles and mass fraction of burned fuel for Fuel2 operating with 15% EGR for n-heptane. ....	64
Figure 31: Mole fractions of NO, NO <sub>2</sub> , CO and CO <sub>2</sub> for Fuel2 running with 15% EGR at different EGR cycles for n-heptane. ....	65
Figure 32: Pressure, temperature and heat release profiles for the combustion of FTD for Fuel1-3 operating with different points of injection. ....	66
Figure 33: Mole fractions of CO, CO <sub>2</sub> and mass fraction of burned fuel at the end of the cycle, and the ignition delay for Fuel1-3 for FTD operating with different points of injection. ....	67

Figure 34: Mole fraction of NO in the end emission when FTD is combusted for Fuel1-3. ....	68
Figure 35: Temperature, pressure and heat release profiles and mass fraction of burned fuel for Fuel1 running with FTD for a base case and a cycle running with 15%EGR. ....	69
Figure 36: Mole fractions of NO, NO <sub>2</sub> , CO and CO <sub>2</sub> during the combustion cycle of FTD for a base case and a case running with 15%EGR (Cycle1). ....	70
Figure 37: Mole fraction of CO, CO <sub>2</sub> and NO <sub>x</sub> in the end emissions for the simulated cases of n-heptane and FTD for Fuel2 compared to experimental values for diesel and 30%FTD. Notice that the CO emission has a logarithmic scale. ....	73
Figure 38: Mole fraction of CO, CO <sub>2</sub> and NO <sub>x</sub> in the end emissions for the simulated cases of n-heptane and FTD, compared to experimental values for diesel and 30%FTD, for a base case and when 15%EGR is applied. Notice that the CO emission has a logarithmic scale. ....	74

# NOMENCLATURE

$A$	The pre-exponential factor in the Arrhenius equation
$A_w$	In-cylinder wall area [m <sup>2</sup> ]
$B$	Cylinder bore [m]
Bio-SNG	Bio-Synthetic Natural Gas
CAD	Crank Angle Degree
CBP	Consolidated Bioprocessing
C/D	Coalescence dispersal
CH <sub>4</sub>	Methane
CI	Compression Ignition
$\dot{c}_i$	The time derivative of concentration of specie $i$ , $c_i(t)$ [mole/m <sup>3</sup> s]
CNG	Compressed Natural Gas
CO	Carbon Oxide
CO <sub>2</sub>	Carbon Dioxide
$c_p$	Specific heat at constant pressure [J/K kg]
DARS	Digital Analysis of Reaction Systems
DI	Direct Injection
DICI	Direct Injection Compression Ignition
DTU	Technical University of Denmark
EGR	Exhaust Gas Recirculation
$E_j$	The energy barrier for a chemical reaction $j$ to occur [J/mole]
$e_k$ and $e_p$	Specific kinetic and potential energy [J/kg]
FAME	Fatty Acid Methyl Ester
FCVs	Fuel Cell Vehicles
FTD	Fischer Tropsch Diesel
GHG	Greenhouse Gas



GTCC	Gas Turbine Combined Cycle
$H$	Enthalpy [J]
$h$	Specific enthalpy [J/kg]
HC	Hydro Carbon
$h_c$	Heat transfer coefficient [W/m <sup>2</sup> K kg]
$h_g$	Woschni heat transfer coefficient [W/m <sup>2</sup> K kg]
$\Delta H_j$	The change in enthalpy of reaction $j$ [J]
$HR$	Heat Release [Kg J/Deg]
$k$	The reaction rate constant [m <sup>3</sup> /mole s]
LCA	Life Cycle Analyses
$L_{cr}$	Connecting rod length [m]
LLNL	Lawrence Livermore National Laboratory
LNG	Liquefied Natural Gas
MDF	Mass Density Function, $F_\phi$
MFB	Mass fraction of Fuel Burned
$M_i$	The molecular weight of specie $i$ [kg/mole]
$n$	The amount of gas present [mole]
$n_j$	A fit parameter in the Arrhenius expression
NO <sub>x</sub>	Nitrogen Oxides
$N_r$	The total amount of reactions $j$
$N_s+1$	Temperature index
OH	Hydroxide
$Of_{pin}$	Piston pin offset [m]
$p$	Pressure [N/m <sup>2</sup> ]
PaSPFR	Partially Stirred Plug Flow Reactor
PDF	Probability Density Function
PM	Particular Matter

PO <sub>4</sub>	Phosphate
PRF	Primary Reference Fuel
$\dot{Q}$	Heat transfer with the surroundings [J/s]
$\dot{q}$	Specific heat transfer [J/kg s]
$R$	The universal gas constant [J/mole K]
$R_{ct}$	Crank radius [m]
R&D	Research and Development
RED	Renewable Energy Directive in the European Union
$r_j$	The reaction rate for reaction $j$ [mole/m <sup>3</sup> s]
RME	Rape Methyl Ester
SI	Spark Ignition
SO <sub>x</sub>	Sulfate Oxides
SRM	Stochastic Reactor Model
$T$	Temperature [K]
$t$	Time [s]
TDC	Top Dead Center
$T_w$	The cylinder wall temperature [K]
$U$	Internal energy [J]
$u$	Specific internal energy [J/kg]
$V$	Volume [m <sup>3</sup> ]
$v$	Specific volume [m <sup>3</sup> /kg]
$V_c$	Clearance volume [m <sup>3</sup> ]
VCO	Volatile Organic Compounds
$\nu_{ij}$	The net stoichiometric coefficient determining to what extent each specie will collide and react for species $i$ in reaction $j$
$\dot{W}$	Work done on or by the system [J/s]
WGS	Water-Gas-Shift

$w^x$	Weighting factor of particle $x$
$Y_i$	Mass fraction
$\varepsilon_r / \varepsilon_Q$	Parameters set for reducing mechanisms
$\theta$	Crank angel degree
$\gamma_x$	Specific heat ratio of particle $x$
$\rho$	Density [kg/m <sup>3</sup> ]
$\phi$	The vector of the random variables in the MDF
$\Phi$	Equivalent ratio
$\Psi$	The sample space variables
$\omega_i$	Global reaction rate for species $i$ [mole/m <sup>3</sup> s]

# 1. INTRODUCTION

## 1.1 BACKGROUND

Burning of fossil fuels is a major contributor to greenhouse gas emissions which lead to climate changes, where CO<sub>2</sub> is the most prominent component with regard to human activities. Oil-based fuel is the dominant energy source used for transportation (95%), and in 2004 this sector alone contributed to 23% of the total GHG emissions [1]. Figure 1 and 2 provides an illustration of the role the transportation sector plays as a CO<sub>2</sub> emitter in Norway. As can be seen from figure 1, the transport sector exceeded the industry as the number one emitter of CO<sub>2</sub> equivalents in Norway in 2006, represented by the red line. Figure 2 shows the contribution from road traffic isolated from the rest of the sector which lies well above the contribution from the remaining emissions from transport, represented by respectively the blue and purple line [2]. This is a representation of the emitters in Norway, but the same trend is seen globally. This emphasizes the importance of regulating the emissions from the transportation sector, with an extra focus on road traffic. With a world population in growth and therefore a higher demand for energy and transportation fuel, the need for a more sustainable and environmental friendly transportation sector increases. This can be realized by improving the efficiency of the engines and introducing a more environmental beneficial fuel.

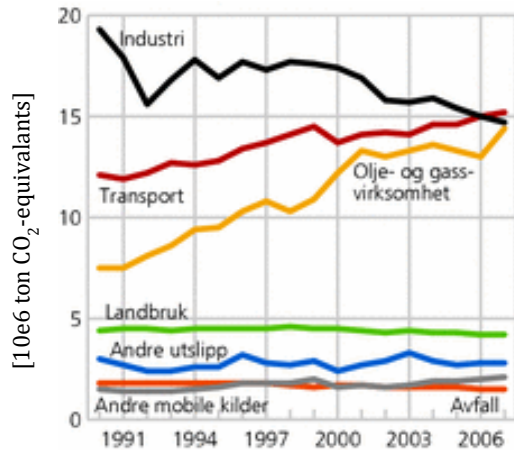


Figure 1: Emission of CO<sub>2</sub>-equivalants in million ton by sector from 1991-2006. Red line represents transport [3].

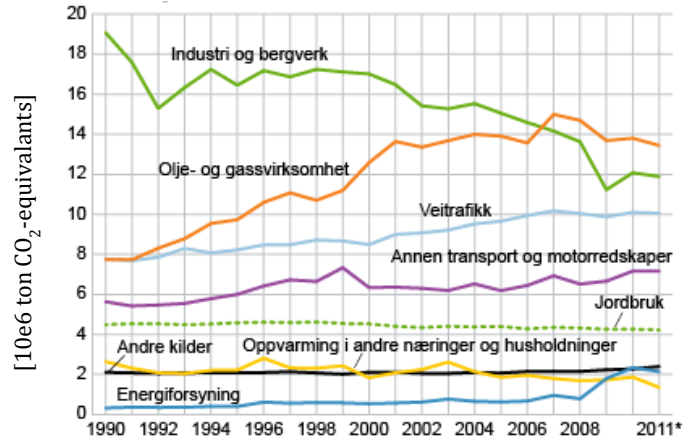


Figure 2: Emission of CO<sub>2</sub>-equivalants in million ton by sector from 1990-2011, isolating road traffic (blue line) [2].

Natural gas, liquefied petroleum gas and electricity for electric cars all have the potential of being beneficial environmental alternatives, but require investments in modification of vehicles and refueling systems [3]. The two former are not renewable, and the sustainability of the electric car depends on the origin of the electric power since the electricity may come from renewable sources such as hydropower, but also from coal and other fossil fuels.

Regardless the electric cars are at the moment an expensive technology and the batteries have a shorter range than a combustion engine, which unable use in airplanes and ships. Biofuels are already available on a large scale today, and because of its similar characteristics to conventional fuel it can easily be introduced to an already existing infrastructure [4].

When evaluating the industries which use engines to combust fossil fuels, the car industry plays the leading role with regard to engine development. This may come from the fact that the emissions from car engines are released in areas in direct contact with humans, whereas energy plants are often being placed in sites shielded from the rest of society [5]. Table 1 shows available technology at different market scales for the car industry today, and prospected in the future. More efficient combustion cars and hybrid cars are projected to be commercially available around 2015, at the same time as electric cars and rechargeable hybrid cars are introduced to a large scale market [6]. The reason for the delay in commercializing new technology arises from the conservatism of the car industry. The development of new and more environmentally beneficial technology does not directly imply that this is the technology being used [3]. The industry will not prioritize these solutions if there is no market demand. The creation of this demand requires an infrastructure that enables easy use, and again the development of this infrastructure will not be initiated if there is no market for it. Today combustion engines are predominant and in a middle term perspective biofuels, with their easy introduction and availability, will be the most important energy source to reduce CO<sub>2</sub> emission from transport [6]. It is projected that biofuels can replace between 13-25% of the total energy demand [1], which will give a reduction of 1800-2300 ton CO<sub>2</sub> [4].

Table 1: European market status for technology, today and prospected [6].

Status of technology	Development of new technology	R&D projects	Small scale production, niche markets	Big scale production introduced to market	Market expansion	Commercial market
2010	Hydrogen	Hydrogen, Rechargeable hybrid cars	Electric cars	Efficient combustion engine cars, Hybrid cars		
2012-2013		Hydrogen	Rechargeable hybrid cars	Electric cars, Rechargeable hybrid cars	Efficient combustion engine cars, Hybrid cars	
2015			Hydrogen	Electric cars, Rechargeable hybrid cars		Efficient combustion engine cars, Hybrid cars
2020				Hydrogen	Electric cars, Rechargeable hybrid cars	Efficient combustion engine cars, Hybrid cars

Biofuels are not a new phenomenon. In 1900 Rudolf Diesel demonstrated an engine running purely on peanut oil, and saw great potential for the use of vegetable oil as engine fuel. In 1912 he said *“The use of vegetable oils for engine fuels may seem insignificant today. But such oils may become in the course of time as important as petroleum and coal-tar products of the present time”* [7]. Due to the availability and low cost of petroleum at Diesels time, it

was not before the World War 2 and the 1970`s oil crises that biodiesel became a field of interest [8]. Biofuels consist of more than biodiesel from vegetable oils, and are divided into four different groups known as generations which differ in feedstock utilized and their technological path. Here follows an overview of the different generations, which is described in more detail in section 2 [9-13].

- First generation biofuels: Biodiesel, bioethanol and biogas
  - Made from food- and oil-seed crops
  - Utilize well established technology
- Second generation biofuels: Bioethanol, synthetic biofuels, biodiesel and bio hydrogen
  - Made from organic waste material and cellulosic material
  - Utilize relatively new and advanced technology
- Advanced biofuels: “third and fourth generation”
  - Can utilize the same feedstock as first and second generation, but their characteristics are changed mainly by gen technology or from gen designed materials.
  - Exists mainly in R&D stage.

First generation biofuels are the commercial available fuels today, but there are uncertainties regarding how environmental beneficial they really are due to their feedstock being food and oil-seed crops. The second generation biofuels are regarded as superior to the first generation when assessing their sustainability, since their feedstock is abundant and not in direct competition with food and feed production. They are not commercial available today, but there is ongoing research in order to make the production cost competitive [12, 14].

Even though biofuels has a long history there are still uncertainties regarding the change of combustion characteristics compared to conventional fuels. Most biofuels are found as blends with even higher uncertainties around their characteristics, making it an important area of research. Both the value chain of the fuel and their end emissions need to be fully explored before increasing their use, and to obtain a complete picture of the sustainability the performance of the engine needs to be assessed as well. As illustrated in table 1 the combustion engine will keep playing a leading role in the future, and with an efficiency in the range of 10-55%, large environmental savings can be achieved by further developing the engine. There is ongoing research to improve this low efficiency as well as reducing emissions, which can be seen in the vast improvement of the car engines in the recent 25 years [15]. This is not only positive for the use of biofuels, but will save energy regardless of the fuel utilized. In today`s world the dependency on fossil fuels makes it unrealistic to expect a complete substitution with a more environmental beneficial alternative, like biofuels, making engine improvements vital.

In order to lower the time and cost of this research work, computational simulation has arisen as an important tool. Here well established knowledge is used to create physical and chemical models so the simulations resemble the process in a real engine. Here information can be withdrawn from the results which may not be possible to achieve by experiments in a real engine. With that said none of today`s models can fully include all aspects of a combustion

engine so experimental data are needed to validate the results, but the simulation models are a powerful supplement in the research work [5, 15].

How reliable the results are depends on the complexity of the models. Although there has been a development in both simulation models and computational power of the computers in the last years, there is a trade-off between the quality of the information retrieved and the time consumption. A conventional hydrocarbon fuel is highly complex and its kinetic data is incomplete. To save computational power and create more reliable models with regard to kinetics, surrogate fuels with similar combustion characteristics as the hydrocarbon fuels are used. For the surrogate fuels both the chemical and physical properties are known, making them more suitable to model. The surrogate fuels are especially useful when developing new fuels like the biofuels, since there will not exist kinetic reaction mechanisms for these new fuel components [5, 16].

With an increased focus on engine efficiency and alternative fuels, the diesel engine has showed to operate better compared to the more widespread petrol engine. Biodiesels easy introduction, better fuel economy, higher engine power and more stable running conditions has created an incremental interest and demand for the diesel engine worldwide [17, 18]. This trend is also seen in Norway, and the report *Klimakur* projects that diesel cars will increase from 30% today, to 70 % of all vehicles in 2020 [6, 18]. Figure 3 and 4 corresponds to this tendency, and show the registered petrol and diesel cars in Norway from 1970 to 2006, and the amount of petrol and gasoline sold from 1952 to 2006. As can be seen from figure 3 the diesel car has had a steady increase in the amount of registered cars since 1980, whereas for the petrol car a decrease is detected from 2004. This coincides with the share of new sold cars in 2007, with diesel engines being 3/4th of the total sale. Figure 4 shows how the sale of petrol and diesel correlates to this trend, and for the first time in 2004 the sale of diesel exceeded the sale of petrol. The figures also imply an increase in both the sum of registered cars and sale of fuel, emphasizing the importance of offering biofuels compatible with combustion engines, especially diesel engines [8].

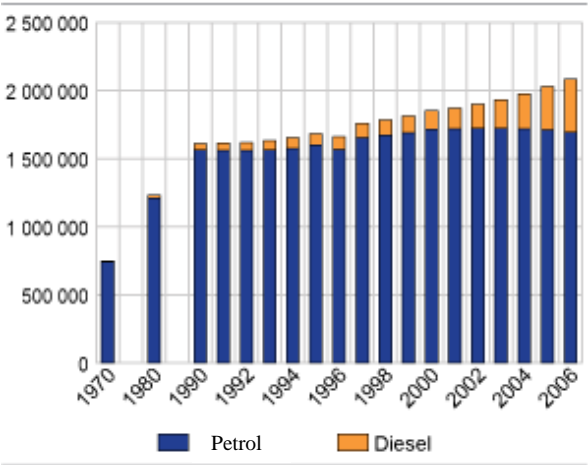


Figure 3: Registered petrol and diesel cars in Norway [8].

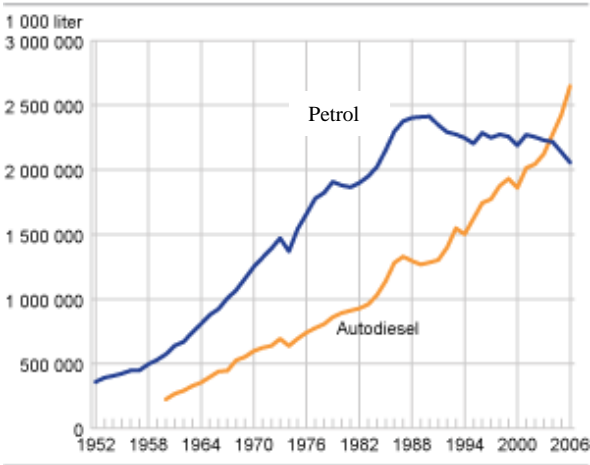


Figure 4: Sale of petrol and diesel fuel in Norway (1000L) [8].

## **1.2 OBJECTIVE**

The objective of this thesis is to investigate how biofuels behave during a combustion process in an engine compared to conventional diesel. Biofuels are mostly found as blend with conventional fuels, and there are uncertainties related to the impact both on the operational conditions and the sustainability when increasing the use. Nevertheless biofuels are a prominent alternative to the fossil fuels in the transportation sector and extensive research is required to ensure their quality. Traditionally this research has been conducted experimentally which is both cost and time consuming. As a complement to this research computational simulations can be used to reduce the cost and time investments, and may even yield information not possible to obtain from experiments [19].

In this thesis simulations will be performed on surrogate fuels representing Fischer Tropsch Diesel (FTD) and conventional diesel. How valid these models are will be discussed since they are simplifications and substitutes, and the results may therefore deviate from the real case. However simplified models can reveal important trends which will be looked into in this thesis. The production and use of FTD is one of the most promising options to reduce the GHG emissions of the transportation sector [11], and here its characteristics when combusted in an engine will be compared to the surrogate fuel for diesel. It is not just the fuel source which can make the combustion more beneficial, also operational conditions plays a big role in the combustion process. Here the engine speed, load, point of injection and exhaust gas recirculation (EGR) will be altered to see the effect it plays on the end emission and engine performance.

It would be preferred if the results from the simulation would reflect all aspects of the operation in a real engine, but this is not the case due to the complexity of the combustion process, as well as computer capacity. The results obtain from the simulations will be compared to experimental data from DTU (Technical University of Denmark) in order to validate the quality of the information withdrawn.

## **1.3 EXTENT AND LIMITATIONS**

This report will only look at alternatives for diesel engine, since these are increasing in number in Europe generally, and especially in Norway.

The simulations will be conducted on surrogate fuels for fossil diesel and the second generation biofuel FTD. The engine used for simulation is a direct injection (DI) engine, which operates with an injection of fuel during a closed cycle, keeping the valves shut during combustion.



For the simulations of fossil diesel n-heptane has been used as the surrogate fuel, instead of the standardized procedure for modelling diesel including both n-heptane and iso-octane. This is due to errors in DARS when applying the standardized fuel composition.

As for the fuel composition for FTD it is strongly simplified and reduced to three fuel species, owing to limitation in computational power. The simplifications have made the fuel less oxygen rich compared to actual FTD. Due to complications when importing two chemical models in DARS simultaneously simulations have been conducted on pure FTD, although it is usually found as a blend with conventional fuel. This was also the intention of this paper. There are only a few cases ran for this fuel due to unexpected errors, license limitation and the given time frame for this work.

## **1.4 REPORT COMPOSITION**

The first part provides an introduction to the existing biofuels, namely first and second generation biofuels and advanced biofuels. The definitions are given along with a description of the different feedstocks and technologies utilized. In the following section the engine and fuels simulated in this paper are presented, i.e. compression ignition engine, and FTD and a primary reference fuel (PRF) used to simulate diesel. Here Exhaust gas recirculation (EGR) is introduced, and a discussion regarding the sustainability of FTD is conducted.

The next section assesses the use of chemical models in simulations, and the trade-off between the quality on the information retrieved and the time consumption. The process of reducing a mechanism in order to limit the computational time while still maintaining an acceptable level of quality is discussed, and the chemical models used for FTD and the diesel surrogate are given.

The next part looks at the physical modeling of the direct injection compression ignition (DICI) engine, where a Stochastic Reactor Model is used. The basic concept of the model is presented with a focus on the Probability Density Function (PDF).

Then a section regarding the setup of the simulation case in this thesis presents the operational conditions in the engine with regard to engine geometry, fuel injected, speed etc., before the results of the simulations are presented and discussed. The results are then compared to experimental data to validate the models used in the simulations.

The thesis finishes of with a discussion around the findings and a conclusion drawn from this work.

## 2. BIOFUELS – AN OVERVIEW

Biofuels are divided into 4 main groups known as “generations”, determined by the technologies and feedstocks utilized for production. First generation is made from food- and oil-seed crops with well-established technology. Second generation is made from organic waste material and cellulosic materials, with relative new and more advanced technology. The third generation uses the same feedstocks as first and second generation, but their characteristics are changed mainly by gen technology. Here genetic material is removed or inserted into the organism to obtain more beneficial characteristics (higher yield, more resistance, etc.). Fourth generation is made from gen designed materials, and both the feedstock and the production process are modified. The terms third and fourth generation biofuels are not an accepted definition, and these biofuels that exist in R&D stage are normally addressed as advanced biofuels [9-13]. An overview of the biofuels conversion routes are shown in figure 5, with an increase in the complexity of the utilized technologies downwards in the figure [20]. The technologies will be explained in this chapter, where the different generations are defined.

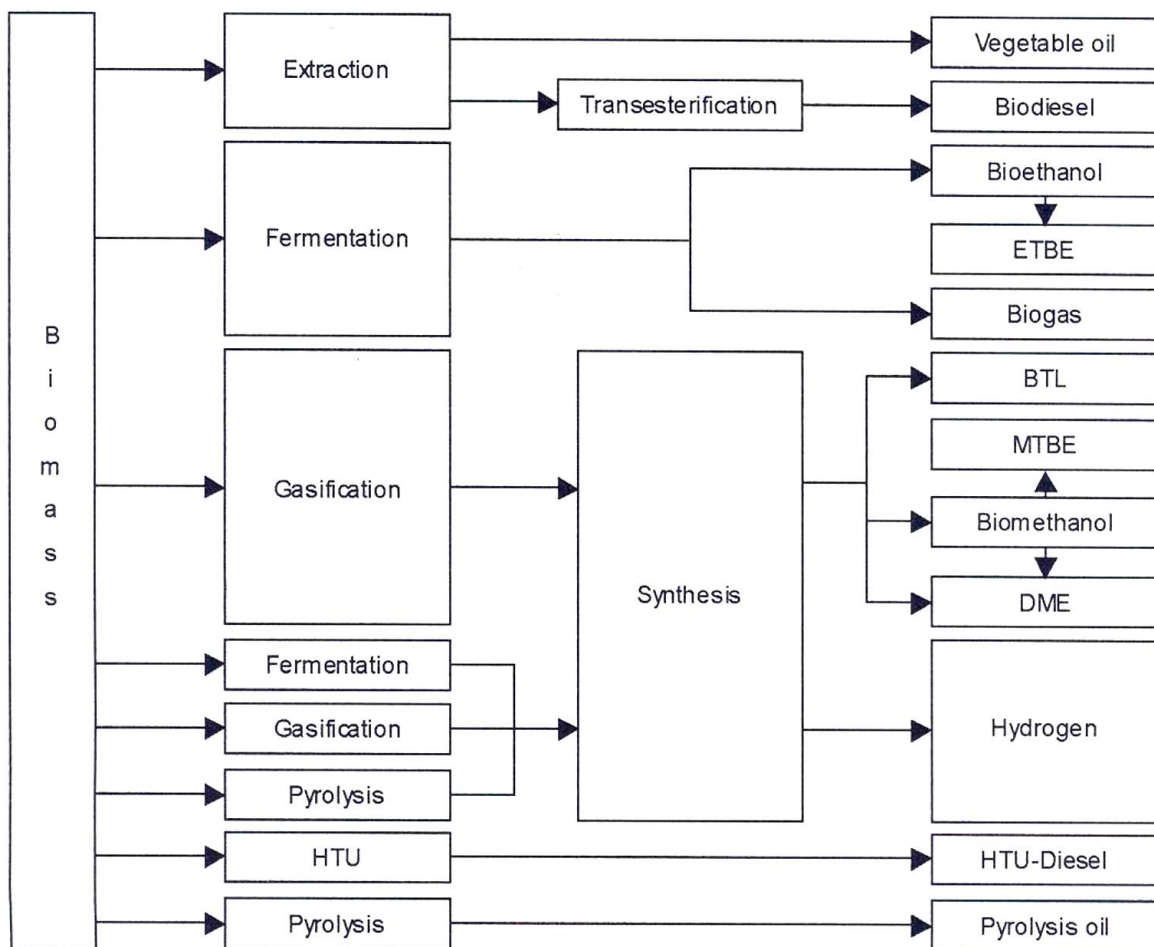


Figure 5: Biofuel conversion routes [20].

## 2.1 FIRST GENERATION BIOFUELS

First generation biofuels are the commercial available biofuels today, and consists of biodiesel, bioethanol and biogas. Their role in the fuel mix is developing with a tripled global demand for liquid biofuels from 2000-2007, which continues to increase [12].

### 2.1.1 Biodiesel

Biodiesel is a substitute for traditional diesel and can be used as B100 (100% biodiesel), but is normally found as a blend with petroleum diesel (5%, 10% and 20%) [3]. It is produced through transesterification, a process where an ester and an alcohol react to produce another alcohol and another ester. For production of biodiesel vegetable oils, residual oils and fats, which contain esters and glycerol, react with an alcohol (mostly methanol). The glycerol is displaced by a short line of alcohol to separate esters of fatty acids, with the glycerol as a co-product [14, 21]. Rape oil is the most used base in Europe and produces the biodiesel Rape Methyl Ester (RME). Fatty Acids Methyl Ester (FAME) is made from other fatty acids [4].

All diesel engines today can run on B7 without compromising the engines performance. At higher concentrations the engine might experience clogging of filters due to a higher solubility in the biofuels releasing deposits from former diesel use, bad fuel quality at cold temperatures due to a higher viscosity and a slightly lower energy output. Positive effects are higher cetane number which yields a low ignition delay, literally no sulfur content, a more complete combustion and better lubricity [14]. Today biodiesel makes up 0.2% of total diesel fuel [12].

### 2.1.2 Conventional Bioethanol

Bioethanol is the biofuel produced at the largest scale today [22], and can replace gasoline in flexi-fuel vehicles or be a base for ethyl tertiary butyl ether (ETBE), which blends better with gasoline. Conventional bioethanol is produced by fermentation of sugar or starch from plants like grain, corn, sugar beet and potatoes [4, 14]. Starch cannot be transformed directly to ethanol, but first converted to glucose by hydrolysis and then fermented [10]. The fermentation of sugar (glucose) is done by enzymes produced from yeast [12]. The conventional ethanol is called grain alcohol and bioethanol produced from cellulosic biomass is called biomass ethanol, which will be discussed under second generation biofuels [14]. Brazil and USA are the biggest producers of bioethanol and their main feedstock is respectively sugar cane and corn [22].

Bioethanol represents 2% of all gasoline fuel [12], and all gasoline cars can run on fuel with 10% bioethanol without modifications [3]. In higher concentrations, bioethanol can degrade elastomeric components and accelerate corrosion of some metals. This is a problem in older

models, but by choosing right materials this can be easily and affordably eliminated. It has a high octane number and can improve fuel economy in re-optimized engines [3].

### 2.1.3 Biogas (biomethane)

Biogas is produced from anaerobic digestion of liquid manure and other digestible feedstocks, such as organic waste, animal manure and sewage sludge or corn, grass and crop wheat [3]. The biogas is often used for generation of heat and electricity, but can also be further processed to fuel. The biogas is then purified by removing CO<sub>2</sub> and hydrogen sulfide to obtain biomethane (CH<sub>4</sub>), and then compressed and used in natural gas engines. Biomethanol is limited in its ability to compete with the liquefied biofuels, due to high production cost and lack of required vehicles and infrastructure [12].

## 2.2 SECOND GENERATION BIOFUELS

Table 2: Classification of 2nd generation biofuels, their feedstock and production path [12].

Biofuel group	Specific biofuel	Biomass feedstock	Production process
Bioethanol	Cellulosic ethanol	Ligno-cellulotic materials	Advanced enzymatic hydrolysis and fermentation
Synthetic biofuels	Biomass-to-liquid (BTL) Fischer-Tropsch diesel (FT) Synthetic diesel Biomethanol Heavier alcohols Dimethyl ether (DME)	Ligno-cellulotic materials	Gasification and synthesis
Biodiesel (hybrid of 1st and 2nd)	NExBTL H-Bio	Vegetable oils and animal fats	Hydrogenation
Bio hydrogen	Hydrogen	Ligno-cellulotic materials	Gasification and synthesis or biological processes

Second generation biofuels are considered to be superior to first generation with regard to sustainability, but are not available on a commercial scale yet. Since first generation biofuels come from food- and oil-seed crops they are in direct competition to food and feed production, which has questioned their true environmental benefits. The second generation biofuels feedstock consists primarily of ligno-cellulosic materials, which are cheap, abundant non-food materials. The process of converting cellulosic materials into fuel is more advanced than for the first generation feedstocks. This comes from the higher complexity in their composition, and there is a need to overcome some of the technological barriers in order to make the process cost competitive. Recently there have been big investments in pilot and demonstration plants with the objective to identify feedstocks, processes and pathways with the potential of being operated at a big scale [3, 12, 14]. In table 2 the most common second generation biofuels are listed, along with the feedstock utilized and production process. The biofuels have ligno-cellulosic feedstocks and are produced through a Bio-chemical or

Thermo-chemical route. These are the main technological pathways and will be discussed in this section [12].

### ***2.2.1 Bio-chemical route***

Producing ethanol from lingo-cellulosic feedstocks demands a different technology than ethanol produced from sugar and starch. Its strong bonds need pretreatment to enable an efficient hydrolysis, and traditional enzymes cannot hydrolyze cellulose. Hence sophisticated cellulose enzymes must be used for hydrolysis, and yeast must be replaced by microorganisms for fermentation. This hinders the production process to be cost competitive, with the result of less than 0.1% of total ethanol produced being of second generation in 2008. The bio-chemical route consists of four steps: pretreatment, hydrolysis, fermentation and purification [12, 23].

#### *Pre-treatment*

Without pretreatment cellulose would convert into sugar at a slow rate. The pretreatment should disorganize the crystalline structure to access the cellulose, remove lignin and hemicelluloses, increase the porosity of the material so enzymes can penetrate into the fibers during hydrolysis and prevent the formation of by-products with inhibitory effects on the hydrolysis and fermentation process [23, 24].

There are several methods for pretreatment and they can be divided into physical, physical-chemical and biological pretreatment. Not all of these are available for commercial use, and how suitable they are depends on the feedstock. In addition they must also be compatible with the method of hydrolysis [23].

#### *Hydrolysis*

The chains of sugar in cellulose are broken down. This can be done by chemical or enzymatic reactions, where the bonds are broken by acid or by enzymes. Enzymatic hydrolysis will have a low presence of by-products, low corrosion problems and low utility consumption due to its mild conditions (pH = 4.8 and temperature 45-50°C) compared to the acid [23].

#### *Fermentation and purification*

The sugar is converted by microorganisms like bacteria, yeast or fungi without the presence of oxygen. The product is referred to as “beer” and consists of ethanol, cell mass and water. Ethanol is recovered in a distillation column, where water remains with the solid parts, and can then be used in fuel cell vehicles (FCVs). For use as a mixture with gasoline it can be further distilled in the presence of an entrainer, dried by a desiccant or pervaporated [25].

## 2.2.2 Thermo-chemical processing

Thermo-chemical processing is on the contrary from the bio-chemical route, based on well-established technology [12]. Figure 6 shows the three main technologies of thermal processing; pyrolysis, gasification and combustion. In combustion biomass is burned in domestic stoves and boilers with the product  $\text{CO}_2$ ,  $\text{H}_2\text{O}$  and heat, so this process is not a part of the biofuel production and therefore not relevant for this paper. Figure 6 also shows the products of the biofuel conversion technologies, primarily bio-oil and fuel gas. Different end uses are listed, but for this thesis only end use in engines will be explored [26]. The thermo-chemical route includes production of syngas which is cleaned, before usually entering a Fischer-Tropsch process (explained later in this section) where mainly synthesis diesel is produced [12].

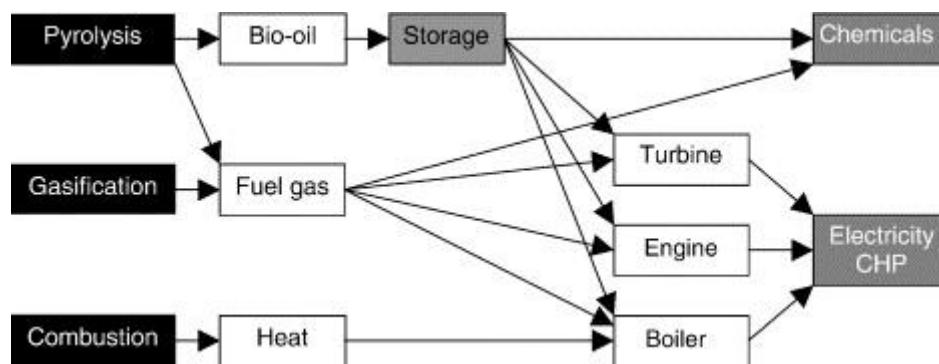


Figure 6: Products from thermal biomass conversion. CHP stands for combined heat and power [26].

### 2.2.2.1 Pyrolysis

Pyrolysis is degradation by heat in the absence of oxygen. The final products are charcoal, bio-oil and fuel gaseous products. The products vary with residence time, heating rate, temperature and composition of the biomass. These different conditions divide the process into conventional, fast and flash pyrolysis. It is not possible to produce diesel fuel directly from pyrolysis, but flash pyrolysis produces crude oil with 70% efficiency. It operates with high temperature, short residence time, fast heating rate and fine particles. After pyrolysis the products are separated in a cyclone. The gas is then cooled down and the condensable components are converted to bio-oil, whereas gases like  $\text{CO}_2$ ,  $\text{CO}$ ,  $\text{H}_2$  and  $\text{CH}_4$  are recycled or used in gas engines. The char can be burned to produce heat, or mixed with crude oil to form bioslurry, which can be converted to syngas in a gasifier.

This process is of interest since the oil can be burned in thermal power station, used in conventional petroleum refinery, burned as gas or upgraded to hydrocarbon fuel, but the challenge is high bio-liquid upgrading cost [27].

### 2.2.2.2 *Gasification – Biomass-to-liquid*

Gasification is conversion of biomass by thermal decay and chemical reformation, in contact with a controlled amount of oxygen. The product is CO, H<sub>2</sub>, CO<sub>2</sub>, CH<sub>4</sub> and higher carbon compounds, and is called producer gas, syngas or synthetic gas depending on its properties. All biomass can be used, but wet biomass (agriculture and municipal waste) will give a lower efficiency [12, 14, 22].

Gasification can be conducted with or without the presence of a catalyst, but it is usually present since it can lower the operation temperature considerably (900°C vs. 1300°C). Steam air, oxygen and hydrogen can all work as gasification agents in the reactor. There are various types of reactors and they need to fulfil requirements around the ratio of CO to H<sub>2</sub>, have the ability to operate with a large scale production and produce clean gas that do not obstruct the catalyst or require an expensive purification process. Cyclone, barrier or electrostatic filters and wet scrubbers can be used to remove impurities like char particles, inorganic ash, sulfur and alkali compounds. Wet scrubbers and cracking can remove tar and nitrogen compounds. Tar is the main obstacle for further processing, but also contains energy that can be utilized by cracking. It is important that technical barriers around clean-up are being addressed, since impurities in the syngas inhibit the FT catalyst and can make the FT process uneconomic [12, 14, 28].

The main routes of converting syngas to biofuel are hydrogen by water-gas-shift (WGS) reaction, hydrocarbons by FT synthesis or hydrocarbon or oxygenated liquid fuel by methanol synthesis with additional processing [14]. In a WGS reaction water reacts with CO to produce CO<sub>2</sub> and H<sub>2</sub>, where CO<sub>2</sub> later is removed. The syngas from gasification has a low ratio of hydrogen, and in order to produce methanol or FT fuel the ratio of hydrogen must be increased since these processes require a H<sub>2</sub>/CO<sub>2</sub> ratio of respectively 3:1 and 2:1. This is done by the WGS process and the gas is compressed before entering the methanol or FT synthesis [29].

#### *Methanol synthesis*

There are technologies being developed to increase the ratio of methanol conversion. The conventional reactor operates in gas phase, but slurry technologies like liquid phase process has a higher conversion. Here the syngas, the methanol produced and the catalyst are in contact with the liquid, which increases the heat transfer from the catalyst. It is important to have a clean syngas in order to protect the catalyst. This technology can obtain a methanol conversion ratio of 95%.

Methanol has similar characteristics as ethanol. It has a slow evaporation rate which gives poor cold start properties, and it needs little oxygen for combustion due to its low stoichiometric air/fuel ratio (even less than ethanol). Compared to petrol it has a higher density, but lower calorific value which will give reduced engine power. Methanol can be used in SI engines, and petrol with 15% methanol can be used without any modifications required. With a higher content it faces the same problems as conventional ethanol, addressed

in sectioned 2.1.2. Methanol has a low cetane number which hinders ignition and makes it unsuitable for diesel (CI) engines [29].

### *Fischer Tropsch synthesis*

Fischer-Tropsch (FT) synthesis is based on already commercial technology from coal-to-liquid process. It is an exothermal reaction that in addition to producing a variety of hydrocarbons, releases a high amount of heat. The reaction occurs in the presence of an iron or cobalt based catalyst. By varying temperature, pressure, feed gas composition ( $H_2/CO$ ), catalyst type and composition of reactants, the product vary. Typically diesel and waxes are produced at 180-250°C, and gasoline and olefins at 300°C [4, 14].

FT petrol has a too low octane number to be used in SI engines, but can be used in a mix with conventional petrol with a concentration up to 15%. FT diesel (FTD) on the other hand has high quality, and is generated from production of waxes followed by selective hydro cracking [29]. The FTD can be used as a mix with conventional diesel, or in modified diesel engines. It has an energy density in the area of conventional diesel, a high cetane number which gives good ignition qualities, it is ideally carbon neutral and has basically no sulfur content [28, 29].

## **2.3 ADVANCED BIOFUELS**

Advanced biofuels are characterized by new feedstocks and advanced technologies. They are still in an R&D stage but may play an important role in the future.

### **2.3.1 Algae**

Algae are divided into macro-and microalgae, where microalgae are unicellular species, while macroalgae are multicellular with plant characteristics (seaweeds) [30]. There is a big interest around microalgae since they possess great feedstock properties with a capacity to yield 16 times more oil than palm oil, and 100 times more oil than traditional vegetable oil crops [12]. Microalgae are regarded as one of the most sustainable feedstock since they require 1% of the water consumed by the latter crops, have a rapid growth, have the ability to capture considerably  $CO_2$  (one kg dry algae employ 1.83 kg of  $CO_2$ ), are not a food crop, do not require pesticides, can function as wastewater treatment (removal of  $NH_4$ ,  $NO_3$  and  $PO_4$ ), can be produced on arable land and all year around [12, 31]. The technologies used for producing biofuels from algae are commercial today, and the main barrier is the availability of the feedstock [4]. Microalgae can be produced in closed photobioreactors where parameters like temperature, sunlight, contamination risk and  $CO_2$  level are regulated and controlled, but this is too expensive compared to the oil extracted. A bigger open-air system which typically takes place in lakes and natural or artificial ponds is cheaper, but then there is no control of the climate conditions or the presence of other organisms that can obstruct the growth. A



possibility is a combined solution with daily transfers from the closed to the open system, in order to maintain a sufficient concentration of the desired culture [12]. The harvest of the biomass makes up 20-30% of the total production cost, which needs to be lowered. The lipids have to be extracted from the algae before they can be converted into energy through either bio-chemical conversion, chemical reaction, direct combustion or thermo-chemical conversion, which are processes described earlier. To commercialize biofuels from microalgae a development regarding photobioreactors design and harvesting is needed [31].

### ***2.3.2 Bio-SNG – Bio-synthetic natural gas***

Bio-SNG can use both wet and dry feedstocks, but with different conversion routes. For wet biomass the conversion is either through anaerobic digestion where methane is generated, or supercritical water gasification (temperature above 374°C and pressure above 221bar) where the product is a hydrogen rich gas [12, 32]. From dry biomass the route is gasification followed by a methanation process, where methane is developed from CO and H<sub>2</sub>. Because of its similarities to natural gas, bio-SNG can utilize already existing natural gas pipelines, and also as fuel it possesses all of the same properties as compressed natural gas (CNG) and liquefied natural gas (LNG). A challenge with bio-SNG is the necessity of compressing or liquefying the gas to reduce the need for storage space, which increases the cost and energy use. Bio-SNG has a low emission of CO<sub>2</sub>, NO<sub>x</sub> and particles [12].

### ***2.3.3 Pyrolysis diesel***

Pyrolysis is, as mentioned under 2.2.2.1, thermal degradation of biomass in the absence of oxygen. In producing bio-oil through fast pyrolysis, bigger particles can be used as input which saves contamination and energy. It can operate with a lower temperature than a gasifier (500°C) and at 1 atmosphere. After the pyrolysis the char is separated, milled and mixed with the bio oil, and therefore the conversion of carbon is increased. The problem with the oil is its strong acidity, which makes it corrosive and the materials used for storage and handling are more expensive. It is therefore common to use the char for heating purposes, and the oil as a base for further development of diesel fuel [12].

### ***2.3.4 Hydrogen***

Hydrogen is considered an important fuel for the future with its high energy concentration per weight and flexibility in use and storage. It is not commercially available today since it does not occur naturally. It is expensive to produce, requires dedicated infrastructure and has a low energy density per volume.

There exist different pathways in producing hydrogen. Among them gasification, thermo chemical cycles where water is split into hydrogen and oxygen, or the conversion of intermediates (ethanol, bio-oil). Gasification and pyrolysis are the most promising pathways in medium term [32].

### ***2.3.5 Consolidated bioprocessing (CBP)***

CBP is a one-step conversion of biomass by CBP microorganisms that can produce cellulase, hydrolyse and ferment the cellulosic biomass. This will be a more cost efficient process due to a simpler feedstock processing and a more efficient conversion [33].

The CBP microorganisms are developed through two routes: engineering naturally occurring cellulolytic microorganisms or non-cellulolytic organisms to increase yield [34]. The technologies are still under development, but metabolic engineering has great potential in producing environmental friendly fuels in the future [33, 34]

The second generation FTD is one of the most prominent alternatives to conventional diesel, and is the biofuel furthered investigated in this thesis. Its combustion characteristics will be compared to conventional diesel and a short discussion regarding its sustainability will be presented.

### 3. ENGINE TYPE AND FUEL SIMULATED

As mentioned in the introduction the diesel engine is projected to strengthen its position in the car market both in Norway and worldwide [6, 18]. It is therefore important to focus on finding and commercializing alternative fuels which can be used in these engines, as well as studying how the engine itself can improve by altering its operational conditions. Consequently in this thesis a direct injection compression ignition (DICI) engine, also known as the diesel engine, has been simulated and tested under different operational conditions. The fuels simulated are a surrogate fuel used to model conventional diesel and a reduced model for FTD. They have been compared with regard to combustion characteristics and emission profiles. FTD can be used as a mix with conventional diesel or in modified diesel engines, and is a high quality fuel [28, 29].

#### 3.1 DIESEL ENGINE

##### 3.1.1 *CI engine*

The diesel engine is a CI (compression ignition) engine, which is an internal combustion engine. Here the oxidizer is sucked into the cylinder before it is compressed, and at the end of the compression stroke the fuel is injected into the cylinder. The fuel atomizes, vaporizes and mixes with the oxidizer before the mixture auto-ignites, due to in-cylinder temperature and pressure above the fuels ignition point [35]. This creates a massive exothermic reaction pushing the piston back, and delivering power to the engine. The diesel engine has a high thermal efficiency compared to other combustion engines, due to its large compression ratio and lean mixture. The large compression ratio is necessary to obtain a high enough temperature to secure auto-ignition, and since a large compression ratio also signifies a large expansion ratio, less thermal energy will be released with the exhaust. As opposed to an SI (spark ignition) engine, the CI engine can operate with a leaner mixture. This is also related to the manner of ignition, where the SI engine requires the mixture to be close to stoichiometric to ensure ignition of the whole mass when spark igniting. The excess of oxygen present in a CI-engine contributes to a more complete combustion, and balances off the in-homogeneities in the fuel distribution. The lean mixture also leads to lower exhaust gas temperatures, which reduce the wear and tear on the components, lowering the maintenance cost. However there are some trade-offs when using a CI engine, like higher  $\text{NO}_x$  and soot emissions. Since the fuel distribution is in-homogeneous local stoichiometric air-fuel ratios will dominate, producing high flame temperatures. These high temperatures along with the abundant oxygen and nitrogen from the air will yield increased  $\text{NO}_x$  emissions. Also the soot emission will be greater owing to the reduced time for mixing fuel and air [17, 18, 36-38].

### **3.1.2 Direct injection (DI) engine**

The CI engine is seldom found without direct injection, and is therefore a DI engine. It is not the only engine that can be operated as a DI engine; this can also be the case for the SI engine although it is not customary. A DI engine can be described as a way of introducing fuel to the combustion chamber, where the engine will directly inject the fuel instead of having it premixing with the oxidizer [5].

A factor that can play an important role in the optimization of the CI engine is the point of injection. After injecting the fuel, there will be a time delay before ignition occurs in the chamber due to the mixing process. In order for the engine to operate at a highest possible efficiency the auto-ignition should take place close to top dead center, localized at a  $0^\circ$  crank angle. An earlier ignition will work against the movement of the piston, and a late ignition will lose power due to the expansion of cylinder volume.

The DI engine is in constant development in order to increase its efficiency, but also to reduce its emissions. These two factors to some extent correlate, since emissions like soot particles, HC and CO represents a loss with regard to engine efficiency due to incomplete combustion, as well as being polluting. However with emissions requirements prohibiting larger fractions than 0,5% soot, 1% HC and 0.5% CO compared to the initial fuel injection due to air-polluting, the engine will only experience limited losses and still operate with an efficiency of 98% [35].

### **3.1.3 Emission and exhaust gas recirculation (EGR)**

As just mentioned an important factor when developing and optimizing an engine is the emission characteristics, which are continually facing stricter requirements. The emissions from an ideal combustion process ( $\text{CO}_2$ ,  $\text{H}_2\text{O}$ ,  $\text{N}_2$ ,  $\text{O}_2$ ) generally make up 99% of the total exhaust, while the remaining 1% is negligible thermodynamically, but significant with regard to the environment [38]. The exhaust from diesel engines is classified as carcinogenic [18], imposing a hazard to human health along with the surroundings. Consequently there is an ongoing development in the technology of preventing the in-cylinder creation of the hazardous components, as well as after treatment.

CO is a product of incomplete combustion and may originate from either a too rich or too lean mixture. In the primer case there is insufficient oxygen present in order to fully oxidize the fuel, and for the latter case the temperature will be too low leading to partial oxidation. Soot is also formed in rich mixtures with high temperature, but can rather easily be reduced by oxidizing in a lean mixture at a high temperature.  $\text{NO}_x$  is produced at high flame temperatures in regions redundant with oxygen and nitrogen, as is the case during a lean combustion in a diesel engine. A problem which arises when trying to reduce the emissions is that reducing one component may have counteracting effect on another. Lowering the temperature and the concentration of oxygen will reduce the  $\text{NO}_x$ , but this may elevate the presence of both CO and soot due to a more incomplete combustion. The soot and CO can be reduced by obtaining

a more complete combustion either by increasing the mixing time or including a post-injection, enhancing the temperature later in the cycle. Both the latter methods will increase the  $\text{NO}_x$  production with elevated temperatures in the presence of oxygen [17, 18, 38, 39].

As discussed above the presence of CO and soot will diminish with a more complete combustion, which is optimal with regard to engine efficiency. New technology such as supercharging and injection systems improving mixing will lead to better operational conditions, but makes the  $\text{NO}_x$  reduction targets even harder to reach [40]. Another factor intensifying the  $\text{NO}_x$  emissions is the increasing traffic in urban areas where the engine runs at low loads, and hence altering the air-fuel ratio. The high loads operates with an air-fuel ratio of 1.5-1.8, which can increase to 10 during idling [38]. Exhaust gas recirculation (EGR) is currently one of the most effective means to reduce the  $\text{NO}_x$  emissions. Here some of the exhaust is redirected back into the combustion chamber as a part of the inlet gas [17, 40]. The goal of EGR is to reduce the emissions by modifying the oxygen concentration and thermodynamic properties in the cylinder, without large trade-offs in engine performance [38]. It is not a new phenomenon but has strengthened its possession due to the stricter requirements set to the  $\text{NO}_x$  emissions, and a development in its technology securing a more reliable operation [40].

The recycled gas is an inert gas and will not participate in the reactions [18]. However their presence will reduce the  $\text{NO}_x$  due to two main factors: 1) The main components in the exhaust gas are  $\text{CO}_2$  and  $\text{H}_2\text{O}$  which possess a higher specific heat compared to air, lowering the temperature of the reaction rate. 2) The dilution effect lowers the concentration of oxygen surrounding the fuel molecules, forcing them to diffuse over a larger area to obtain sufficient oxygen to combust. Accordingly the reaction rate and temperature will be lowered since the heat will be released over a larger time frame. Another factor yielding temperature decrease is the enhancement in mass, which will absorb the energy released during combustion. This is due to the presence of  $\text{CO}_2$ ,  $\text{H}_2\text{O}$  and the additional amount of  $\text{N}_2$  in the enlarged diffusion area. The diffusion effect is shown to have the most prominent contribution in the reduction of  $\text{NO}_x$  [17, 18, 40, 41]. Other less important effects come from an increase in soot formation and the prolonged ignition delay. Additional soot is produced due to a more incomplete combustion, which decreases the flame temperature as a result of enhanced radiation. The ignition delay effects the emissions in two manners: The delay may cause the combustion to occur in the exhaust stroke where the temperature is lower, and thereby reducing the  $\text{NO}_x$ . Another effect is a more complete combustion owing to the longer mixing time. This normally increases the flame temperature, but the additional molecules absorbing the heat released ensures a temperature reduction, lowering the emissions [41].

There are several trade-offs when applying EGR such as worse specific fuel consumption, engine durability, aggravating lubricating oil qualities and higher soot emissions. EGR is usually found with a cooler, lowering the temperature of the exhaust before it mixes with the intake air. Even with cooling the exhaust temperature exceeds the air-intake temperature, decreasing the density of the mixture. This reduces the total mass introduced to the cylinder, lowering the engine performance. The durability of the engine is affected by the sulfur oxide and other aggressive substances presence in the exhaust, which when reintroduced in the

combustion chamber will wear the engine. Also the concentration of sulfur oxide present in the oil increases with EGR, causing it to deteriorate. The most severe trade-off is however found in the soot emissions due to the counteracting correlation between the production/reduction of soot and  $\text{NO}_x$ , explained earlier in this section. Some tests however have demonstrated a lower soot emission for very high EGR ratios, which is a result of the flame temperature being below what is required for soot formation (1800K). Although this provides a reduction in soot as well as  $\text{NO}_x$ , such high EGR ratios impose instability in the combustion process, especially at high loads where more fuel is injected. Consequently the  $\text{NO}_x$  reduction can be defined as load dependent, where the lower load requires a more extensive use of EGR due to the higher oxygen concentration and lower concentration of combustion products. This also implies that it can withstand a higher degree of EGR. For the higher load the use of EGR will be limited due to the soot trade-off and unstable conditions, even though the  $\text{NO}_x$  emission still will be significant [17, 38, 40, 41].

Despite the negative effects accompanied with the introduction of EGR, it is the most efficient way of reducing  $\text{NO}_x$ . Another incentive for the appliance of EGR came in 1990, when the emission of particulates was decided to be measured in mass flow rather than concentration. This favors EGR since it limits the exhaust mass flow, thereby reducing the mass flow of particles. The problem to be resolved is to what extent EGR should be used with regard to engine load, and it should be combined with after treatment like soot traps and catalytic filters [17, 38, 40].

## 3.2 FUEL

Since a CI engine does not utilize an external source for ignition, the fuel has to withhold good combustion quality in order to self-ignite. This is determined by the cetane rating of the fuel, which reflects the ignition delay of the fuel after injection. Biofuels often show great qualities with regard to combustion process and end emissions, and in this thesis one of the most promising alternatives to conventional diesel, FTD, is tested and compared to the combustion of a surrogate fuel representing conventional diesel. FTD has a high cetane rating, low sulfur and toxic content and withholds more oxygen in its composition which yields a more complete combustion [16, 42]. It can be used as a blend or even as a pure fuel without requiring modifications in the diesel engine, although yielding minor challenges in the combustion process [43]. Its production path is already addressed in section 2.2.2.2.

There has been an increased skepticism regarding the sustainability of biofuels since they often turn out be less environmental friendly than first assumed when the whole life cycle is investigated. This has led to stricter requirements to the feedstocks and their origin, induced by the Renewable Energy Directive (RED) in the European Union [44]. To insure that the fuels are within the limitations set, it is important to truly assess the sustainability of the fuel in question. Here follows a discussion regarding the true benefits of FTD.

### 3.2.1 Sustainability of FTD

FTD is a second generation biofuel, and as mentioned before more environmental beneficial than the first generation biofuels. When assessing the true benefits of biofuels it is important to evaluate the whole life cycle from cradle to grave. It is said that all biofuels are carbon neutral since their feedstock absorbs the same amount of CO<sub>2</sub> that is emitted when combusted in an engine. However this is not true when assessing the whole life cycle. Here cultivation, transportation and distribution are included, which are non-carbon neutral processes and will aggravate the results [45]. The GHG savings for different life cycle analyses (LCAs) found in literature vary greatly. This is due to the lack of a standardized method for calculating the effect imposed by different parameters (direct and indirect land use change, use of fertilizers, etc.), and the fact that they often do not include the same parameters [46]. The direct land use change comes from emissions related to cultivating new areas, like CO<sub>2</sub> stored in trees or in the soil itself. The indirect land use change arises from the need for cultivating new areas for food and feed production, as already cultivated land is being used for biofuel production. These are complicated parameters and their true effect is difficult to assess. Consequently different conclusions are found in reports including the same parameters, and some effects are also commonly omitted due to the insecurity they inflict on the results. In a report from Menichetti and Otto (2009) [47], excluding land use change and indirect effects, the FTD yields a reduction in GHG emission of 90%. In an LCA performed by Wu et al. (2006) [48], comparing FTD made from switchgrass where direct land use change is included, the savings are reduced to 84%. These are only two examples and greater variations can be found in other reports, but regardless they show that FTD can reduce the GHG emissions substantially.

From the LCA of FTD from Wu et al. (2006) [48] some emission characteristics are compared to conventional diesel, and can be seen in figure 7. This is the emission profile when tested in a DICI engine, and figure 7 shows the change in percentage of fossil fuel consumption, emission of GHGs, volatile organic compounds (VOCs), CO, NO<sub>x</sub>, PM<sub>10</sub> and SO<sub>x</sub>. The reduction in GHG emissions is as mentioned above 84%, and also a significant reduction in fuel consumption is present with a decrease of 88%. The emissions of criteria pollutants show an increase of VOCs, CO and NO<sub>x</sub>, while the rest decreases. Most LCAs conclude with a doubling of NO<sub>x</sub> emission compared to conventional fuels, which is caused by their increased oxygen content [49]. Here a much lower increase is present (45%), which is the result of a reduced use of fertilizers and the usage of gas turbine combined cycle (GTCC) power co-production. The fertilizers can be reduced due to the ability of the root system of the switchgrass to retain nutrients and prevent runoffs, reducing the level of nitrogen used. The GTCC power co-production can replace power from coal fire boilers and save 9-34 times the NO<sub>x</sub> emissions.

Also the vast reduction in SO<sub>x</sub> emissions observed is related to the factors mentioned above. SO<sub>x</sub> shows the biggest reduction of the criteria pollutants with a saving of 49%. The diesel used today contains a low percentage of sulfur so the savings in the end use are minimal. Accordingly the reduction mainly originates from the change in feedstock and production stage, where less fertilizer and the GTCC play the leading role. Coal is the biggest emitter of

SO<sub>x</sub>, and the electricity production will reduce the demand of coal based electricity (which in 2006 made up 30% of the energy mix in the US). Use of less fertilizers with phosphorous will give a lower potential for SO<sub>x</sub> [48].

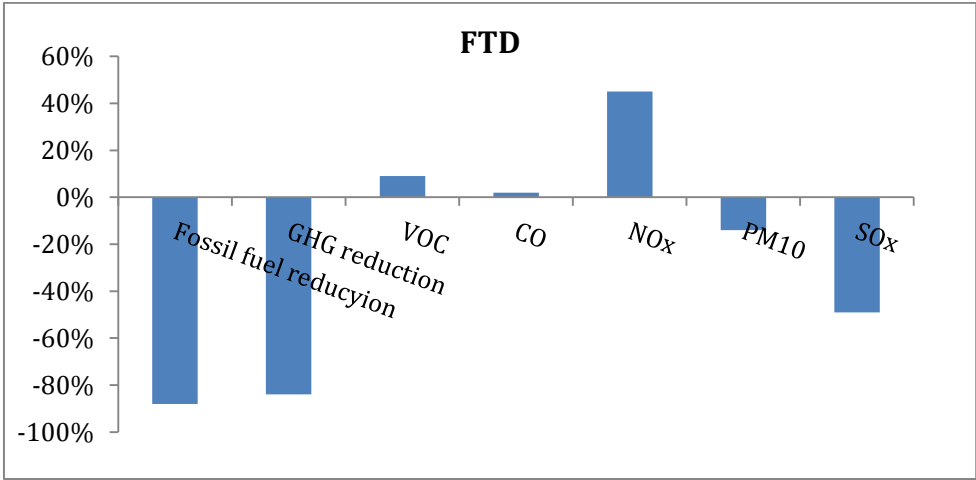


Figure 7: Percentage change in energy use, GHG emission and emissions of criteria pollutants per mile driven of BIO-FTD, relative to diesel in a conventional DICI engine [48].

There has been an increasing awareness around the environmental potential of second generation biofuels. RED has targeted a 10% renewable energy share by 2020, and to increase the interest and development of these second generation biofuels they are rewarded doubled credit. In the same target only 5% can come from biofuels based on starch rich crops, sugars and oil crops, i.e. first generation biofuels [44, 50].



## 4. CHEMICAL MODELING

In order to run simulations on the desired fuels, chemical models need to be obtained which withhold the same characteristics as the original fuel. With a chemical model containing reaction chemistry, important information like ignition quality, pollutant emissions and combustion characteristics can be obtained. Even new information may be provided, compared to what is obtainable from experimental data [15, 16, 51]. There has been a huge development and improvement of the detailed kinetic mechanisms, and with that an increase in their complexity and time required for calculation [15, 52]. Although more reactions are known and defined, not all play an equally important role in the process. A detailed description of the kinetics is needed as a starting point, but can be simplified by eliminating less important species and reactions through a reduction of the models [53-55].

The chemical kinetics and the thermodynamics provide the basis for which reactions that will occur. In a chemical reaction molecules and/or atoms collide, and if the collision energy exceeds that of the chemical bonds they will break, rearrange and create new product species. In these reactions atoms like C, H, O and N are released and redistributed, but unlike the molecules which can be broken up and transformed, the atoms are always preserved [51, 56]. The thermodynamically aspect is fulfilled by the collision energy exceeding the energy in the chemical bonds, and the chemical kinetic model will for all species determine at which rate the product species are produced. This is resolved by the concentration of the reacting species, since a higher concentration will increase the likelihood of a collision occurring. Another parameter is the rate constant which holds information regarding parameters like temperature and pressure dependency [5, 56]. Here follows a derivation of the reaction rate, which is collected from [5, 56]:

Here two species  $A$  and  $B$  collide and form the product specie  $C$ :



The reaction rate when the two species collide is given as  $r$ :

$$r = k(T)[A]^{v_A}[B]^{v_B} \quad (4.2)$$

Where  $v$  is a stoichiometric coefficient determining how much of each specie that will collide and react, and  $[A]$  and  $[B]$  give the concentration of the species. The rest of the factors influencing the reaction rate are included in  $k$ , which is the reaction rate coefficient determined by the Arrhenius equation:

$$k = Ae^{-E/(RT)} \quad (4.3)$$

Where  $A$  represents the physical aspects (molecular size, angular effects, average molecular speed, etc.),  $E$  is the energy the collision needs to overcome in order to break the chemical bonds,  $R$  is the gas constant and  $T$  the temperature. A modification of the Arrhenius equation gives the reaction rate coefficient for reaction  $j$  as:

$$k_j = A_j T^{n_j} e^{-E_j/(RT)} \quad (4.4)$$

Here the temperature dependency of  $A$  is expressed individually, where  $n_j$  is a fit parameter.

A specie  $i$  can play the part of both the product and the reacting specie, hence a species concentration  $c_i$  is the sum of all reactions where it is involved. The concentrations time derivative is therefore expressed as the sum of all reaction rates for a specie  $i$  in reaction  $j$ :

$$\dot{c}_i = \sum_{j=1}^{N_R} (v''_{ij} - v'_{ij}) r_j = \sum_{j=1}^{N_R} v_{ij} r_j \quad (4.5)$$

Here  $v'_{ij}$  and  $v''_{ij}$  represents the reactant and product side respectively for specie  $i$  in reaction  $j$ , where  $v_{ij}$  represents the sum of reactants and products in a net stoichiometric coefficient and  $N_r$  is the total amount of reactions. The reaction rate expressed in equation (4.2) can for reaction  $j$  be expressed as:

$$r_j = \prod_i^{N_i} c_i^{v'_{i,j}} k_j \quad (4.6)$$

The consumption and production of all species in the system is then given as:

$$\omega_i = \sum_j^{N_r} v'_{i,j} r_j \quad (4.7)$$

The pre-exponential factor  $A$  in the Arrhenius equation represents the rate at which collisions occur when disregarding their kinetic energy. That is the molecular size and average molecular velocities. In the definition of  $A$  the boltzmanz factor is included, which relates the fraction of collisions to the amount occurring with energy above  $E_j$ . This amount will be of greater size with higher temperature in the cycle, since this denotes the molecular speed.

A differential equation needs to be solved for each specie introduced, which will yield a huge set of coupled differential equations. The time derivative of specie A is given as:

$$\frac{d[A]}{dt} = \omega_A \quad (4.8)$$

#### 4.1 REDUCING CHEMICAL MODELS

From the equations above it can be understood that each specie introduced will prolong the computational time when running a simulation. An increase in the number of species will actually give an exponentially increase in computational time. There are two factors which will determine the complexity of the chemical model, that is: 1) the complexity of the fuel

investigated and 2) to which extent you would like to include factors like  $\text{NO}_x$ ,  $\text{SO}_x$  and soot [5].

The quality of the obtained results from simulations will be determined by how accurate the chemical model is, and a problem that always arises is the trade-off between quality and time consumption. Recent years there has been a huge development within the computational power of computers, and also substantial research has been put into reducing the size of the chemical models, without sacrificing too much of the quality [5, 19].

The goal of reducing the kinetic mechanism is to simplify the calculations by eliminating the insignificant species and reactions, without altering the global properties of the process [53]. In a reaction there will be a great number of intermediate species which will not be a part of the end product, but they all possess a more or less significant contribution to the combustion process. Heat is released when the species react, which is important for the development of the combustion process and the engine performance. Some species will play a more important role than others and occur with a larger mass fraction, but accurate calculation has to be conducted on all species regardless of mass fraction to get the optimal quality. However the correlation between the number of species included and time consumption is not linear. When looking at the complexity of a chemical model with respect to the size of the systems numerical matrix, its size will be the number of species and unknowns (like temperature, pressure, etc.) included, to the power of two. Another important factor regarding the time consumption is the variance in the size of the species concentration in the system. This owes to an increased time for calculation when solving larger mass fractions, at the same time as it solves very small mass fractions with the same accuracy. Here also the number of species included will play a role, since a large number of species present will yield an increased difference in the mass fractions [5].

There are different approaches to reducing a mechanism, and often several methods are applied together. Some are mentioned here in this section. The oldest and a simple method is a sensitivity analysis, where the role of the parameters is quantified. The analysis looks at the sensitivity of a chosen parameter (e.g. flame temperature or ignition timing), to a change in the species investigated. But a specie is not only rated by the impact of the specie itself, also its role in producing or consuming other important species will increase its importance [55, 57]. The slower reaction elimination method, analysis and identifies optimal sets of reactions. The detailed reduction compares the reaction rates for important atomic species (like C, H, O and N), with predefined critical values. The minor flows can often be removed however some important reactions which have a slow reaction rate should not be neglected. Another approach is lumping, where species with similar properties can be represented by one lumped specie. Here the reaction path and not the single species are of importance, so species of interest should not be lumped together [5, 53, 55].

To illustrate the course of such a reduction the requirements used in a paper by Wang et al. (1991) [54] are provided in the following equations. To determine which reactions and species that should be removed, two criteria reflecting the reaction rate and heat released from reaction  $j$  have been used:

$$|r_j| < \epsilon_r |r_{ref}| \quad (4.9)$$

$$|r_j \Delta H_j| < \epsilon_Q \dot{Q}_{max} \quad (4.10)$$

The equation (4.9) looks into how significant reaction rate of reaction  $j$  is compared to a reference reaction rate, while equation (4.10) compares the size of the heat released. Here  $r_j$  is the rate of reaction  $j$ ,  $r_{ref}$  the rate of a reference reaction,  $\Delta H_j$  is the enthalpy change of reaction  $j$  and  $\dot{Q}_{max}$  is the maximum heat released when considering all reactions and  $\epsilon_r$  and  $\epsilon_Q$  are chosen parameters. If a reaction fulfills both of the two criteria it will be removed from the model, and as can be seen from (4.9) and (4.10) smaller values for  $\epsilon_r$  and  $\epsilon_Q$  gives stricter criteria for reducing the mechanisms.

The general process of reducing a mechanism follows the proceeding five steps [53]:

- 1) Identify important species and reactions from the base mechanism.
- 2) Eliminate insignificant species and reactions.
- 3) Run the reduced mechanism at operating conditions and validate the results by comparing with reference data.
- 4) Improve the reduced mechanism by adding or removing species and reactions in order to correspond better with the reference data.
- 5) Alter reaction rate constants to correspond better with reference data.

#### ***4.1.1 Important factors for this paper***

The factors important to include depend on what you want to retrieve from the simulations. When the fuel species are injected and mixed with the oxidizer, they will be transferred into different intermediates depending on the reactions involved. Regardless of what the product species are, the reaction molecules will have a smaller number of carbon atoms than the reactant molecules. For a complete combustion with air, the end products should be CO<sub>2</sub>, H<sub>2</sub>O and N<sub>2</sub>, but this only occurs under ideal conditions and is never the real case. In this thesis simulations will be run for a diesel surrogate and a reduced model for FTD, and the impact of different operational conditions on important aspect like the emissions of the essential greenhouse gases and criteria pollutants, combustion characteristics and engine performance will be investigated. The species that will be of extra important for this thesis are [56]:

- The fuel species: They are the basis for the reaction occurring.
  - N-Heptane, (nC<sub>7</sub>H<sub>16</sub>), a primary reference fuel (PRF) for the diesel surrogate.
  - N-Alkane (nC<sub>14</sub>H<sub>30</sub>), I-Alkane (C<sub>14</sub>H<sub>30-2</sub>) and Alkene (C<sub>14</sub>H<sub>28-1</sub>) for the FTD surrogate.
- CO<sub>2</sub>: One of the final products of the complete combustion process. It is the most prominent component with regard to anthropogenic greenhouse gases.

- CO: A toxic molecule which is a product of incomplete combustion, hence its presence represents a loss of energy in the process.
- NO<sub>x</sub>: Collective term for NO and NO<sub>2</sub>. By-products in the combustion process and are formed by an endothermic reaction, which requires high temperatures. NO is most prominent in the emissions, but rapidly oxidizes to NO<sub>2</sub> in the atmosphere, increasing its toxicity by a factor of 5. In the atmosphere NO<sub>x</sub> can also react to form nitric acid which contributes to acid rain, ozone and a range of other toxic components [18, 58, 59].
- OH: A very reactive specie which basically does not exist before the point of ignition, after which it quickly reaches its maximum share. It is therefore a good indicator to determine where the ignition is initiated.

## 4.2 DIESEL SURROGATE

For the simulation of diesel a chemical kinetic mechanism has been collected from Lawrence Livermore National Laboratory (LLNL). To model the diesel a primary reference fuel (PRF) consisting of n-heptane is used, which is a well understood fuel with accurately defined chemical kinetic reaction rates [15]. N-heptane is an alkane, which is saturated hydrocarbons, with the chemical formula nC<sub>7</sub>H<sub>16</sub>. It has an octane rating of zero and requires therefore a low activation energy for ignition, and burns explosively [15, 56]. This makes it unsuitable for petrol engines, but is a fairly good model for diesel.

## 4.3 FTD SURROGATE

For novel fuels only few reliable chemical models are available, and for FTD these are found as complex models difficult to utilize due to their large size. This is a consequence of the nature of the fuel and the fuel production, since its composition varies with the process conditions and catalyst used. Accordingly comprehensive chemical models with regard to chemical species included are required in order to obtain a general representation of FTD. In this thesis a reduced model for FTD is employed with the fuel composition 0.772 n-Alkane (nC<sub>14</sub>H<sub>30</sub>), 0.047 i-Alkane (C<sub>14</sub>H<sub>30-2</sub>) and 0.181 Alkene (C<sub>14</sub>H<sub>28-1</sub>). In the original model obtained from LLNL 7200 species were included, but through a reaction flow and sensitivity analysis the model was reduced to 1535 species. This is nearly an 80% reduction in species, providing a 90% reduction in time consumption. The reduced models reliability have been ensured by a qualitative analysis by Malik et al. (2013) [43], where the main features of the more complex model were still observed. Even though the model for FTD has undergone a large reduction it is still relatively complex when compared to other biofuels like biodiesel, which can be reduced to less than 100 species while still possessing a satisfying quality [43].

## 5. PHYSICAL MODELING

### 5.1 MODEL DESCRIPTION

This section provides a description of the simulation approach with regard to engine type applied and its physical properties. A combustion process is highly complex; therefore approximations have to be done in order to run a simulation process. These simplifications will be addressed, along with important calculations performed in the model.

DARS version 2.08 has been used as the simulation tool when assessing the combustion process, and this section is mainly based on manuals from DARS [60-62].

The model chosen for this paper is the Stochastic Reactor Model (SRM), and the engine type used is a Direct Injection Compression Ignition (DICI) for a passenger car. Some simulation models assume homogeneity inside the cylinder as a simplification for the calculations, whereas in a SRM the homogeneity is replaced by statistic homogeneity. This is based on the Partially Stirred Plug Flow Reactor (PaSPFR) where the volume in the cylinder is divided into a number of smaller volumes, known as particles. A particle has its own chemical composition, temperature and mass, but due to the fact that the SRM is a 0-dimensional model no characteristics regarding the position in space are given. Although no exact position in space is present, the Probability Density Function (PDF) gives a distribution of the properties of the particles and enables them to mix and exchange heat with the cylinder walls. By doing so the model takes into account in-homogeneities and turbulence.

A DI-SRM is a good approach when simulating a diesel engine since it includes a model for direct injection of fuel. Here new particles are added under the assumption that the fuel is fully vaporized during injection, and the new particles consist of the new fuel injected combined with already existing gas in the cylinder. The fuel is injected during a closed cycle, and no inlet or exhaust flows through valves are included in the model. It follows from the injection of fuel that the combustion process is determined by the mixing process as well as the chemical kinetics, which will decide the combustion initiation. It is therefore important to have a sufficiently accurate model for both the kinetics and the mixing process.

One of the most important aspects of the SRM is its capability to include in-homogeneities. For a DI engine the in-homogeneities arises from the injection of the fuel, the inlet charge itself being in-homogeneous and from the heat exchange with the cylinder walls. To ensure that in-homogeneity is accounted for, it is important to have good models for the fuel injection and heat transfer. One essential characteristic regarding the SRM is its ability to include these factors while still retaining a low computational cost.

To simplify the solving of the equations for the PDF, a time stepping operator splitting technique is employed. This means that for each time step the differential operator is split into several operators representing different physical aspects which are solved sequentially. These are piston movement, fuel injections, mixing, chemical reaction and heat transfer.

For academic work as well as in the industry, the SRM has received increased attention later years due to its ability to imitate the combustion characteristics and end emissions [15]. In a comparison to a VW engine parameters such as ignition delay, heat release rate and emission of  $\text{NO}_x$  were predicted quite well, as opposed to the emissions of HC and CO which were under predicted.

## 5.2 CALCULATION

### 5.2.1 Energy and mass conservation in a closed system

The model consists of one zone, i.e. no transport of gas between zones, so the numerical model is a set of zero dimensional time dependent differential equations. Newton's method is applied for solving the balance equations, and higher order backward differential functions are used to determine the time. The laws of thermodynamic are obeyed when simulating in DARS, and the balance equations for mass, energy and momentum are based on the Navier-Stokes equation for reactive flow:

$$\frac{\partial W}{\partial t} + \frac{\partial J}{\partial x} = Q \quad (5.1)$$

Where for a variable  $V$ ,  $W$  is the density ( $[V]/\text{cm}^3$ ),  $J$  is the flux density ( $[V]/\text{cm}^2$ ) and  $Q$  is a source term describing production ( $[V]/\text{cm}^3\text{s}$ ).

For the calculations the ideal gas law is always assumed to be valid.

$$pV = nRT \quad (5.2)$$

Here  $p$  represents the absolute pressure of the gas,  $V$  the gas volume,  $n$  the amount of gas present in mole,  $R$  the ideal gas constant and  $T$  the absolute temperature of the gas [37].

As mentioned the simulated combustion cycle operates as a closed cycle with no inlet or exhaust flow through valves. When operating with a closed system the balance equations for mass and energy are simplified to conservation equations. These equations are used as a base when deriving differential equations used for the mass density function in the PDF, and consequentially the origin of these conservation equations will first be described here.

#### 5.2.1.1 Mass conservation

The general mass balance of a chemical specie  $i$  is described by the inlet and outlet flux, and the formation/consumption of the specie.

$$\frac{\partial m_i}{\partial t} = \sum_l^{N_{in}} \dot{m}_{i,l} + \sum_k^{N_{out}} \dot{m}_{i,k} + \omega_i M_i \quad [\text{kg/s}] \quad (5.3)$$

Where  $m_i$  represents the mass of specie  $i$ , the two first terms represents the total mass flux in and out of the control volume  $V$ ,  $l$  represents the inlets and  $k$  the outlets. The last term represents the formation of the specie, where  $\omega_i$  is the net reaction rate and  $M_i$  is the molecular weight for specie  $i$ .

Here the engine will operate as a closed system so there will be no inflow or outflow, i.e. the two former terms will equal zero. When accounting for this, while introducing the density as  $\rho = m/V$ , and the mass fraction  $Y_i$  as the mass of specie  $i$  divided by the total mass,  $\frac{m_i}{m}$ , the conservation equation for the mass fraction of specie  $i$  can be expressed as:

$$\frac{\partial Y_i}{\partial t} = \frac{\omega_i M_i}{\rho} \quad [1/s] \quad (5.4)$$

### 5.2.1.2 *Energy conservation*

Before determining the energy conservation the general form of the energy balance is first provided:

$$\frac{dE}{dt} = \dot{Q} - \dot{W} + \sum_l^{N_{in}} \dot{m}_l (h + e_k + e_p)_l - \sum_k^{N_{out}} \dot{m}_k (h + e_k + e_p)_k \quad [J/s] \quad (5.5)$$

Where

$$\dot{W} = p \frac{dV}{dt} \quad [J/s] \quad (5.6)$$

The energy balance is derived from heat transfer with the surroundings  $\dot{Q}$ , work done on or by the system  $\dot{W}$  and energy transfer connected to the inlet and outlet flow. The  $e_k$  and  $e_p$  are the specific kinetic and potential energy and  $h$  is the specific enthalpy for the inlet  $l$  and outlet  $k$  of the control volume. These two latter terms regarding inlet and outlet flow in the system will equal zero due to the closed system, hence the total energy can be expressed by the change in internal energy  $U$ , and (5.5) reduces to:

$$\frac{dU}{dt} = \dot{Q} - \dot{W} \quad [J/s] \quad (5.7)$$

The internal energy  $U$  can be expressed as the specific internal energy  $u$ , times the total mass  $m$ . The change in internal energy can then be given by:

$$\frac{dU}{dt} = m \frac{du}{dt} + u \frac{dm}{dt} \quad [J/s] \quad (5.8)$$

When using the definition for enthalpy  $h=u+pv$ , where  $p$  and  $v$  represent respectively the pressure and specific volume, the previous equation can be expressed as:



$$\begin{aligned}\frac{dU}{dt} &= m \frac{d(h - pv)}{dt} + (h - pv) \frac{dm}{dt} = m \frac{dh}{dt} - m \frac{dpv}{dt} + h \frac{dm}{dt} - pv \frac{dm}{dt} \\ &= m \frac{dh}{dt} + h \frac{dm}{dt} - \frac{dmpv}{dt} \quad [J/s] \quad (5.9)\end{aligned}$$

The previous equation gives the total change in energy, where the terms represent the change in enthalpy, mass and work. The middle term which gives the change due to mass transfer will equal zero.

The total specific enthalpy can be given as the summation of each species specific enthalpy, times their mass fraction ( $h = \sum_i^{Ns} Y_i h_i$ ). Hence the change in specific enthalpy can be given as:

$$\frac{dh}{dt} = \frac{d}{dt} \left( \sum_i^{Ns} Y_i h_i \right) = \sum_i^{Ns} Y_i \frac{dh_i}{dt} + \sum_i^{Ns} h_i \frac{dY_i}{dt} \quad [J/s \text{ kg}] \quad (5.10)$$

Where  $N_s$  is the total amount of species. The specific enthalpy is defined by the enthalpy at a reference temperature, represented by the index 0, and the specific heat at constant pressure for a given specie,  $c_{p,i}$ . The relation is given by:

$$h_i = h_i^0 + \int_{T^0}^{T'} c_{p,i} dT \quad [J/kg] \quad (5.11)$$

The ideal gas behavior gives  $h_i = h_i(T)$ , and when combined with equation (5.11), an expression for the change of the specific enthalpy of specie  $i$  is given as:

$$\frac{dh_i}{dt} = \frac{\partial h_i}{\partial T} \frac{dT}{dt} = c_{p,i} \frac{dT}{dt} \quad [J/s \text{ kg}] \quad (5.12)$$

When inserting equation (5.12) above and the mass fraction conservation equation (5.4) into the equation for the change of specific enthalpy (5.10), and applying that the specific heat equals the summation of each species specific heat times their mass fraction ( $c_p = \sum_i^{Ns} Y_i c_{p,i}$ ), equation (5.10) can be expressed as:

$$\frac{dh}{dt} = c_p \frac{dT}{dt} + \sum_i^{Ns} \frac{h_i \omega_i M_i}{\rho} \quad [J/s \text{ kg}] \quad (5.13)$$

When inserting (5.13) into the expression for internal energy (5.9) and setting this equal to (5.7), also expressing the change in internal energy, while using the relation  $V = v \cdot m$ , the expression for energy balance changes into the expression for energy conservation, given by:

$$\frac{dU}{dt} = m \left( c_p \frac{dT}{dt} + \sum_i^{Ns} \frac{h_i \omega_i M_i}{\rho} \right) - \frac{dVp}{dt} = \dot{Q} - p \frac{dV}{dt} \quad [J/s] \quad (5.14)$$

The heat transfer  $\dot{Q}$  is defined as:

$$\dot{Q} = \dot{q}m = mh_c A_w (T - T_w) \quad [J/s] \quad (5.15)$$

Where  $\dot{q}$  is the specific heat transfer,  $h_c$  is the heat transfer coefficient,  $A_w$  is the in-cylinder wall area,  $T$  is the in-cylinder temperature and  $T_w$  is the cylinder wall temperature.

When inserting (5.15) into (5.14) and rearranging the terms one gets:

$$m c_p \frac{dT}{dt} + m \sum_i^{N_s} \frac{h_i \omega_i M_i}{\rho} - V \frac{dp}{dt} - mh_c A_w (T - T_w) = 0 \quad [J/s] \quad (5.16)$$

And finally the conservation equation for energy can be given as:

$$\frac{dT}{dt} = -\frac{1}{c_p} \sum_i^{N_s} \frac{h_i \omega_i M_i}{\rho} + \frac{1}{c_p m} V \frac{dp}{dt} + \frac{1}{c_p} h_c A_w (T - T_w) \quad [K/s] \quad (5.17)$$

Equations (5.4) and (5.17), providing the conservation of mass fraction and energy, represents equations for the full set of variables usually presented as the variable vector  $\phi$ , applied in the next section.

### 5.2.2 PDF

In the SRM a PDF gives a distribution of particle properties, which resembles a space variation of the cylinder mass. A mass density function (MDF) is a discretized function of the particles and can be written as:

$$F_\phi = (\psi_1, \dots, \psi_{N_s+1}, t) \quad (5.18)$$

where

$$\phi(t) = (\phi_1, \dots, \phi_{N_s+1}; t) \quad (5.19)$$

gives the vector of the random variables in the MDF. Here  $\psi_1, \dots, \psi_{N_s+1}$  are the sample space variables of the corresponding variables  $\phi_1, \dots, \phi_{N_s+1}$ .  $N_s$  is the number of species in the model,  $N_s+1$  is the temperature index and  $t$  is time. When assuming statistical homogeneity and applying the conservation of mass fraction and energy given by equation (5.4) and (5.17), the time development of MDF is given by:

$$\frac{\partial}{\partial t} F_\phi(\psi, t) + \frac{\partial}{\partial \psi_i} (Q_i(\psi) F_\phi(\psi, t)) = \text{mixing term} \quad (5.20)$$

Where  $Q_i$  represents the changes of the MDF due to chemical reactions, heat transfer and the volume work:

$$Q_i(\psi) = \frac{M_i}{\rho} \omega_i(\psi), i = 1, \dots, N_s \quad [1/s] \quad (5.21)$$

$$Q_{N_s+1}(\psi) = -\frac{1}{c_p} \sum_i^{N_s} \frac{h_i M_i}{\rho} \omega_i(\psi) + \frac{1}{c_p m} V \frac{dp}{dt} + \frac{1}{c_p} h_g A_w (T - T_w) \quad [K/s] \quad (5.22)$$

Equation (5.21) and (5.22) represents respectively the balance of mass fraction for specie  $i$  and the energy balance. Here  $h_g$  is the Woschni heat transfer coefficient. The Woschni model is an empirically derived heat transfer model, which is widely used for determining the heat transfer coefficient [63].

### 5.2.2.1 Operator splitting technique

To simplify the calculations in the equations for the MDF a time stepping operator splitting technique is used. This implies that when solving the differential equation for MDF, the different physical processes are split into differential operators. This results in one time step being divided into piston movement, fuel injection, mixing, chemical reaction and heat transfer, which are solved sequentially. In figure 8 the operator splitting loop is demonstrated. The first step is determining the initial conditions which are provided by the user, and these values are here collected from the operational conditions of the experimental tests from DTU. Then the mass inside the cylinder is divided into particles, before the differential operators for the different physical processes are solved, each followed by a pressure correction calculation. These different operators will be handled in more detail in the following sections.

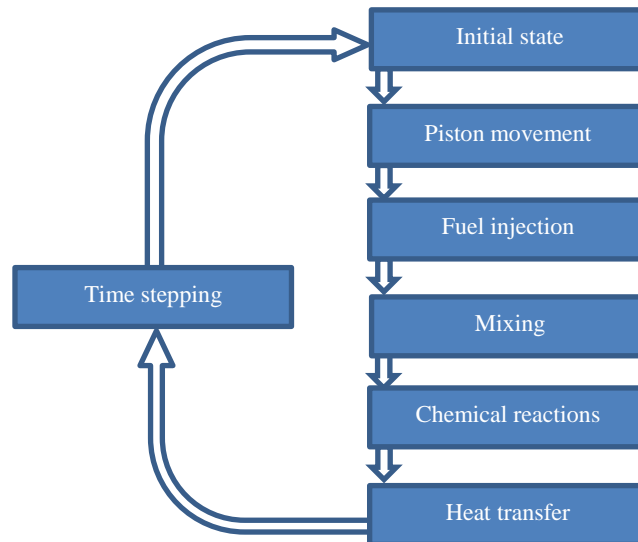


Figure 8: Operator splitting loop.

### 5.2.2.2 *Piston movement*

The piston decreases the cylinder volume as it goes from a crank angle of  $-180^\circ$  to  $0^\circ$ , and thereafter the volume expands until the piston reaches  $180^\circ$ . By doing so the pressure increases as the piston approaches  $0^\circ$ , and thereby decreases again. Consequently the gas inside the cylinder compresses, combusts and expands, which are the fundamentals in a combustion engine and hence important to model. This requires an accurate calculation of the piston volume, and an important parameter to include is the pin offset. This refers to a technique used to decrease mechanical stresses on the cylinder walls, friction and noise by offsetting the cylinder axis in relation to the crank center. In the model this is allowed for when determining the engine geometry, which changes with the crank angle degree  $\theta$ , and is given in the equation below:

$$V = V_c + \frac{\pi B^2}{4} \left( \sqrt{(L_{cr}^2 + R_{ct}^2) - Of_{pin}^2} - \sqrt{L_{cr}^2 - (R_{ct}^2 \sin(\theta) - Of_{pin})^2} - L_{cr}^2 \cos(\theta) \right) \quad (5.23)$$

Where  $V_c$  is the clearance volume,  $B$  the cylinder bore,  $L_{cr}$  is the connecting rod length,  $R_{ct}$  is the crank radius and  $Of_{pin}$  is the piston pin offset.

### 5.2.2.3 *Direct injection model*

One of the main characteristics of the DI-SRM is the direct injection model. When the fuel is injected it is assumed to vaporize instantaneously, which implies that the input model must be a vaporized injection curve and the energy required to vaporize the fuel needs to be included in the calculations. In order to include the vaporization energy the temperature of a sufficient amount of mass from the cylinder gas, referred to as the mixing mass, will be lowered to the fuel vaporization temperature and subtracted from its original particle. The mixing mass will form a new particle with the mass of injected fuel. The particle last created can have a smaller mass compared to the others, so this will be filled further at the next time step. Each of the particles are only allowed to grow to a size where their weight equals the other particles, and from that point the remaining fuel mass is assigned to another particle. As the injection progresses the mass of the existing particles decreases, but the number of particles increases.

The fuel injection model consists of several steps which are shown in figure 9. They include injection time, amount of vaporized fuel, vaporization temperature, mass needed for vaporization and then an update of the particles. The algorithm for the fuel injection, which is a step in the global time step, will be as followed:

- 1) Check if the time range is within the time range of any injection events. If true follow step 2-5, otherwise step out.
- 2) Calculate the amount of vaporized fuel from the externally described vaporization rate.
- 3) Determine the vaporization temperature corresponding to current pressure.

- 4) Calculate the amount of mixing mass corresponding to vaporization energy.
- 5) Update the particles properties.

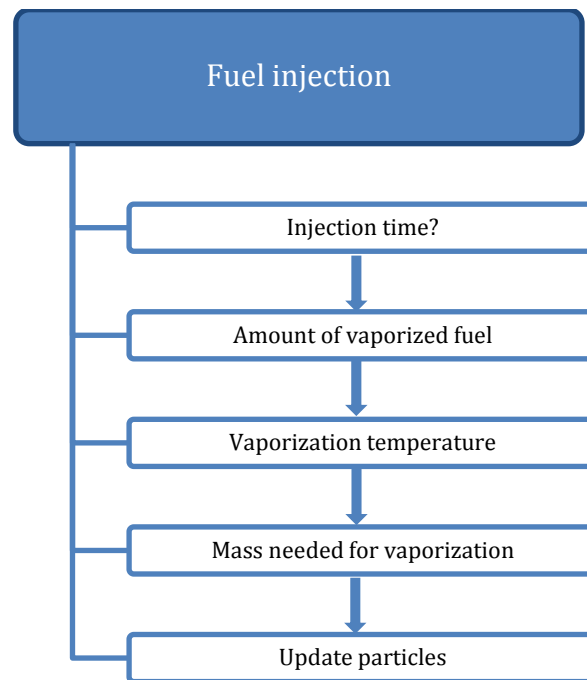


Figure 9: Steps in the fuel injection model.

#### 5.2.2.4 *Mixing*

The mixing model includes turbulence which is essential for the combustion in an engine like the DICl. Here the incoming charge is not premixed and a fast mixing of fuel and cylinder gas is preferred, which is enhanced by the presence of turbulence. Both mixing and turbulence have a high degree of complexity and several models can be used in an SRM. For DARS three different models are included, and in this work the coalescence/dispersal (C/D) model will be used. More information is given about the other models in the DARS manual – book 3 [60].

#### *C/D Mixing Model*

The C/D is a simple model and assumes that out of  $N$  particles,  $n$  random particle pairs will be mixed and obtain a mutual mean. This gives a PDF consisting of delta functions rather than being a continuous model.

In DARS for each time step the C/D model will execute the following tasks:

- 1) Calculate a time jump parameter
- 2) Advance a randomly calculated sub time step,  $t_{\text{sub}}$
- 3) Randomly select two distinct particles

4) Perform mixing:

$$Y_i^o(t + t_{sub}) = Y_i^x(t + t_{sub}) = \frac{w^o Y_i^o(t) + w^x Y_i^x(t)}{w^o + w^x} \quad (5.24)$$

$$h^o(t + t_{sub}) = h^x(t + t_{sub}) = \frac{w^o h^o(t) + w^x h^x(t)}{w^o + w^x} \quad (5.25)$$

Here the mass fraction of specie  $i$  and the specific enthalpy for the two chosen particles, denoted by  $o$  and  $x$ , will mix and obtain a mutual mean. Here  $w$  is a weighting factor determining the impact of each particle.

5) If  $t_{sub} < \Delta t$ , set  $t_{start} = t_{start} + t_{sub}$ , return to step 2.

Here  $\Delta t$  is the global time step.

#### 5.2.2.5 Chemical reactions

When solving for the chemical reactions, a set of non-stationary equations are solved for each particle giving them a new chemical composition after the current time step. Here a standard backward differential function method and a Newton algorithm is used to solve the set of equations, and the partial differential equations calculated for the chemical reactions are given as:

$$\frac{\partial}{\partial t} F_\phi = \frac{\partial}{\partial \psi_{N_s+1}} \left( \frac{1}{C_p} \sum_{i=1}^{N_s} h_i \frac{M_i}{\rho} \omega(\phi) F_\phi(\psi, t) \right) - \sum_{i=1}^{N_s} \frac{\partial}{\partial \psi_i} \left( \frac{M_i}{\rho} \omega(\phi) F_\phi(\psi, t) \right) \quad (5.26)$$

#### 5.2.2.6 Heat transfer

As mentioned earlier heat transfer is one of the sources to the in-homogeneities in a DI engine. It is therefore important that the heat transfer is modeled at a level of accuracy which gives realistic results. Here the Woschni heat transfer model is used to define the total heat transfer, but a stochastic approach determines the distribution of heat transfer over the particles.

#### 5.2.2.7 Pressure Correction Calculations

After each step the MDF`s are revised under the assumption of constant pressure, but an error arises since these steps are occurring sequentially and not simultaneously as in the real case. To eliminate this small error a pressure correction calculation is performed between each step, which recalculates the pressure and gives all the differential operators the same pressure condition. This eliminates the error that the constant pressure assumption introduces, as opposed to solving the MDF differential equation (5.20) directly. When the pressure is corrected the temperature and density of the particles are revised.

In the pressure correction calculations the pressure change will be divide between the different steps in the loop, that is:

$$\begin{aligned}
& -V \frac{1}{C_p} \left( \frac{dp}{dt} \right) \\
& = -V \frac{1}{C_p} \left( \frac{dp}{dt} \right)_{pistonmov} - V \frac{1}{C_p} \left( \frac{dp}{dt} \right)_{fuelinj} - V \frac{1}{C_p} \left( \frac{dp}{dt} \right)_{mix} \\
& \quad - V \frac{1}{C_p} \left( \frac{dp}{dt} \right)_{chem} - V \frac{1}{C_p} \left( \frac{dp}{dt} \right)_{heatt}
\end{aligned} \tag{5.27}$$

This is solved by the constraints regarding adiabatic compression of all particles and the sum of total volume, which has to be equal to the cylinder volume. Each particle  $x$  has its own specie composition and temperature, specific heat ratio,  $\gamma_x$  and pressure,  $p_x$ . For the adiabatic compression the following equation is given:

$$p_x V_x^{\gamma_x} = \bar{p} (V_x + \Delta V_x)^{\gamma_x} \tag{5.28}$$

And then to obtain an expression for  $\bar{p}$  the sum of the volume is used:

$$\sum_{x=1}^{N_{part}} \left[ V_x \left( \frac{p_x}{\bar{p}} \right)^{1/\gamma_x} \right] = V_{tot} \tag{5.29}$$

Where  $N_{part}$  is the total amount of particles. The pressure can by these correlations be corrected, followed by an update of the temperature and density with the new pressure.

#### 5.2.2.8 *Total differential operator for MDF*

When deriving the total differential operator for the DI-SRM, all factors mentioned above are included. Here the MDF given in equation (5.20) is divided into differential operators calculated at each time step, evaluating the impact of piston movement, fuel injection, mixing, chemical reaction and heat transfer, each followed by a pressure correction calculation. The total equation can be found in DARS manual - book 3 [60], where the different terms are furthered derived.

### 5.2.3 *Heat release*

The heat release is a measure of the engine performance and is a complex process to model. The atomization and vaporization of fuel, along with air entrainment, fuel-air mixing and ignition chemistry, will all affect the heat release process in a real engine. The basic understanding of this process is not adequate to model it from its fundamental base [35]. In DARS the total heat release is measured as the sum of the chemical heat release from each particle determined by their enthalpy, over one crank angel degree (CAD).

$$HR = \sum_{x=1}^{N_{part}} \frac{m_x (H_x^f - H_x^a)}{\Delta CAD} \quad [kgJ/Deg] \tag{5.30}$$

Where  $x$  is the particle index,  $m$  is the particle mass,  $H^f$  is the particles enthalpy after the chemistry step and  $H^a$  is the particles enthalpy before the chemistry step. The size of the heat release depends on the kinetics, and varies with the reactions occurring due to the difference in enthalpy for the atoms involved.



## 6. CASE SETUP

For the simulations conducted in this thesis the specifications regarding engine size, speed and load have been collected from experiments conducted in a real engine. The injection profile and amount of fuel being injected have been adapted for these simulations in order to approach the case of the real engine. These specifications are not easily determined from the real case since they are automatically adjusted by the engine control unit, ECU [64]. The engine specifications used in this work are given in this chapter.

### 6.1 ENGINE GEOMETRY

The basic engine geometry specifications are gathered from FORD engine data to match the experiments from DTU. The values used are defined in table 3:

Table 3: Engine geometry specifications.

Bore	75mm
Stroke	88.3mm
Compression ratio	17.4
Connecting rod length	136.8mm

### 6.2 ENGINE SPEED

The engine speed will vary with the driving conditions. When considering a real engine it will idle when operating at 900rpm, and will typically operate around 2000-3000rpm. Since the running conditions of the engine will differ for the various engine speeds, simulations have been performed for 900, 1500 and 2500rpm. The combustion characteristics for these changing engine velocities will be evaluated and compared.

### 6.3 LOAD

An engine will operate with different loads with regard to the driving conditions. From engine experiments the power consumption can be determine by the following equation:

$$Power [watt] = torque[Nm] * rpm * 2 * \frac{\pi}{60} \quad (6.1)$$

As mentioned above three engine speeds will be looked into here, which was also the case for the experimental data from DTU. The real engine was tested at five different power consumptions determined by the torque and speed, namely:

900rpm at 0 Nm	=	0kW (idle conditions)
1500rpm at 40 Nm	=	6kW
1500rpm at 80 Nm	=	13kW
2500rpm at 80 Nm	=	21kW
2500rpm at 120 Nm	=	31kW

There is no parameter for predetermining the load in the engine setup in DARS, hence as an approximation the amount of fuel injected during the combustion cycle has been used. Since these cases are not running with a fuel mass equivalent to the amount injected for the real engine at the different loads, the load will be a denominator of the case rather than the actual load of the engine. The amount of fuel injected is also defined in the injection profile, and for the different engine speeds the following fuel will be injected:

900 rpm:	3.492E-05 kg/cycle
1500 rpm:	5.50E-05 kg/cycle and 8.50E-05 kg/cycle
2500 rpm:	1.70E-04 kg/cycle and 3.50E-04 kg/cycle

#### **6.4 INJECTION INPUT FILE**

The injection of fuel occurs at different piston positions and is distributed at altered quantities during the combustion cycle. In table 4 and figure 10 the base injection profile used in the first simulations is given, and defines the fraction of mass injected at a given CAD. This is a dual injection profile, with a pilot injection starting at -5.6CAD followed by a main injection initiated at -2.7CAD. The point where fuel first is introduced into the cylinder (here -5.6CAD), is defined as the point of injection, although only a limited amount is injected here. The numbers marked in green in table 4 represent the pilot injection, which is only a small portion of the total injection (usually 5-10%). This is also illustrated by the first peak in figure 10. The goal of this pilot injection is to increase the temperature and pressure in the cylinder before the main injection, in order to diminish the ignition delay. The largest fuel fractions are injected slightly past top dead center (TDC), which is seen from the highest peak in the injection graph in figure 10 occurring at 0.3CAD.

The fuel injection file describing the injection point and quantity, will inject the fuel regardless of the in-cylinder conditions. In a real engine however, the injection will be altered automatically by the ECU, providing optimal running conditions. In this thesis the base case represented in the table 4 will be compared for the different engine speeds and fuel injected, and it will be tuned for each specific case with the aim to approach real engine conditions.

Table 4: Base fuel injection profile defining the fraction of fuel injected at each CAD.

Crank Angel	Fraction of fuel injected
-5.6	0.006760451
-5.2	0.037182479
-4.7	0.067604507
-4.3	0.037182479
-3.9	0.006760451
-2.7	0.006760451
-2.2	0.040562704
-1.8	0.084505634
-1.4	0.128448563
-1	0.175771718
-0.6	0.216334423
-0.2	0.256897127
0.3	0.28393893
0.7	0.273798254
1.1	0.239996
1.5	0.19605307
1.9	0.152110141
2.3	0.101406761
2.8	0.054083606
3.2	0.027041803
3.6	0.006760451

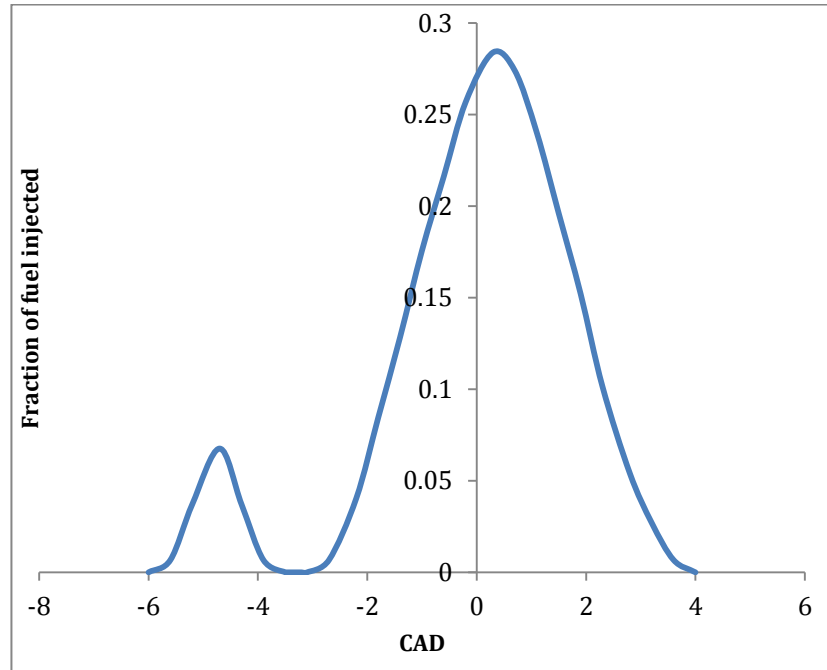
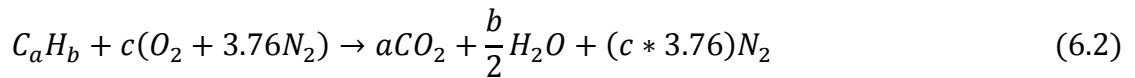


Figure 10: Illustration of the base fuel injection profile, defining the fraction of fuel injected at each CAD.

## 6.5 EQUIVALENCE RATIO, $\Phi$

In a complete combustion with air where hydrocarbon is used as fuel, the products will be carbon dioxide, water and nitrogen. In this case the equivalent ratio,  $\Phi$ , is 1, i.e. the amount of air present is exactly the amount required to fully combust the fuel. The reaction follows the equation below [5]:



To balance this equation it is easily seen that:

$$c = a + \frac{b}{4} \quad (6.3)$$

To achieve different combustion properties the equivalent ratio can be shifted to either work with a lean or rich mixture, respectively with an  $\Phi$  lower or higher than 1.  $\Phi$  is defined from

the ratio of mass fraction of fuel to oxidizer before reacting, compared to the case with complete combustion. The amount of carbon and hydrogen to the amount of oxygen is used to determine the ratio [60]:

$$\Phi = \frac{\frac{Y_{(C,H)}}{Y_{(O)}}}{\frac{Y_{(C,H)}}{Y_{(O)}}_{compl}} = \frac{\frac{m_{(C,H)}}{m_{(O)}}}{\frac{m_{(C,H)}}{m_{(O)}}_{compl}} = \frac{\frac{n_{(C,H)}}{n_{(O)}}}{\frac{n_{(C,H)}}{n_{(O)}}_{compl}} \quad (6.4)$$

As mentioned the mixture is rich if  $\Phi > 1$  and lean if  $\Phi < 1$ , with the rich mixture operating with an excess of fuel and the lean with an excess of oxidizer. This will change the combustion characteristics and the emission profiles. In this thesis the equivalence ratio will change with the amount of fuel being injected, making the fuel-air mixture richer as more fuel is being inserted into the engine.

## 6.6 EXHAUST GAS RECIRCULATION, EGR

EGR is widely used in engine operation and involves recycling some of the exhaust gas back into the combustion chamber, as explained in section 3.1.3. When the recycled gas participates in the combustion process once more, the emission characteristics can be improved, which will be looked into in this thesis. There are several ways of defining the EGR, and here it is defined by the mass fraction of gas recirculated, with regard to the total mass of recirculated gas, fuel injected and oxidizer [60]:

$$EGR = \frac{m_{EGR}}{m_{EGR} + m_{fuel} + m_{oxidizer}} \quad (6.5)$$

## 7. RESULTS SIMULATING N-HEPTANE

### 7.1 BASE INJECTION PROFILE

The simulations were first conducted with a fuel composition consisting of 0.8 n-heptane and 0.2 iso-octane, which is the standardized composition when modelling diesel. Due to errors in DARS when using this mechanism the fuel composition had to be reduced to only include n-heptane.

To save computational time the cycles are ran from -20 to 60 CAD, with gas inlet properties at  $T_i=700\text{K}$ ,  $P_i=2.33\text{E}6\text{N/m}^2$ . These were collected from the motored cycle, and since the variations of the conditions at -20CAD for the different engine speeds are negligible, the same inlet conditions are used for all cases.

#### 7.1.1 Gas properties

Here follows an overview of the cases investigated:

Table 5: Overview of simulated cases with regard to engine speed, injected fuel and load representation.

Case name	Engine speed (rpm)	Injected fuel mass (kg/cycle)	Representing load (Nm)
Fuel1	900	3.49E-05	0
Fuel2	1500	5.50E-05	40
Fuel3	1500	8.50E-05	80
Fuel4	2500	1.70E-04	80
Fuel5	2500	3.50E-04	120

Table 5 defines the engine speed, amount of fuel injected and load of the five main cases simulated in this thesis. As mentioned previously the fuel mass in the simulations will not be equivalent to the amount injected in the real engine at the different loads. The load is therefore only a denominator for the case it represents with regard to low, medium and high load. To avoid confusion the cases are given names associated with the amount of fuel injected, which will be used to address the different cases. Temperature, pressure and heat release profiles will be presented and analysed to retrieve information regarding how the engine operates under the different conditions.

In order to see the effect the equivalence ratio impose on the combustion cycle, simulations were intended to be run with both a rich, lean and stoichiometric mixture of fuel and air. When testing for different equivalence ratios however the point of ignition occurred previous to the injection of fuel, which is not feasible without the presence of fuel in the chamber. This

is explained by how DARS accounts for the equivalence ratio. It considers the ratio to exist at the beginning of the cycle, so here a mixture of air and fuel were already present in the start of the cycle, before additionally fuel were added by direct injection. Therefore in order for DARS to assume no fuel in the chamber until the predetermined injection point, the equivalence ratio has to be set to zero in the case settings. To illustrate the impact of this error figure 11 shows the cycles for 900rpm with an equivalence ratio set at 1 and 0. Here the values for the temperature and pressure profiles can be read from respectively the left and right axis. As can be seen from figure 11 the advancement of ignition is significant for the case operating with fuel already present in the chamber, i.e. the case with an equivalent ratio set to 1. This alters the combustion characteristics of the cycle giving higher peaks for temperature and pressure, due to better mixing conditions and a larger amount of fuel present in the chamber. It is therefore not possible to evaluate the effect of altered equivalence ratios in the results of this thesis, although the ratio will vary for the different cases since  $\Phi$  increases as more fuel is injected into the cylinder.

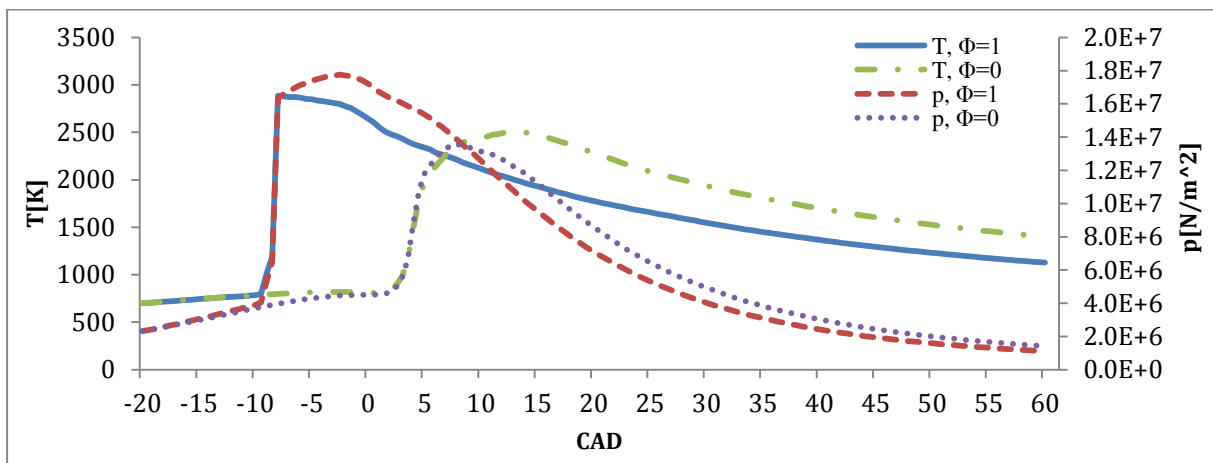


Figure 11: Temperature and pressure profiles for n-heptane running at 900rpm with equivalence ratio,  $\Phi$ , set to 1 and 0 in the case settings.

### 7.1.2 Pressure profiles

A combustion is defined either by the presence of a visible flame or, as in this case, where a significant pressure rise is detected. A combustion can be defined by three phases, namely the delay period, the rapid combustion and the combustion which burns at a rate controlled by its access to oxygen [36]. In the delay period injected fuel atomizes, vaporizes and mixes with the air, before self-ignition occurs. This is the time after the fuel is injected until a vast pressure increase is detected. In figure 12 the pressure curves of the cases defined in table 5 are presented as the piston moves from -20CAD to 60CAD. The minimum delay period exist for case Fuel1, which is as expected. Fuel1 represents idling, hence running with the lowest load and lowest engine speed. When the engine speed increases, the time available for mixing diminishes, and the ignition delay is prolonged to a wider range of CAD.

In the second stage of combustion the fuel burns rapidly, creating a steep pressure gradient. The length of this phase will be determined by the degree of pre-existent mixing between air and fuel, however this correlation is not straightforward to determine from figure 12. Here several variables interact, such as the already addressed engine speed, the amount of fuel injected and piston position when igniting. With an incremental amount of fuel being injected, more time will be required to obtain the same local air-fuel ratio in order to ignite. The piston position also strongly affects the pressure of combustion, since the compression and expansion stroke will respectively lower and raise the cylinder volume. Here all cases simulated ignite in the expansion stroke, where the pressure diminishes.

Fuel1 has as mentioned the shortest delay period which might reflect less mixing taking place, but since it operates at lower engine speed and also has less fuel injected, this is most likely not the case. It reaches the highest maximum pressure of 136bar, which may be explained by a more complete combustion due to better mixing, but might also be a result of its point of ignition. Fuel1 ignites at 1.5CAD which is the earliest point of the cases simulated, hence at the smallest cylinder volume.

At the point of maximum pressure the last phase of the combustion starts. Here the fuel will burn at a slower rate, determined by the accessibility of oxygen. Under optimal conditions the fuel will burn at a rate which provides constant pressure in the cylinder until all fuel is burned [36]. Figure 12 shows that neither of the cases maintains a constant pressure at the third phase of combustion, which is hindered by the position of piston moving downwards in addition to other non-optimal burning conditions.

When looking at the pressure profiles for Fuel2 and 3, the maximum pressure of Fuel3 exceeds the maximum pressure of Fuel2, with their values reaching respectively 125bar and 122bar. They both operate at an engine speed of 1500rpm, but Fuel3 has a larger fuel injection. It is unexpected that these cases ignite approximately simultaneously, and also that the pressure increase is larger for Fuel3.

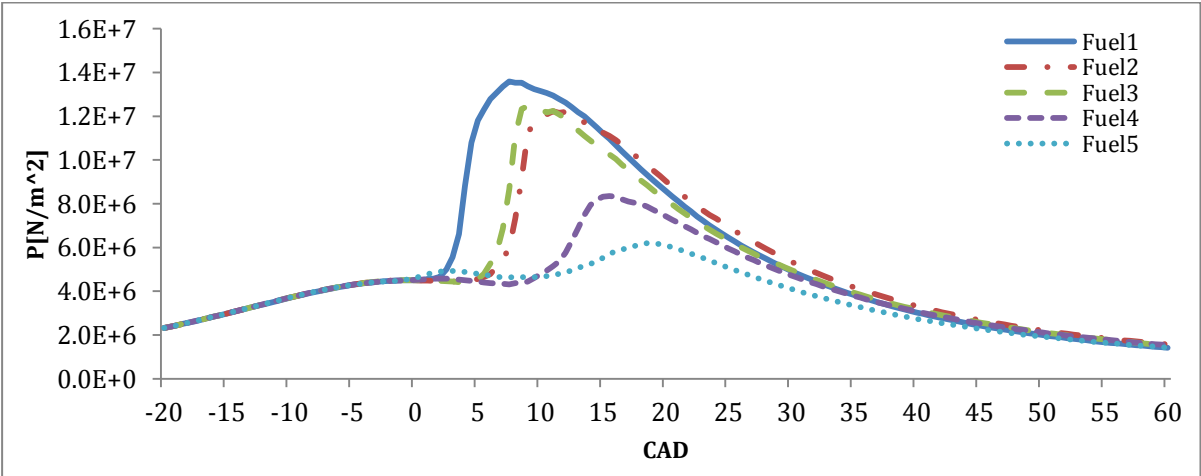


Figure 12: Pressure profiles for n-heptane for the cases Fuel1-5.

For Fuel4 and 5 both operating at 2500rpm, it appears that none of them fully ignite. This is seen from the limited pressure rise, which is especially evident for Fuel5. Fuel5 has the highest amount of fuel injected, requiring the longest mixing period of all the cases simulated when considering both speed and load. The extensive delay period will result in a too low in-cylinder pressure and temperature to enable combustion, due to the pistons position.

**7.1.3 Temperature profiles**

The temperature profiles can also be useful in order to get an indication of the point of ignition, as well as to what degree the mixture of air and fuel ignites. As can be seen from figure 13 the temperature profiles correlate well with the pressure profiles in figure 12. The earliest point of ignition and the highest maximum temperature both occur for Fuel1, which reaches a maximum temperature of around 2500K.

For Fuel2 and 3 running at 1500rpm the maximum temperature is higher for the case representing the lowest fuel amount (Fuel2). The lower maximum temperature for Fuel3 may indicate that the fuel has not fully combusted, and as explained earlier this can be the effect of the increased fuel injection requiring additional time to obtain the same degree of mixing between air and fuel. The steep increase in temperature at the beginning of the combustion for both cases indicates that ignition has occurred; such an increase is not present for the cases representing 2500rpm.

For Fuel4 and 5 there is no steep pressure rise for neither of the cases. This again implies that an ignition has not occurred. They will as mentioned both have an increased engine speed and amount of fuel being injected compared to the previous cases, which have caused problems for the initiation of combustion. Just from looking at their maximum temperatures it can be concluded that combustion has not taken place, since the maximum temperatures of Fuel4 and 5 are in the magnitude of respectively 1500K and 1200K.

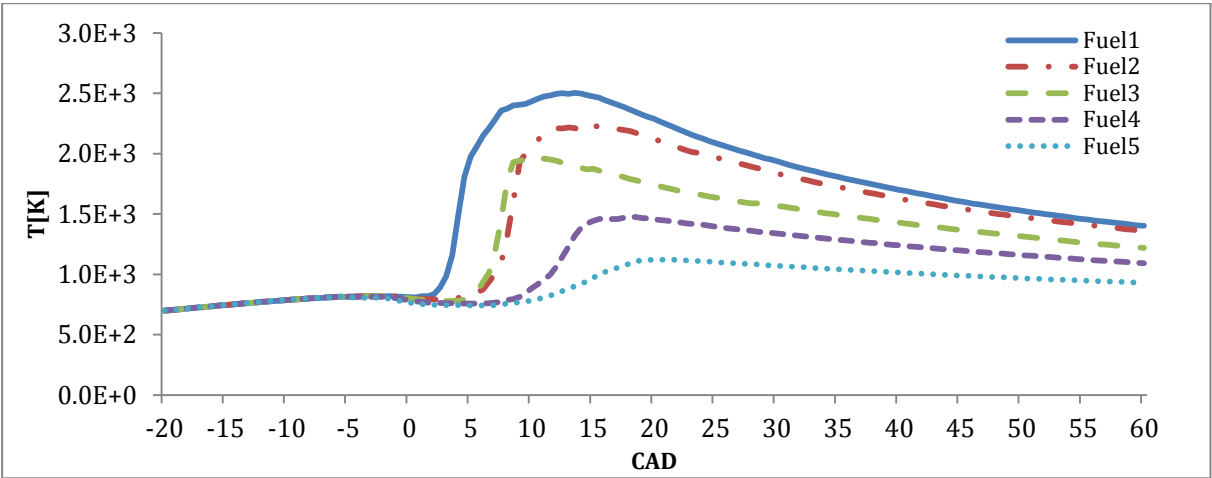


Figure 13: Temperature profiles for n-heptane for the cases Fuel1-5.



#### 7.1.4 Heat release per crank angel degree

To measure the performance of the engine, the heat release per CAD is employed. The more optimal the engine operates the higher amount of heat is released, and the heat release profiles for Fuel1-5 are seen in figure 14. It is important to remember that the heat release is determined by the kinetics, and the enthalpy of the molecules and atoms involved in the reactions. Different reactions will be initiated when certain temperatures and/or pressures are reached, and the primer reactions will determine the reaction path. When changing the in-cylinder conditions the reactions first initiated may alter, and even when increasing temperature and pressure, which favours combustion taking place, the heat release may diminish. This is a consequence of the primer reactions hindering other more energy rich reactions to occur.

As expected from the previous discussion Fuel1, which reaches the highest maximum temperature and pressure, achieves a high heat release of 360J/Deg. This case has favourable mixing conditions of fuel and air owing to its low engine speed, which may explain the beneficial heat release curve. However it does not possess the highest heat release of the cases, which can be a result of its relatively low amount of fuel.

The cases for 1500rpm have the highest heat release of the cases simulated, with values for Fuel2 and 3 of respectively 415J/Deg and 480J/Deg. This was not necessarily the expected result since their temperature and pressure profiles were exceeded by Fuel1, but this is as mentioned determined by the kinetics and due to a higher amount of fuel present it is reasonable that the case for Fuel3 has the highest heat release of all.

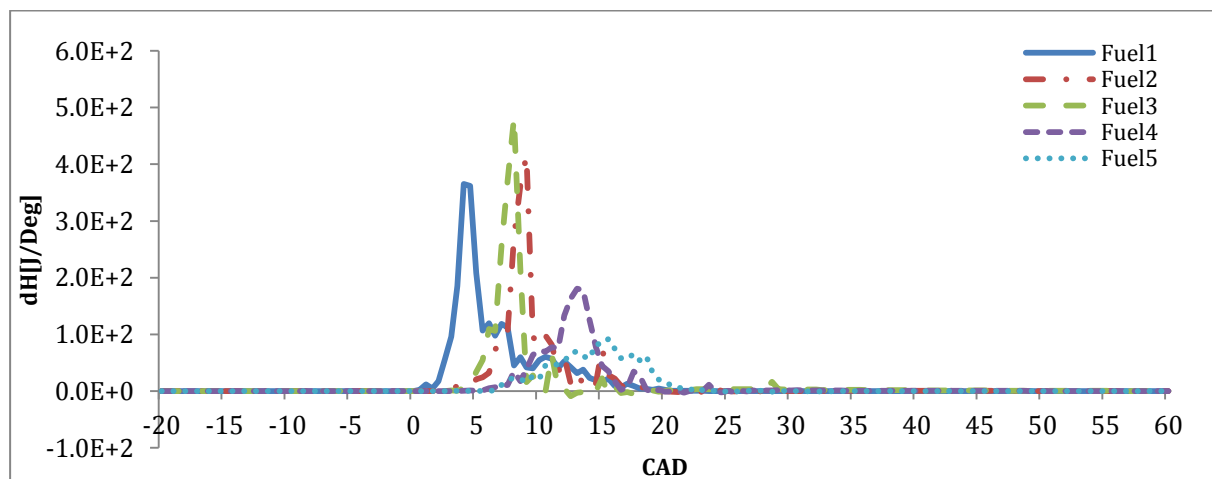


Figure 14: Heat release profiles for n-heptane for the cases Fuel1-5.

Figure 14 reveals a significant drop in heat release for the cases running at 2500rpm. As discussed previously neither of these cases are likely to ignite properly, which explains their low heat release. As opposed to the results for 1500rpm, the case for 2500rpm representing the highest fuel injection, Fuel5, releases the smallest amount of heat. This coincides with the

previous discussion where both the temperature and pressure increase is found to be especially limited for this case.

To support the discussion regarding incomplete combustion the mass fraction of fuel burned, CO and CO<sub>2</sub> emissions for the cases in question are presented in the next section. This will be especially interesting for Fuel3 since it obvious ignites, but might not fully combust. It is important to remember that the temperature and pressure are good indicators for what is occurring during the process, but do not provide the whole picture and inconsistent results may turn out to be the opposite if more information is retrieved.

#### ***7.1.5 Mass fraction of fuel burned (MFB), emission of carbon monoxide (CO) and carbon dioxide (CO<sub>2</sub>).***

The mass fraction of fuel burned given to the left in figure 15 shows that the three cases with the least fuel has basically no fuel left when the combustion is terminated. Also the MFBs for the two cases running at 2500rpm are rather high, even though they do not experience a proper ignition. This can be explained by the kinetics since reactions will occur even without a proper ignition, but the characteristics and time frame of the reactions do not equal the ones of a combustion process. Even though the MFB is relatively high, still a decrease is seen for Fuel4 and 5 compared to the other cases. This strengthens the conclusion that they do not combust.

For the cases Fuel1-3 it is interesting to look at the quantity of CO in the end emissions since this is a strong indicator of incomplete combustion. CO represents a loss in engine performance since a complete combustion would oxidize the CO to CO<sub>2</sub> in an exothermic reaction. As seen in figure 15 Fuel1 has the lowest mole fraction of CO in its emissions, which corresponds well with the previous results. The cases for Fuel2 and 3 contain a higher mole fraction of CO in their end emissions, where as expected the latter case possesses the most significant amount. This demonstrates that neither Fuel2 nor Fuel3 fully combust, hence they both possess a higher potential regarding their engine performance. The CO emissions of Fuel4 and 5 are not as high as Fuel2 and 3, which implies that the reactants have not been converted into CO in the same extent for Fuel4 and 5, rather than their degree of combustion. As mentioned the amount of CO and CO<sub>2</sub> represent the opposite with regard to complete combustion, and the amount of CO<sub>2</sub> in the end emissions are also showed in figure 15. This strengthens the discussion since the same tendencies are seen here, with the highest mole fraction of CO<sub>2</sub> for Fuel1 and lowest for Fuel5.

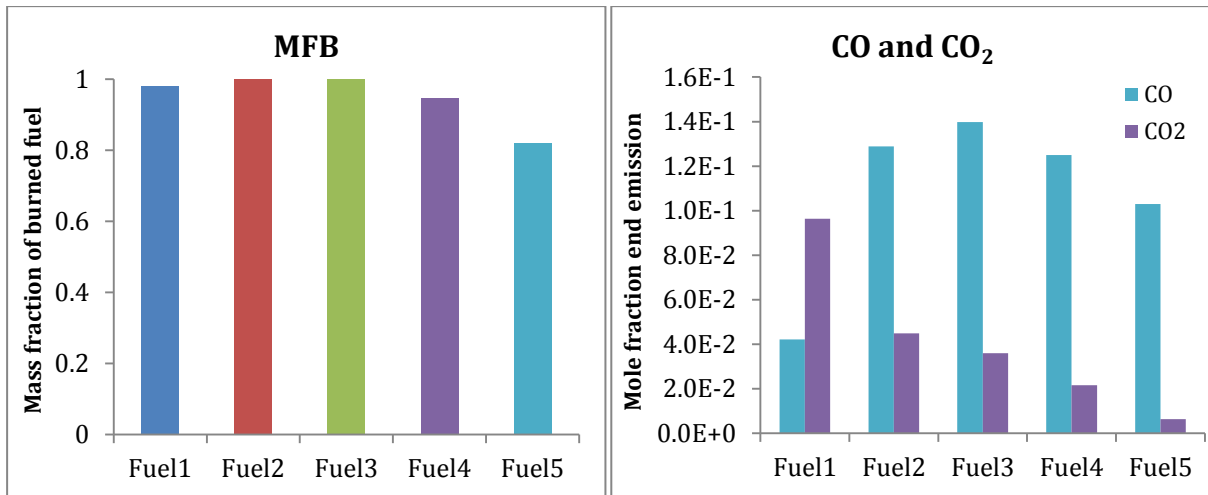


Figure 15: Mass fraction of burned fuel at the end of the cycle, and mole fraction of CO and CO<sub>2</sub> in the end emissions for Fuel1-5 for n-heptane.

It can be concluded from the results presented in the section that all cases need an advanced injection of fuel in order to mix properly and optimize the cycle. This comes from the optimal point of ignition occurring close to TDC, since an early ignition will work against the movement of the piston and a late ignition will lose power due to the expansion of the cylinder volume. In the following section the injection profile will be tuned for each case to yield more beneficial combustion characteristics, and to approach real engine conditions. But first the chemical specie has to be altered to include NO<sub>x</sub>.

## 7.2 MODIFIED MECHANISM INCLUDING NO<sub>x</sub>

Since the mechanism used for the simulations discussed in the previous section does not include NO<sub>x</sub>, modifications were required to incorporate this important factor. Reactions and properties for NO and NO<sub>2</sub> were added in the reaction and thermal file, as well as defining N as a specie.

To see the effect imposed on the operational conditions of the cycle by this small alteration, the pressure distributions for Fuel1 and 2 when both including and excluding NO<sub>x</sub> are shown in figure 16. Here the cases excluding NO<sub>x</sub> experience an earlier ignition and a more rapid combustion in the second stage of combustion. This yields a steeper pressure increase.

Due to the relatively large alterations in the operational conditions for the mechanism including NO<sub>x</sub>, the tuning of injection points for each case will be conducted with the modified mechanism, since they most likely will respond different to the changes.

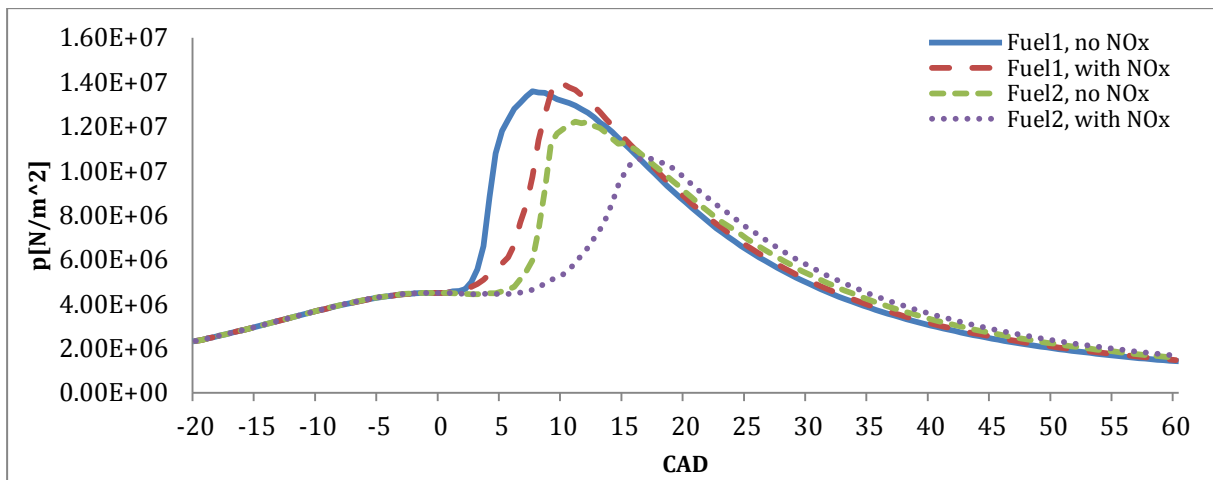


Figure 16: Pressure profiles for n-heptane for Fuel1 and 2 with the initial chemical model and a modified mechanism including  $\text{NO}_x$ .

### 7.3 TUNING N-HEPTANE

As became obvious in the last section the base injection profile is not optimal for neither of the relevant cases. Some performed more poorly than others, and it was clear that each case needs an adapted injection profile in order to run optimal. All of the investigated cases with regard to engine speed and load are in the operational region of a normal engine, where the injection profiles will automatically be adjusted by the ECU. In this section the injection points will be tuned for each case in order to approach the injection occurring in a real engine, and their results will later be compared to verify the models applied.

#### 7.3.1 Fuel1

Fuel1 still operates with the same amount of fuel being injected at 900rpm as defined in table 5. In the last section it was showed that Fuel1 was the first of the tested cases to ignite, but still it occurred after the piston had passed TDC. Adjustments in the injection profile are required in order to improve the cycle, where the injection of the fuel should be advanced compared to the original profile used in the last section. Cases with a later injection will also be tested in order to match the injection points employed in the real engine. Another modification related to the injection profile is to omit the pilot injection, and rather operate with one main injection. This is the common course of injection when operating at such a low engine speed and load.

In figure 17 the pressure, temperature and heat release curves for Fuel1 are given for a number of different injection points. Here also injection at  $-23.4\text{CAD}$ ,  $-31.4\text{CAD}$  and  $-35.4\text{CAD}$  are included, even though they are premature when considering the operational

region of a real engine. However they are included to see whether the trend of incremental pressure, temperature and heat release peaks continues with advanced injection profiles.

As expected the earlier injection points lead to advanced points of ignition. This is seen for all cases until the case injecting at -23.4CAD, where the cases with the following injection points, at -31.4CAD and -35.4CAD, have the same point of ignition. All cases reach a temperature in the area or above 2600K implying that combustion is present, which is additionally confirmed by the steep pressure increase obtained. For the cases with an injection between +0.6CAD and -15.4CAD, the maximum temperature and heat release are in the same area. A small drop in heat release is however detected for the cases with injection at -7.4CAD and -11.4CAD, where the primer also shows a minor drop in temperature. In order to evaluate these small differences, the MFB, CO and CO<sub>2</sub> emissions are given in figure 18 to check for an incomplete combustion. Here also the ignition delays are given as a mean for evaluating the cycles.

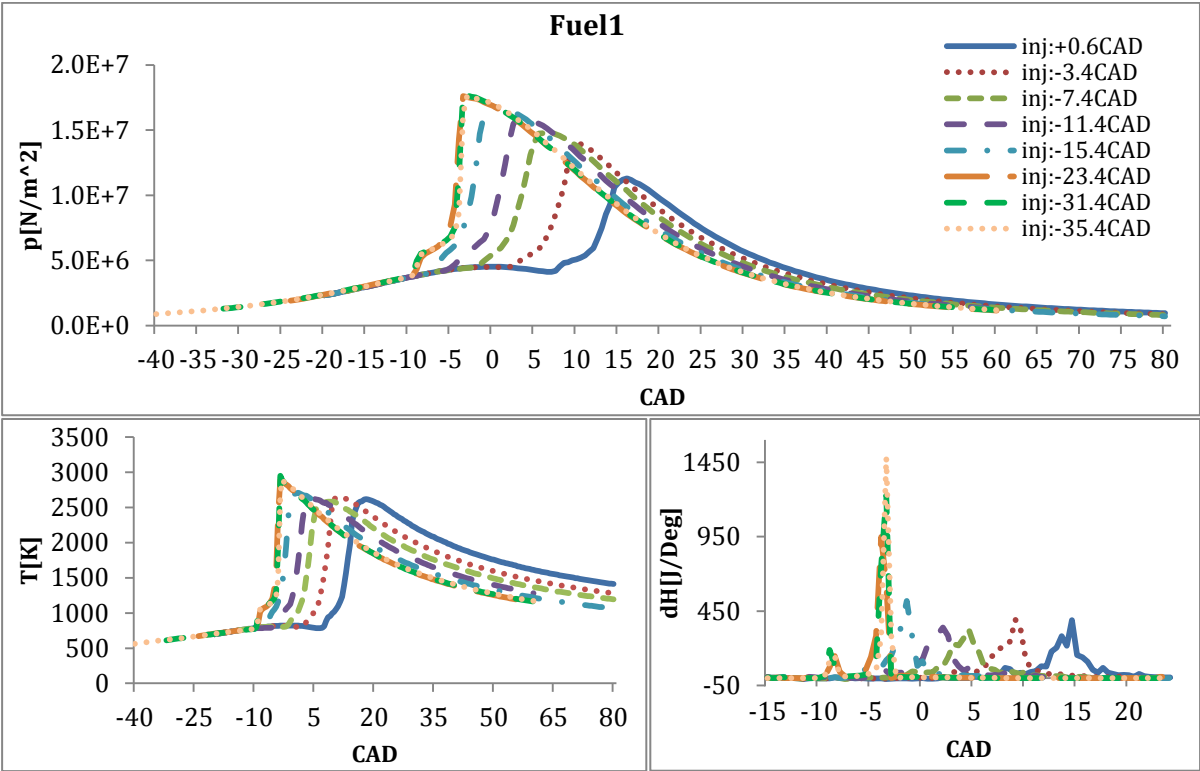


Figure 17: Pressure, temperature and heat release profiles for Fuel1 operating with different injection points for n-heptane. The heat release is given for a smaller CAD than the two others due to a smaller window of interest.

In figure 18 only small differences are detected, as is the case in the figure above, and they may be neglectable. However what is worth noticing is that the case with injection at -7.4CAD has the lowest MFB, and the case with injection at -11.4CAD has the highest CO and lowest CO<sub>2</sub> fractions at the end of the combustion cycle. These are all indications of incomplete combustion, and for the injection at -7.4CAD this may explain the small temperature drop. But as mentioned these differences are small and may be insignificant.

The ignition delay is given to investigate whether the smaller MFB and CO fraction can be linked to insufficient mixing time. The delay is measured from the point where fuel is first introduced into the cylinder, to the point where the pressure and temperature curves first experience a proper increase. The presence of OH has also been considered since it is a highly reactive specie which basically is not present before ignition, after which it quickly reaches its maximum share. These parameters give an indication of the ignition delay, however it is hard to fully assess based on the data from these simulations and the delays are just approximations.

From figure 18 the ignition delay of the case injecting at -7.4CAD has, together with the case injecting at -3.4CAD, the lowest ignition delay. This raises the potential for incomplete combustion due to lack of mixing time. However the latter case has the highest MFB, which may be an effect of a higher degree of mixing when injecting at -3.4CAD, since it mixes as the piston passes TDC. Here the temperature and pressure level inside the cylinder will be elevated compared to the case injecting at -7.4CAD, which ignites when reaching TDC. It is important to mention that these variations are small and other parameters not available for this thesis may give a more complete picture.

The pressure curves in figure 17 behave as expected with increasing profiles as the combustion approaches TDC, with a continuing increase as the fast combustion fully occurs before the piston reaches the expansion stroke.

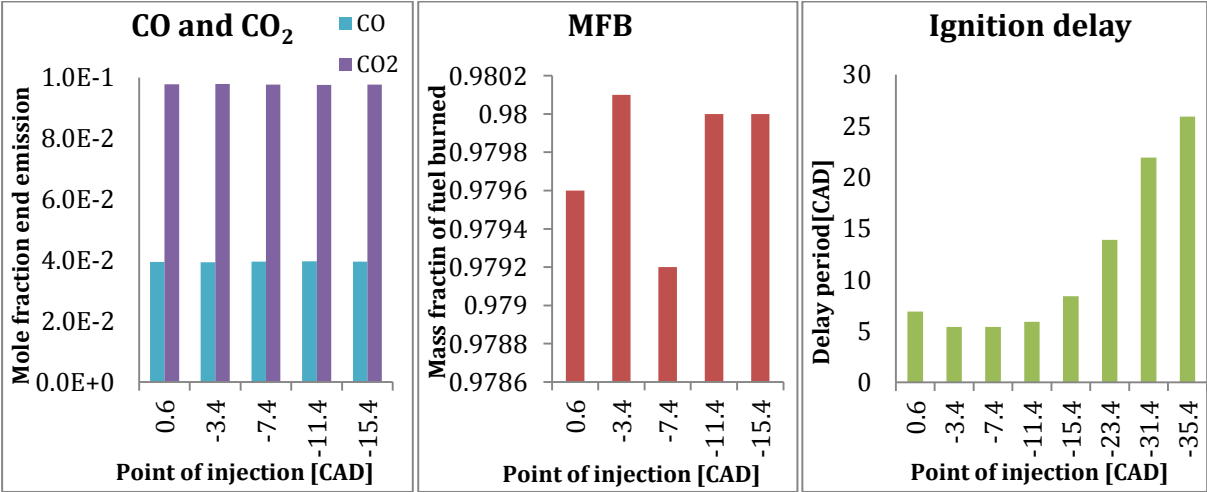


Figure 18: Mole fraction of CO, CO<sub>2</sub> and mass fraction of burned fuel at the end of the cycle, and the ignition delay for Fuel1 operating with different injection points for n-heptane.

From the ignition delays in figure 18 it is seen that the delay for the latest injections decrease slightly when the injection is advanced, before it increases greatly with the extreme advancements. This is reasonable since the latest point of injection will occur after the in-cylinder pressure and temperature have started to decay, prolonging the mixing. For the cases injecting slightly before TDC, their mixing will occur past TDC. Here the pressure and temperature during the delay are at their highest, minimizing the time required for mixing. When the injection is further advanced, the fuel is again introduced to the cylinder at lower

temperature and pressures, since the piston is still approaching TDC. This re-magnifies the time needed for mixing. This also explains the trend seen for the three latest injections where the point of ignition stabilizes, even though the point of injection advances 12CAD between -23.4CAD and -35.4CAD.

When evaluating these three latter cases, figure 17 shows a very steep increase in both temperature and pressure after ignition, and they produce the highest maximum values. Here the fast combustion takes place before the piston reaches TDC, so the process is not stretch like seen for the other cases. As already mentioned the pressure and temperature will decrease in the expansion stroke, which may explain the degenerating combustion conditions for the other cases. Both maximum pressure and temperature for these three cases with extremely advanced injections are in the same region as the others; however the heat release increases substantially. The heat release for the cases with injections at -23.4CAD, -31.4CAD and -35.4CAD are respectively 950J/Deg, 1220J/Deg and 1480J/Deg, while the highest heat release obtained for the other cases is 450J/Deg for the injection at -15.4CAD. Hence the heat release more than doubles when the injection point is advanced to -23.4CAD, which is probably mainly a result of the pistons position during combustion. The continuing heat release increase for the succeeding cases may be a result of increased time for mixing, yielding a more complete combustion. The results for these three earliest injections will not be discussed further since they exceed the limits for the injection in a real engine. Another reason for not investigating these results further is the huge losses such an early combustion would produce in a real engine. It would work against the movement of the piston, which also creates wear and tear in the engine.

#### *7.3.1.1 Effect of a dual injection profile*

In a dual injection profile a pilot injection is used to raise the temperature and pressure in the cylinder before the main portion of the fuel is injected, to ensure a more complete combustion. However the low load and engine speed during idling conditions diminish the need for a pilot injection, and as mentioned the most common way of introducing the fuel into the cylinder is with one main injection. Consequently the primer peak in the injection profile shown in figure 10 will not be present since all fuel is inserted unabatedly.

In figure 19 three cases with different points of fuel injection for Fuel1 are displayed; each case ran both including and excluding a pilot injection. Regardless of applying a pilot injection or not, the point of injection is still defined as the point where fuel is first introduced into the cylinder. Accordingly the cases operating with a dual injection will start their pilot injection at the same time as the cases operating with one unabated injection start their main injection. Consequently the main injection will be advanced for the latter case, and here the dual injection will initiate its main injection respectively 3CAD later.

In figure 19 the effects of the alteration in fuel introduction are demonstrated with regard to pressure, temperature and heat release. Here a small advancement in the ignition for the blue lines, representing one main injection, compared to the red lines, representing a dual injection,

is observed when injecting at the same CAD. This is most likely due to the delay in the main injection of the duel injection profile.

When injecting at -7.4CAD the difference in the point of ignition for the two cases is around 3CAD, i.e. around the same as the delay in the main injection of the fuel when applying a duel injection. An interesting occurrence is approximately simultaneous ignition for the two manners of injecting when injecting at both +0.6CAD and -15.4CAD. Here the in-cylinder pressure and temperature will be relatively low where ignition occurs, and the pilot injections pre-heating and increase in pressure may be of larger importance to initiate the ignition. Especially for the earliest injection at -15.4CAD the two cases ignite very close. This may also be an effect of the increased delay when advancing the injection, as showed in figure 18, prolonging the delay period for the case with one main injection. The increased time for mixing when operating with one main injection can be the factor providing the higher maximum values achieved for pressure, temperature and heat release for both the earliest and latest injection.

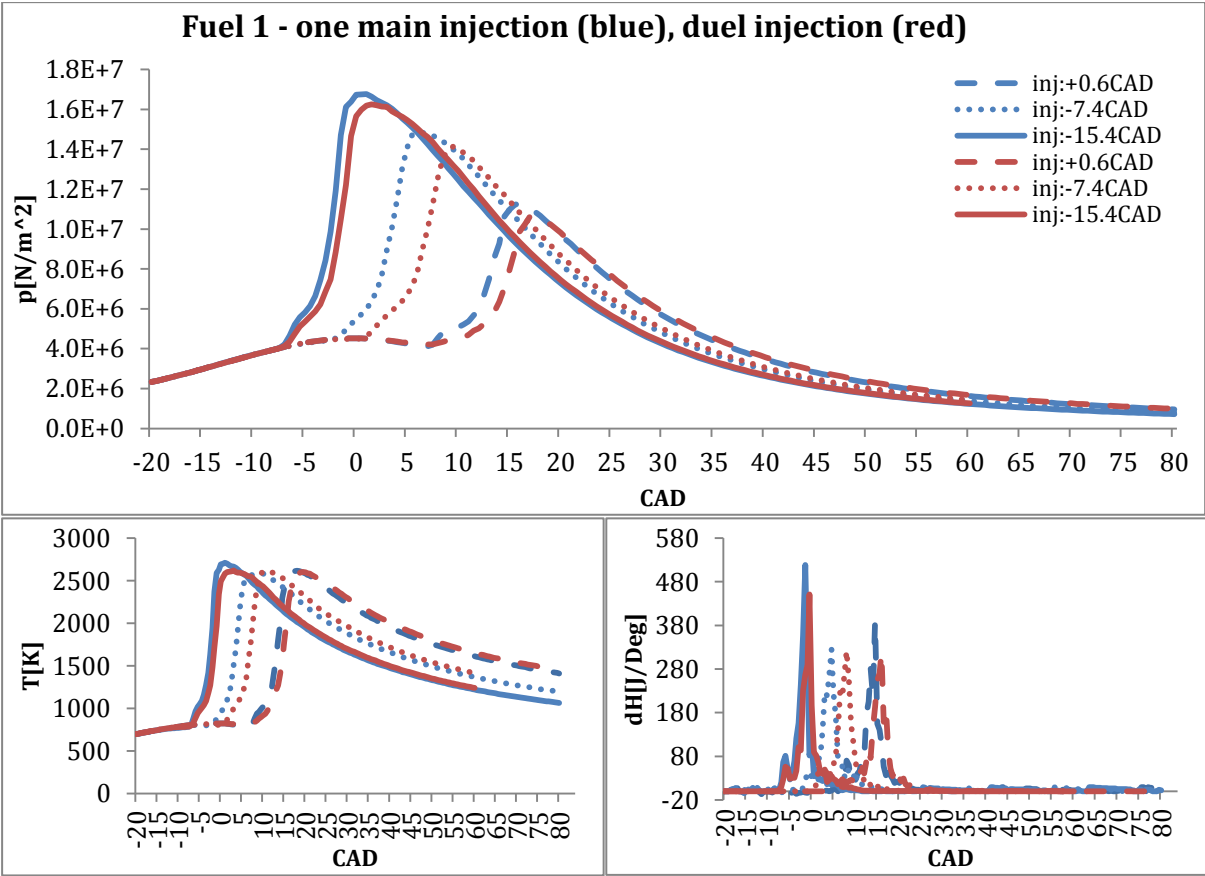


Figure 19: Pressure, temperature and heat release profiles for Fuel1 operating with different injection points given for two manners of injecting fuel: one main injection and a duel injection of n-heptane.

The ignition profiles for the two manners of introducing fuel are more similar than expected. When applying a dual injection profile, a pre-ignition is usually apparent before the major pressure and temperature increase owing to the pilot injection. As observed in figure 19, this



pre-ignition is not more evident for the dual injection compared to the unabated injection. Actually for the injection at +0.6CAD, the unabated injection seems to experience this pre-ignition at a higher degree than the dual injection. This may be due to calculation effects in DARS, an effect of the low amount of fuel injected or the low engine speed.

A more illustrative comparison would exist if the main injection of the dual injection profile would be initiated at the same CAD as the unabated injection starts, hence their main injections would be inserted simultaneously. This data is however not obtained in this thesis, but an advancement in ignition would be expected for the cases operating with a dual injection rather than the delay observed here.

### 7.3.2 Fuel2

Fuel2 has as defined in table 5 a higher amount of fuel injected, as well as a higher engine speed compared to Fuel1. The cases ran for Fuel2 is four cases corresponding with injection points tested in a real engine, as well as one further advanced. Fuel2 operates with a dual injection profile, as is the case for Fuel3-5.

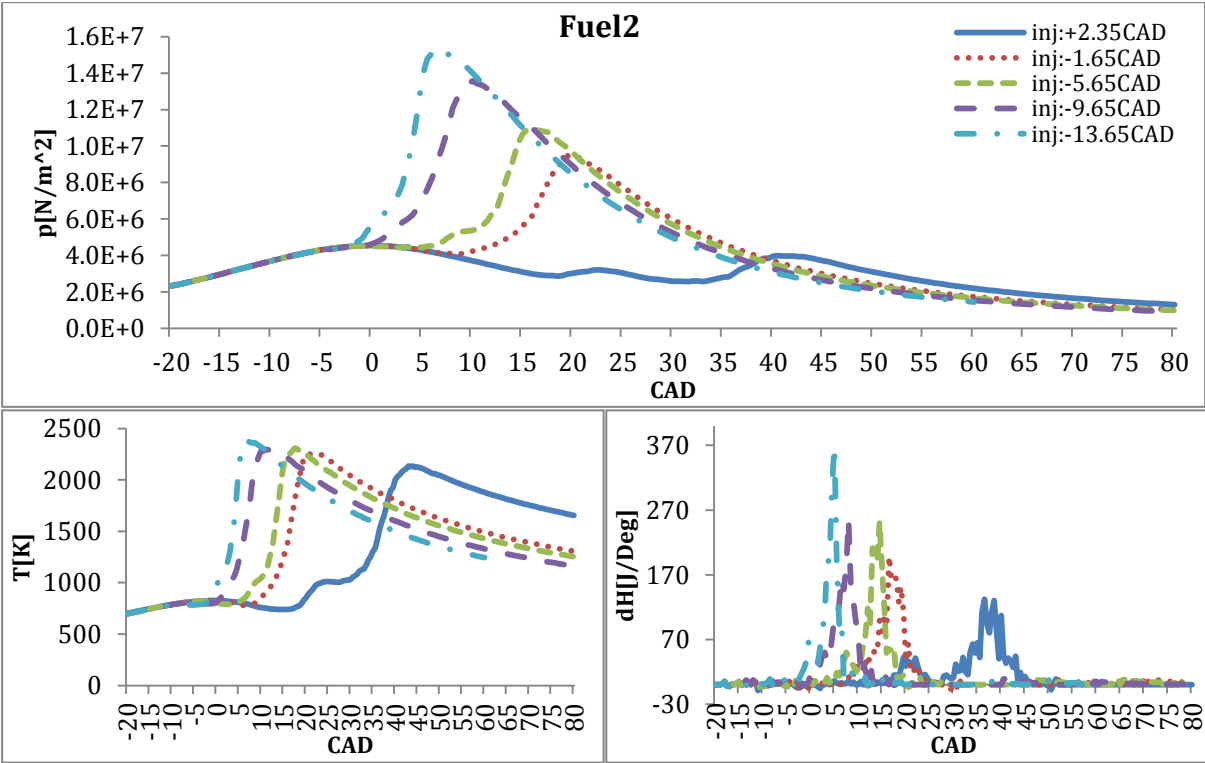


Figure 20: Pressure, temperature and heat release profiles for Fuel2 operating with different injection points of n-heptane.

In figure 20 the pressure, temperature and heat release curves are given for the five different points of injection. Also here the point of ignition advances for the earlier injections, as was the case for Fuel1. When looking at the pressure profiles, the case with the earliest injection

does not seem to ignite, however it reaches a high flame temperature of 2130K as well as having a relatively high heat release. These are inconsistent results and data from this case should be interpreted with caution.

The rest of the cases however show expected results with increased maximum values for all three combustion characteristics given in figure 20, when combustion occurs closer to TDC. In figure 17 it was seen that the temperatures for the cases of Fuel1 injected between +0.6CAD and -15.4CAD all reach maximum values in the area of 2600K. When comparing with the temperature profiles for Fuel2 in figure 20, the maximum temperatures are in the area of 2300K, i.e. 300K lower than for Fuel1. This is a reasonable result since the adiabatic flame temperature, which approximately equals the peak local temperature, will be higher for a leaner operation [65]. This will also increase the expected NO<sub>x</sub> level for Fuel1, which will be looked further into in section 7.8.

The ignition delays are given to the right in figure 21. They show the same tendencies as for Fuel1 in figure 18, with the lowest delay periods found for injection slightly prior to TDC and ignition slightly after. However the delays are generally longer when injecting around the same CAD, which is consistent with the assumption of incremental time for mixing with a higher fuel amount, as well as higher engine speed. The lowest delay for Fuel2 is in the area of 9CAD, whereas for Fuel1 the shortest delay is 4CAD less.

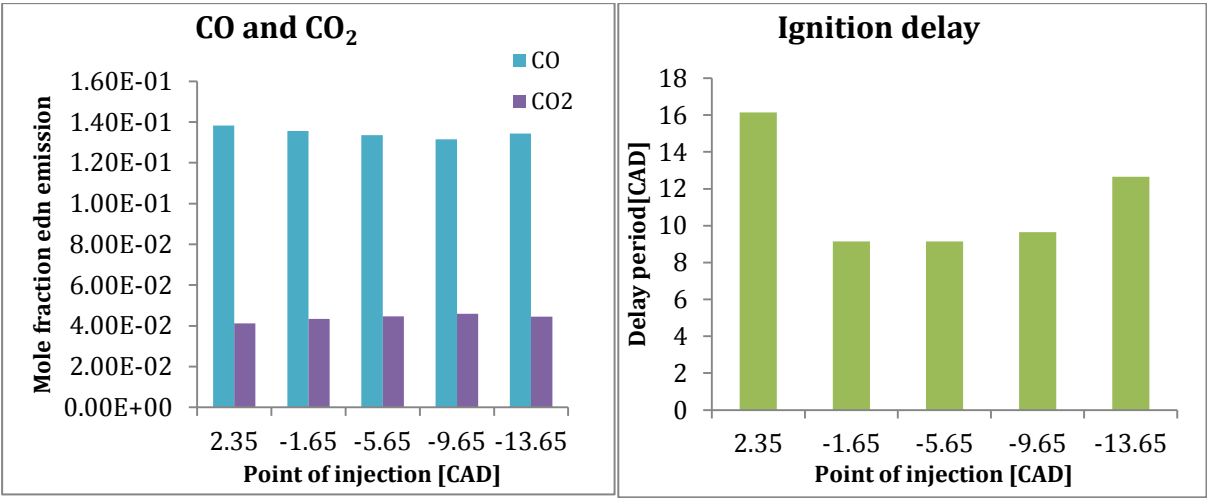


Figure 21: Mole fraction of CO and CO<sub>2</sub> in the end emissions and the ignition delay for Fuel2 operating with different injection points for n-heptane.

As for the indicators of incomplete combustion all cases have a MFB of 0.9999, and CO and CO<sub>2</sub> mole fractions in their end emissions in the same area. When comparing to Fuel1 in figure 18, the fractions of CO<sub>2</sub> and CO show the opposite trends. Here the CO fraction is dominating, implying a more incomplete combustion. The fraction of CO has multiplied by a factor of around 3.4 compared to Fuel1, which may be a result of less oxygen present to oxidize it further.

### 7.3.3 Fuel3

Fuel3 operates at the same engine speed as Fuel2, i.e. 1500rpm, but with an increased amount of fuel injected, as defined in table 5. Its pressure, temperature and heat release curves are given in figure 22. Here no significant pressure increase is detected for the case with the latest injection at +3.4CAD, which is the only case starting injection after TDC. This was also the case when injecting around the same CAD for Fuel2 (+2.35CAD), however here only limited increases are detected in both the temperature and heat release profiles as well, reinforcing the assumption of no ignition. Otherwise the remaining cases run as anticipated, but now the maximum heat release takes place for the injection at -8.6CAD, before it decreases slightly for the earliest injection at -13.65CAD. The maximum values of the temperatures are in the range of 2000K, which is around 300K lower than for Fuel2. Since more fuel is injected this is anticipated results since the oxygen concentration will be less dense, yielding lower local flame temperatures.

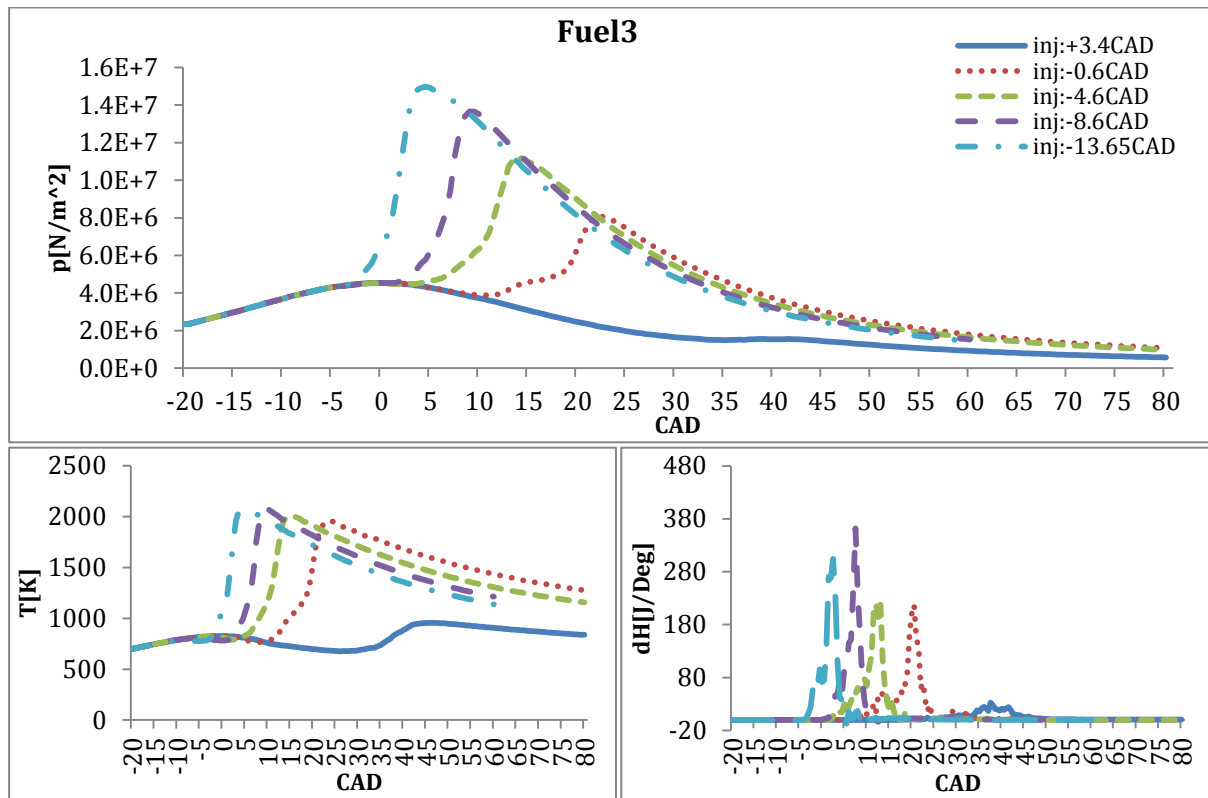


Figure 22: Pressure, temperature and heat release profiles for Fuel3 operating with different injection points of n-heptane.

From figure 23 an expected decrease in the MFB for the earliest injection is detected, with its fraction being 0.52. This does not necessarily indicate that this is the share burned, but the conditions in the cylinder have provided a state where the fuel has started to react. The low values of CO and CO<sub>2</sub> from figure 23 for this earliest injection also indicate that the conversion of fuel has been limited. As for the other cases the MFB is 0.9999 and the CO fraction is increasing with earlier injections. This is the opposite trend with regard to Fuel2,

and indicates that less CO is oxidized into CO<sub>2</sub>. This represents unexploited energy and may cause the heat release to decline for the earliest ignition, even though it burns closest to TDC.

When looking at the ignition delay also represented in figure 23, a generally increase in CAD is detected for Fuel3 compared to Fuel2. This agrees with the increased amount of fuel injected, requiring longer time for mixing. The delays show the same trends as for the previous cases, with the shortest delays occurring with an injection slightly before TDC and an ignition slightly after.

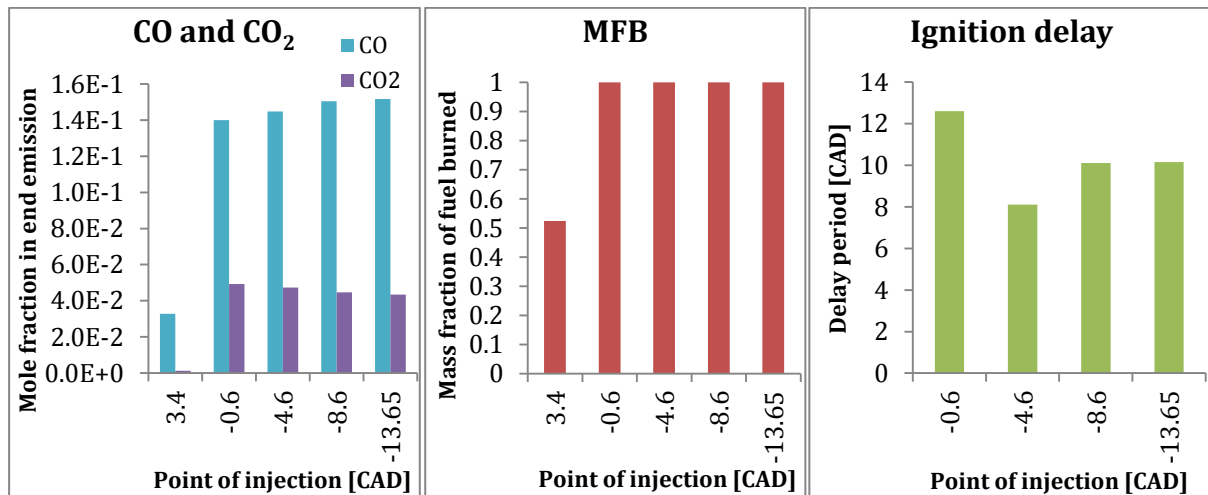


Figure 23: Mole fraction of CO, CO<sub>2</sub> and mass fraction of burned fuel at the end of the cycle, and the ignition delay for Fuel3 operating with different injection points of n-heptane.

### 7.3.1 Fuel4 and 5

For Fuel4 and 5 the engine speed is 2500rpm and the amount of injected fuel is further increased from the previous case, where Fuel5 has the largest fuel injection of all cases investigated. In figure 24 the temperature and pressure profiles from the combustion cycles of Fuel4 and 5 are given for five different points of injection. For both Fuel4 and 5 the two cases with the latest ignition coincide with the most delayed and advanced injection ran in a real engine. They are represented by the blue and red lines, where no significant pressure or temperature lifts are detected during the cycle. Hence neither of these cases experience a proper ignition. Since they represent the outer edge of the injection profiles in the real engine, it appears that none of the cases gathered from the real engine experiment operating at 2500rpm will ignite when simulating in DARS.

Two cases with advanced injection profiles have been run for Fuel4 and 5 to see whether they reach a proper combustion. The injection points are -8.8CAD and -16.8CAD, and the only difference between Fuel4 and 5 in these cycles are the amount of fuel being injected. Fuel4 which has the least fuel injected, i.e. a leaner operation, reaches both higher temperature and pressure peaks, but still a relatively low maximum temperature at 1600K. This occurs at the earliest injection, which is widely advanced compared to the cases in the real engine. The highest temperature reached for an injection at -8.8CAD is 1540K. These higher temperatures

achieved for Fuel4 agree with the observation made earlier, with higher temperature peaks for leaner mixtures. However from the low maximum values it may seem that even for these cases with an advanced injection, a fully combustion does not take place. This is especially evident for Fuel5 with a maximum temperature for the earliest injection at -16.8CAD at 1170K.

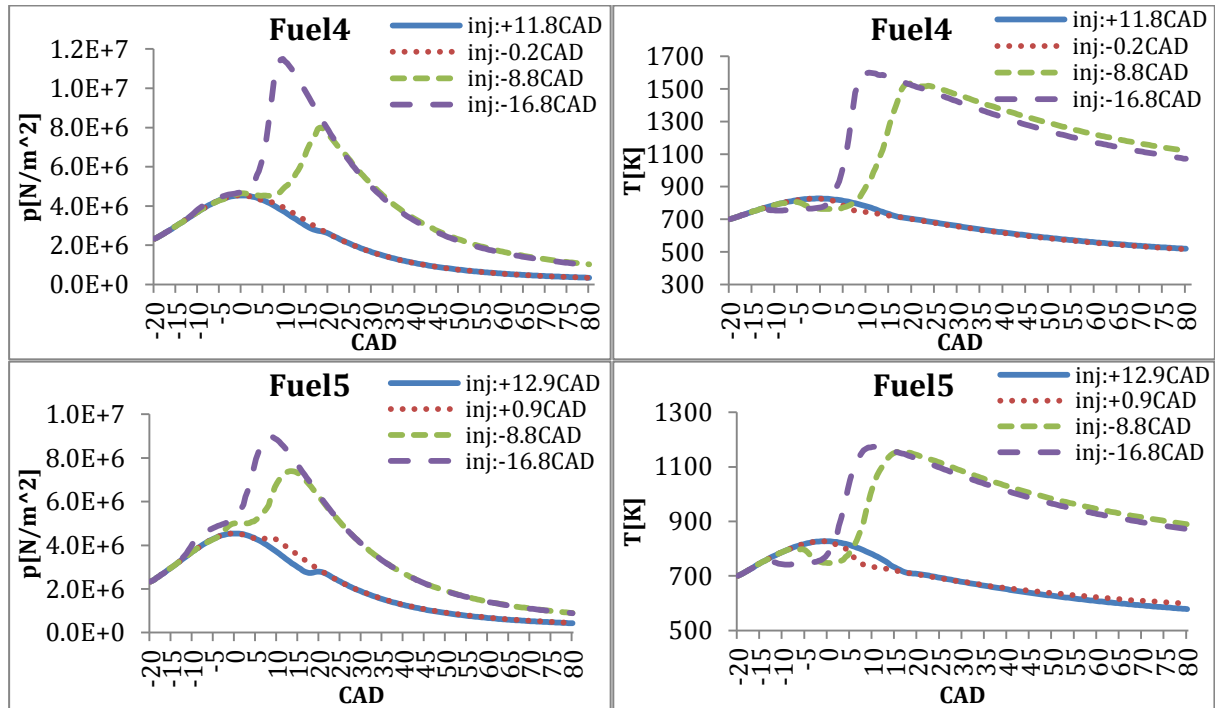


Figure 24: Pressure and temperature profiles for Fuel4 and 5 at altered points of injection of n-heptane.

To further verify this discussion the MFB and the mole fractions of CO and CO<sub>2</sub> in the emissions are given in figure 25. The MFBs of Fuel4 and 5 for their two latest injections are in the range of 28-44%, and it is safe to conclude that they never ignite. This is further reinforced by their neglectable CO and CO<sub>2</sub> fractions. For the two earlier injections the MFB is close to 100% for Fuel4, while 85% for Fuel5. Fuel5 also has a low fraction of CO<sub>2</sub> in its end emissions, indicating an incomplete combustion. These results largely agree with the low maximum temperatures of 1170K and 1150K, demonstrating that a proper combustion has not been present for Fuel5. Fuel4 has basically all fuel converted, but relatively high amount of CO and low amount of CO<sub>2</sub> in its end emissions, also indicating an incomplete combustion. Since both these advanced injection points are beyond the operational conditions in a real engine the importance of their results are limited. However since 2500rpm is a common engine speed it has been further tested for a lower amount of fuel injected (lower load), to investigate whether a leaner operation would yield more favorable results. This is shown in figure 26.

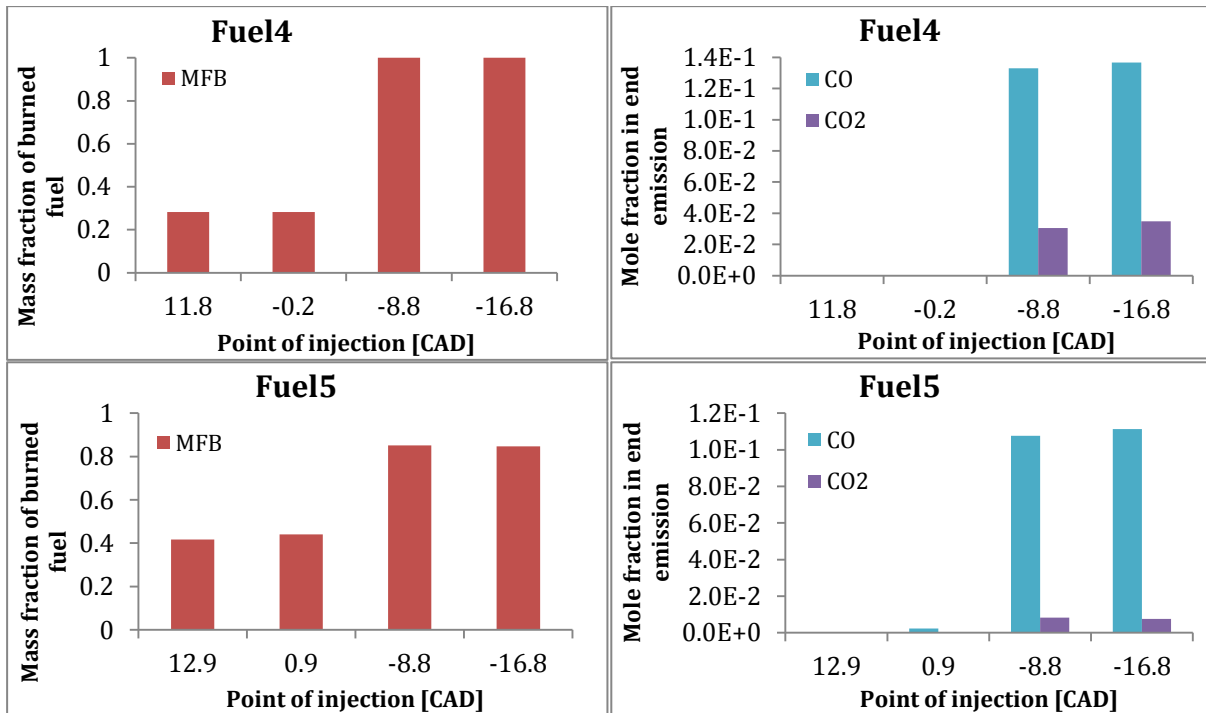


Figure 25: The mass fraction of burned fuel and the mole fraction of CO and CO<sub>2</sub> in the end emissions for Fuel4 and Fuel5 at altered injection points for n-heptane.

These leaner cases are run with the same quantity of fuel injected as for Fuel1-3. They have been tested with an injection at +3.8CAD and -0.2CAD, which basically have the temperature and pressure profiles of a motored cycle. Of these only the results for the injection at -0.2CAD are given in figure 26, where its temperature and pressure profiles are provided. Also the case with the advanced injection at -8.8CAD was tested and displayed in figure 26. Here the case with the lowest fuel amount injected (3.492kg/cycle represented by the purple line) neither seems to ignite. The rest of the cases for the injection at -8.8CAD, experience both a temperature and a pressure increase. However the highest pressure increase, and thereby the greatest potential for mechanical work, is still occurring for the original fuel amount of Fuel4, represented by the blue line (1.7e-4kg/cycle). The temperature peaks for the cases operating with injection at 8.5e-5 and 5.5e-5kg/cycle are substantially increased. This yields an operation with a lower amount of work being produced seen from the lower pressure curves, and at the same time composing larger amount of NO<sub>x</sub> due to the higher temperature and oxygen available. This is further verified by the heat release curves diminishing for these two latter cases, so the fuel reductions tested here are far from optimal for the engine operation. Again the interesting results are found for an injection profile starting at -8.8CAD, which is beyond the operational regime of a real engine. From this it appears that 2500rpm is an engine speed which exceeds the limits in DARS for our area of interest, and the cases Fuel4 and 5 will not be discussed further in this thesis.

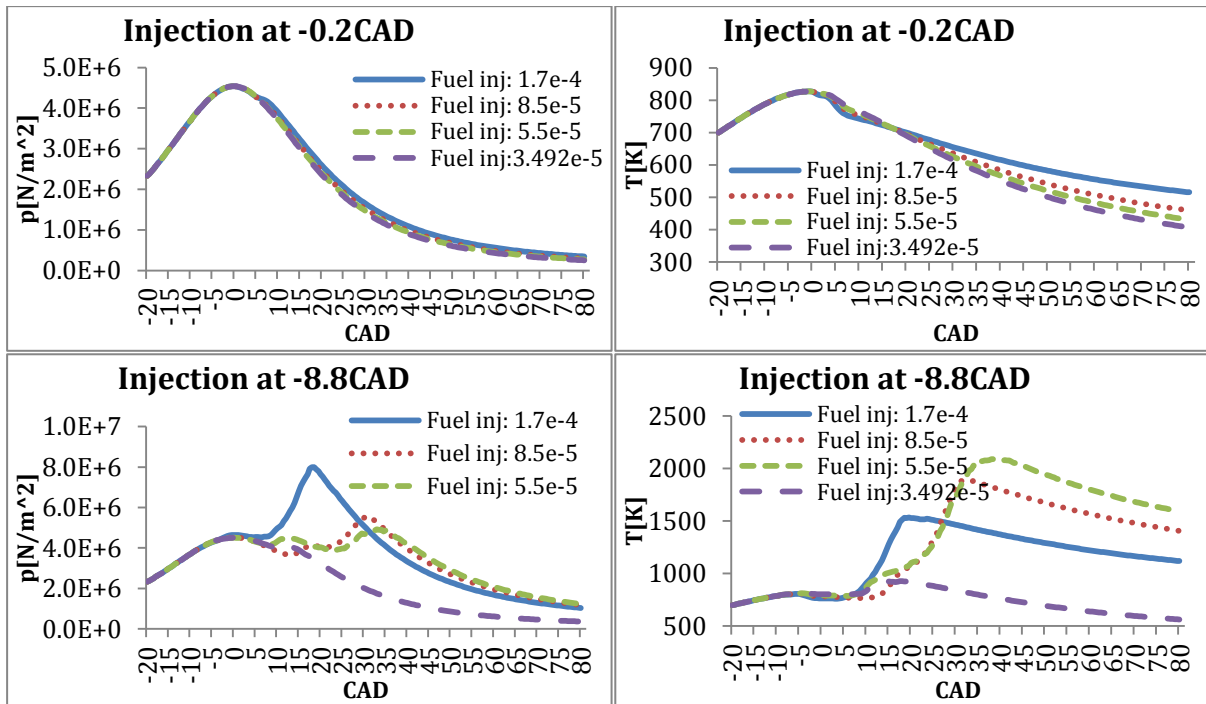


Figure 26: Pressure and temperature profiles for an engine speed of 2500rpm with an injection at -0.2CAD and -8.8CAD when reducing the amount of n-heptane injected from case Fuel4.

## 7.4 NO<sub>x</sub> EMISSIONS

NO<sub>x</sub> is one of the most important components in the exhaust emissions, and is one of four regulated emissions (as well as PM, CO and HC, where the two latter is of less importance since they are easily oxidized) [65]. As mentioned previously there are huge trade-offs between NO<sub>x</sub> and PM when trying to reduce either of these emissions. Accordingly the emissions of PM are reduced while NO<sub>x</sub> are increased by the measures of improving engine efficiency, making NO<sub>x</sub> the most challenging component to reduce. Temperature and oxygen concentration are key factors in the generation of NO<sub>x</sub>. Before EGR will be looked further into in the next section, the current NO<sub>x</sub> emissions of the cases Fuel1-3 will be analyzed.

In figure 27 the NO emissions are shown for Fuel1-3. NO<sub>2</sub> emissions are not included here since they exist in such low quantities that their contribution to the NO<sub>x</sub> level is insignificant compared to NO. Fuel1 has the lowest injection of fuel, i.e. the highest concentration of oxygen, and reaches the greatest temperature peaks of the three cases shown below. Consequently it possesses the highest fractions of NO at the end of its combustion cycles, with a mole fraction up to 1.32E-3 (1320PPM). When looking at the NO profiles of Fuel1 their values are in the same area, as is the case for their temperature peaks in figure 17.

For Fuel2 the latest injection shows practically no NO emissions, however it reaches a temperature of 2130K, which should be above the limit for NO production. As was seen in figure 20 this case shows inconsistent results, which may be the case for the NO fraction as well. It might not have fully converged, and will not be used for further comparison. For

Fuel2 the temperature peaks are increasing with advanced injection, a trend also seen for the NO emissions. Also for Fuel3 increasing temperatures correlate with increasing NO concentrations, but at lower levels compared to Fuel2. This fits with its generally lower temperature profiles and oxygen concentration.

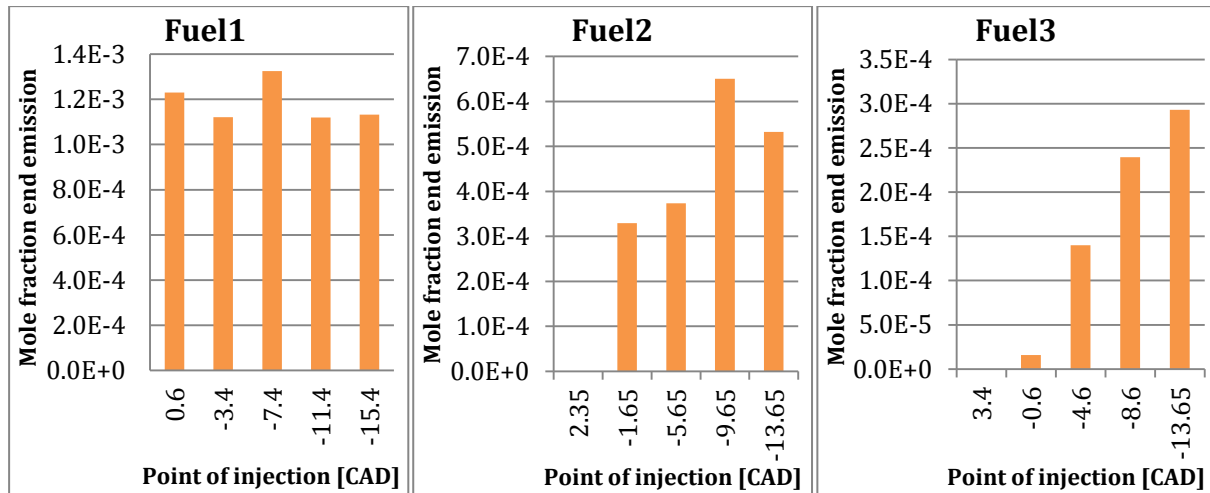


Figure 27: Mole fractions of NO in the end emissions for Fuel1-3, at different injection points of n-heptane. Be aware that the values on the y-axis show different ranges.

The NO emissions have shown a strong correlation with the maximum temperatures achieved, which again is affected by the equivalence ratio. The air/fuel ratio also directly effects the NO production through the concentration of available oxygen.

## 7.5 EGR

As a mean to reduce the NO<sub>x</sub> emissions illustrated above, EGR has been employed. The aim is to lower the temperature during combustion by limiting the oxygen concentration surrounding the fuel molecules, and thereby reduce the two prime parameters creating high NO<sub>x</sub> emissions; temperature and available oxygen.

In this section Fuel1-3 has been tested with an EGR ratio of 15%. Fuel1 was run with 5 EGR cycles, whereas the more time consuming Fuel2 and 3 were run with 2 EGR cycles. Their injection points are -3.4CAD for Fuel1, -1.65CAD for Fuel2 and -0.6CAD for Fuel3, which are the base cases for the experimental testing. When running EGR the gas composition at 180CAD in the previous cycle is partially redirected back into the intake for the next cycle, hence the intake composition is altered when running multiple cycles.



### 7.5.1 Fuel1

When running an EGR cycle the dilution of oxygen will most probably lead to a more incomplete combustion, increasing the emissions of CO and soot. This is a trade-off when utilizing EGR and needs to be assessed when determining the extent of desired EGR use. For Fuel1 five EGR cycles have been run to see the effect each step induces on the  $\text{NO}_x$  emissions, as well as the trade-off with regard to incomplete combustion (here represented by the MFB, CO and  $\text{CO}_2$  concentration). In figure 28 the temperature, pressure and heat release profiles are given for 6 cycles, the base case being the reference cycle with no EGR. Also the MFB is presented here, whereas the  $\text{NO}_x$ , CO and  $\text{CO}_2$  concentrations during the cycles are given in figure 29.

As can be seen from the temperature profiles a clear reduction is present in the peak values from the base case to cycle 1, where EGR is first introduced. For the following cycles the temperature profiles coincide with cycle 1, indicating that the change in  $\text{NO}_x$  emissions for the proceeding cycles will not be as prominent as when first introducing EGR. The same trends as seen from the temperature profiles are also detected for pressure and heat release, revealing a loss in engine performance when applying EGR.

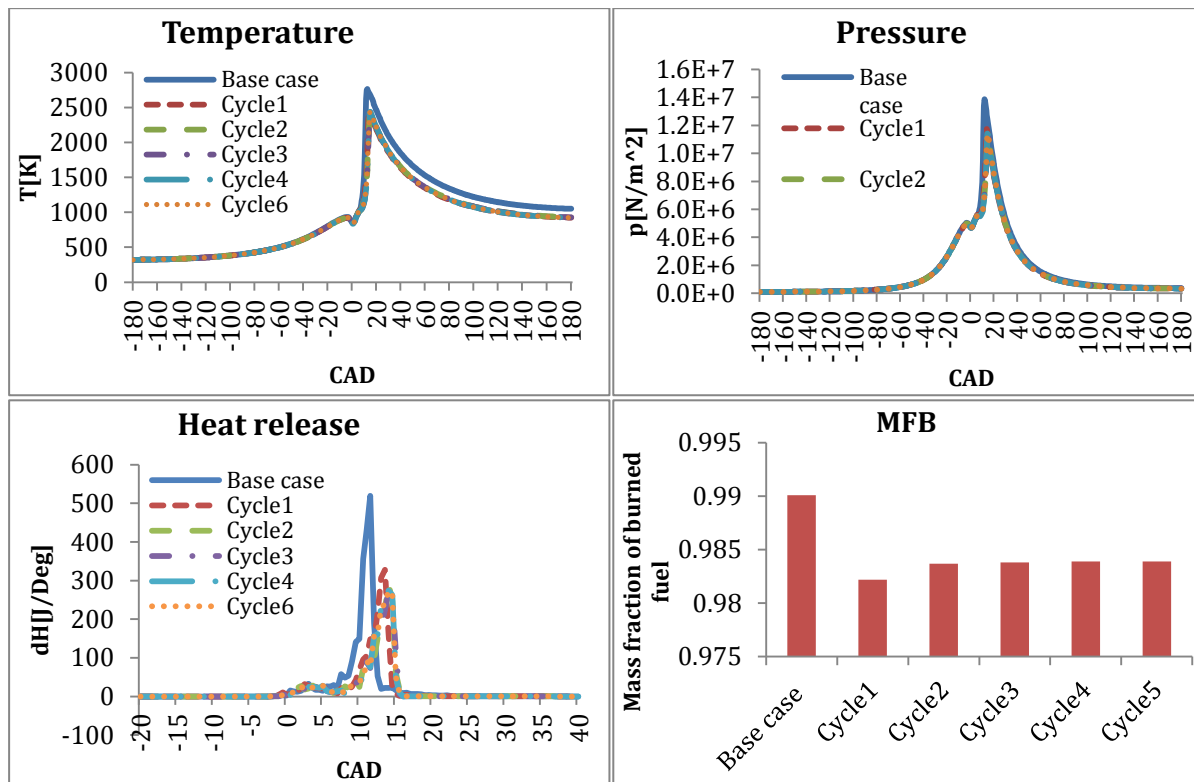


Figure 28: Temperature, pressure and heat release profiles and mass fraction of burned fuel for Fuel1 operating with 15% EGR for n-heptane.

The  $\text{NO}_x$  emissions mainly consist of NO, which is seen from the  $\text{NO}_2$  fractions approaching zero at the end of the cycles in figure 29. When comparing to the base case, cycle 1 obtains a

large NO reduction of 81%. The trade-offs are seen in the CO and CO<sub>2</sub> profiles, with an increase of 98% in the CO fraction and a 24% reduction in the CO<sub>2</sub> fraction. In the proceeding cycles, cycle 2 coincides with cycle1, whereas cycle 3-5 stabilizes at a NO saving of 96% compared to the base case. Here the CO level increases with 116% and the CO<sub>2</sub> reduces by 28%. Due to a much higher concentration of CO and CO<sub>2</sub> compared to NO, their reduction will impose a larger impact on the total emission composition (with a factor of around 100). Due to these large trade-offs when applying EGR, which increases further with multiple cycles, as well as limitation in time consumption when running simulations, only one EGR cycle should be included.

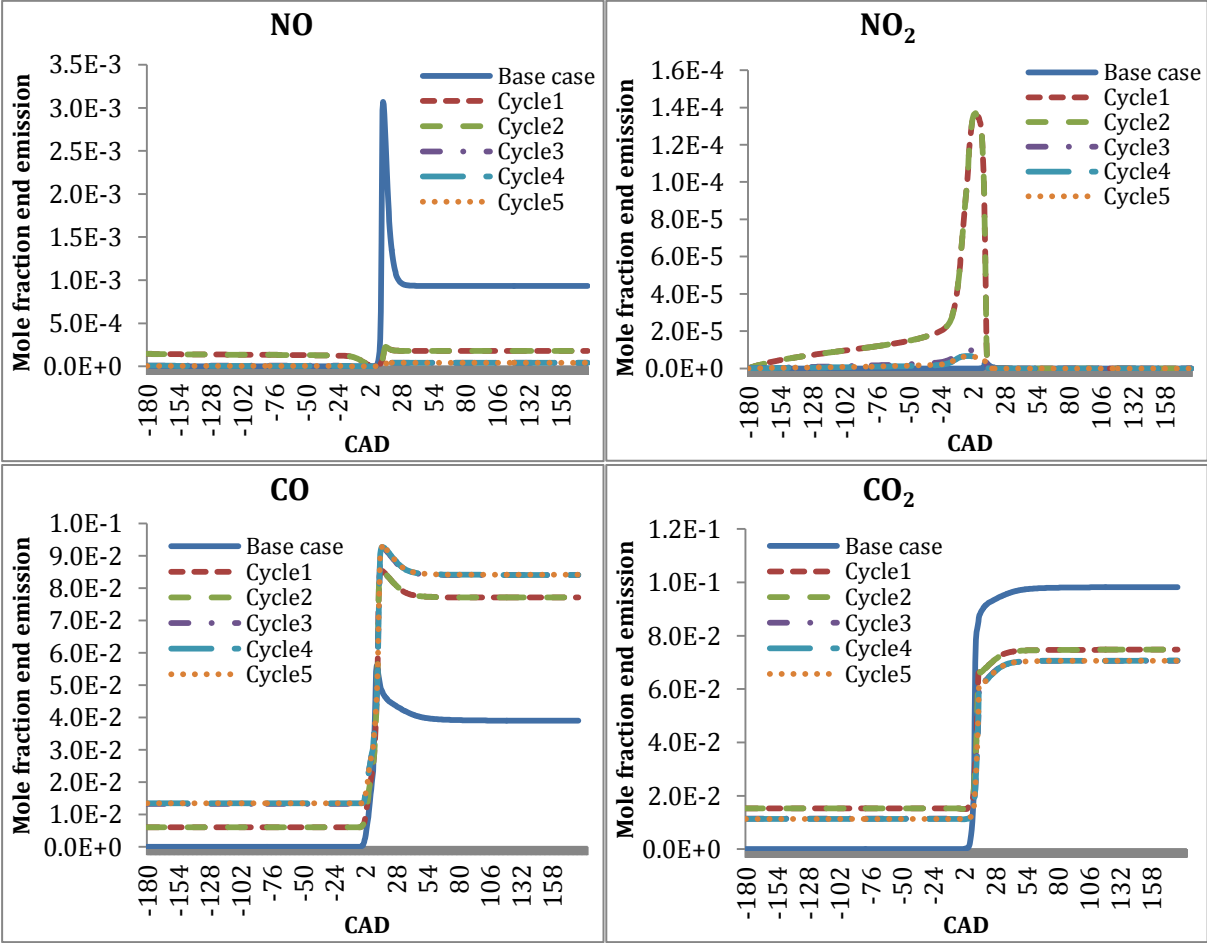


Figure 29: Mole fractions of NO, NO<sub>2</sub>, CO and CO<sub>2</sub> for Fuel1 running with 15% EGR at different EGR cycles for n-heptane.

### 7.5.2 Fuel2 and 3

When applying 15% EGR for Fuel2 and 3, a proper combustion is no longer present. This is especially evident for Fuel3, making its results irrelevant for this thesis. Therefore only the data for Fuel2 are provided here, and will be briefly discussed. When looking at the temperature profiles for Fuel2 in figure 30, only the base case experiences a proper temperature increase. The temperature profiles for Cycle1 and 2 approximately follow the

temperature profile of the motored cycle, except from the cooling effect observed when the fuel is introduced in the cylinder. This cooling effect is also observed for Fuel1 in figure 28, however not present in the tuning of the injection profiles in chapter 7.3. This is probably a result from how the fuel temperature has been determined, which is set equal to the in-cylinder temperature of the gases at the beginning of the simulation. In the tuning part the starting conditions were set at -20CAD, where the gas has an increased temperature compared to at -180CAD, which is applied here. It was anticipated that this would impose a neglectable effect since the amount of fuel injected is relatively small, although the observations here imply otherwise. Here the base case has a delayed point of ignition, and decreased maximum temperature, pressure and heat release compared to the tuning case showed in figure 20 for the injection at -1.65CAD. Due to the reduced temperature, also the NO<sub>x</sub> level of the base case given in figure 31 reduces with regard to what is obtained in figure 27. This cooling effect may also be the triggering factor for not obtaining a proper ignition when EGR is applied.

The same observation is made from the pressure profiles and heat release curves, where only the base case experiences a proper increase. The pressure increase does not occur before 40CAD, and its maximum value is around half of what is obtained for the tuned case in figure 20. When looking at the MFB for Cycle1 and 2 they both have a fraction slightly above 0.4, underlining that an ignition has not been present.

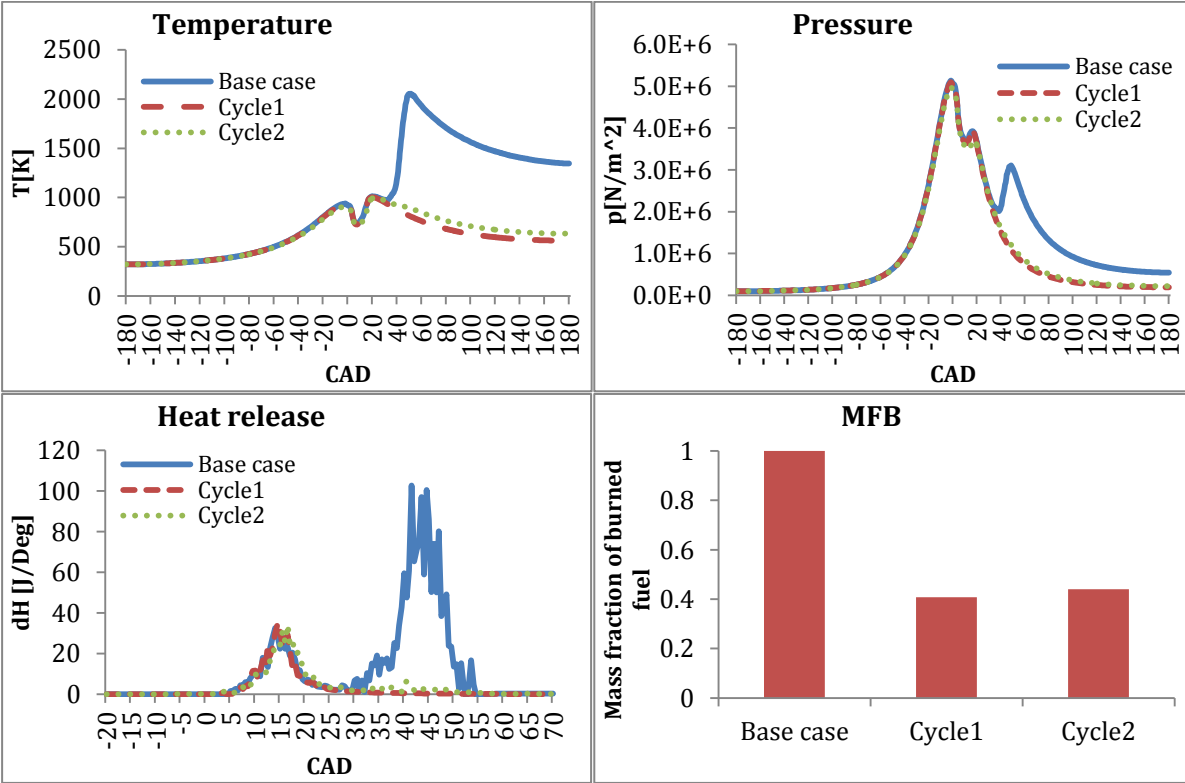


Figure 30: Temperature, pressure and heat release profiles and mass fraction of burned fuel for Fuel2 operating with 15% EGR for n-heptane.

From figure 31 it is seen that the level of  $\text{NO}_x$  in all the cycles is very low, especially for the two cycles running with EGR where  $\text{NO}_x$  is practically not present. This correlates with the observation of no combustion since high temperatures are required for the formation of  $\text{NO}_x$ . The CO and  $\text{CO}_2$  levels decrease, which again arises from the mixture never igniting.

The results obtained for Fuel2 are limited in their relevance since a proper combustion is not present, which can be a result of several factors not discovered here, especially when EGR is applied. Accordingly more emphasize should be put on the results obtained for Fuel1 since they better reflect the effect of EGR.

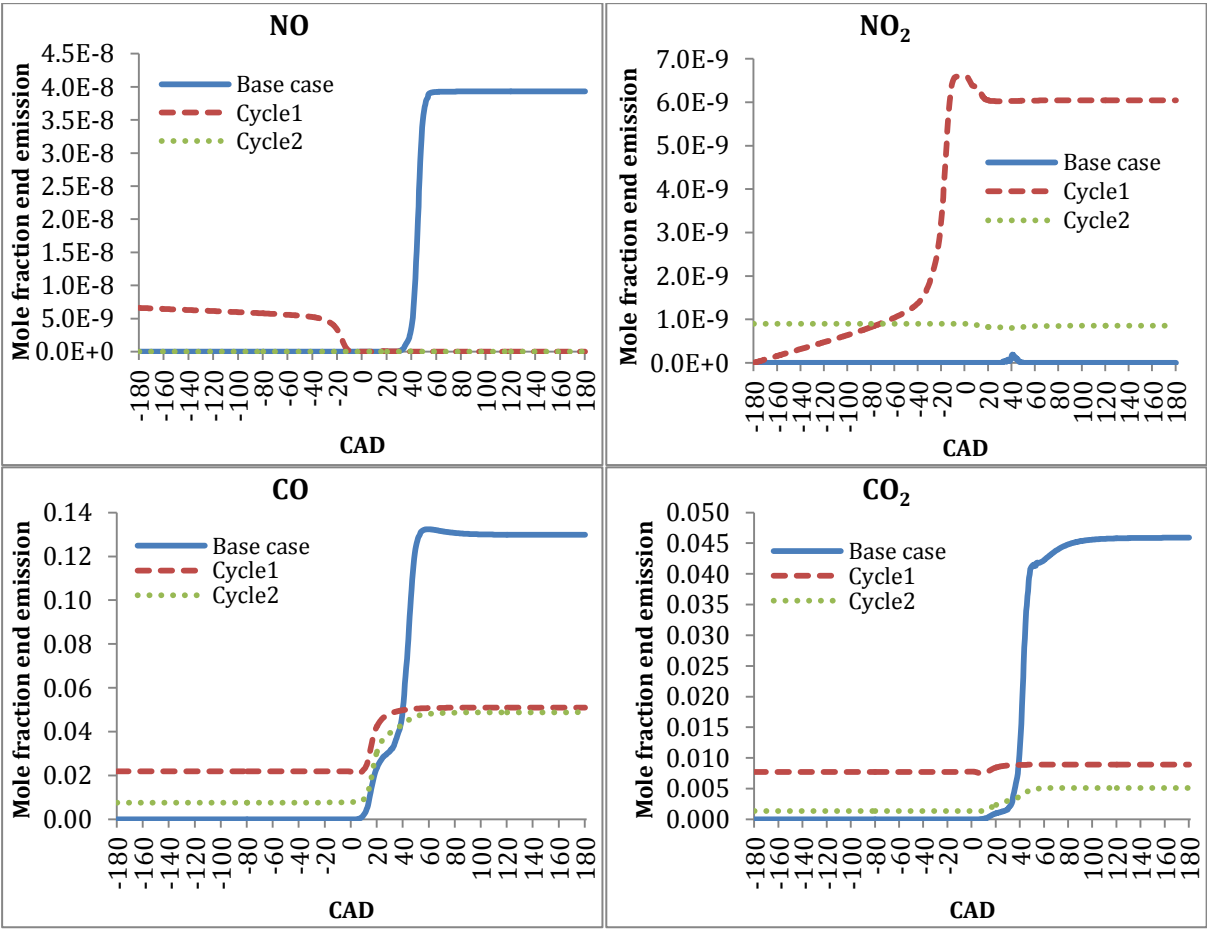


Figure 31: Mole fractions of NO, NO<sub>2</sub>, CO and CO<sub>2</sub> for Fuel2 running with 15% EGR at different EGR cycles for n-heptane.

## 8. RESULTS – SIMULATING FTD SURRUGATE

FTD has also been tested in DARS, although with a more limited set of cases. This is due to the short timeframe for this work and the relatively vast time required for running the simulations. However sufficient cases have been run to evaluate the FTD surrogate with regard to both n-heptane, experimental data and the effect of EGR. Here a base case is presented for each of the conditions Fuel1-3, with injections at -3.4CAD for Fuel1, -1.6CAD for Fuel2 and -0.6CAD for Fuel3. 15%EGR was applied for Fuel1 to assess its effect, and the results are compared to the experimental data later on.

### 8.1 BASE CASE FUEL1-3

For n-heptane better mixing conditions were observed for the cases ran with the lowest speed and load, yielding shorter ignition delays, higher temperature and pressure profiles, a high degree of heat release and lower CO levels. This trend is also observed in figure 32, where the temperature, pressure and heat release profiles for each of the base cases for FTD are presented. As defined above, Fuel1-3 operate with different points of injection, so their ignition delays should be evaluated with caution if assessed directly from figure 32. However approximations of the ignition delays are given to the right in figure 33.

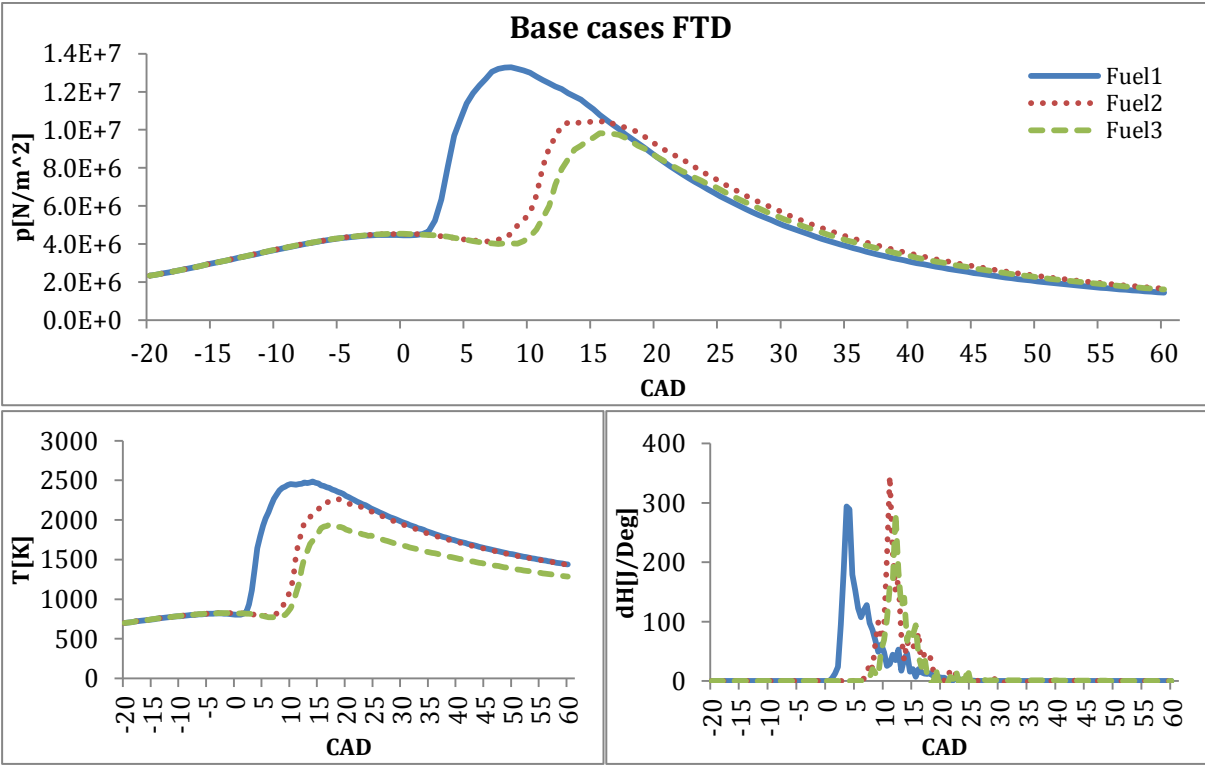


Figure 32: Pressure, temperature and heat release profiles for the combustion of FTD for Fuel1-3 operating with different points of injection.

From figure 32 it is seen that Fuel1 achieves the highest temperature and pressure peaks, and that Fuel2 has a superior heat release. The higher temperature and pressure for Fuel1 can be an effect of it igniting first, hence combusting earlier in the expansion stroke where the losses in temperature and pressure due to change in volume are smaller. The higher temperature for Fuel1 can also originate from its lean operation and therefore a higher concentration of oxygen in the chamber, yielding higher local flame temperatures, as described earlier.

Biofuels are known to have a generally higher degree of oxygen in their fuel composition compared to conventional fuels. Accordingly higher local flame temperatures and a generally more complete combustion are expected, as for a lean operation. However when comparing the temperature levels from figure 32 to the temperature levels of Fuel1-3 for n-heptane (seen in figure 17, 20 and 22), a decrease is actually observed in the temperature peaks for all cases except for Fuel2, which has a small increase of 70K. Also the CO and CO<sub>2</sub> levels in figure 33 remain fairly stable compared to the same cases ran for n-heptane (represented in figure 18, 21 and 23). Again the results are partially contradictory with a higher oxygen content for FTD compared to diesel, since a slight increase is detected in the CO level for Fuel2 and 3, and also a decrease in CO<sub>2</sub> level for the latter case. This indicates a more incomplete combustion of FTD for some of the cases, which probably occurs due to the lack of including the higher degree of oxygen in the strongly reduced model for FTD.

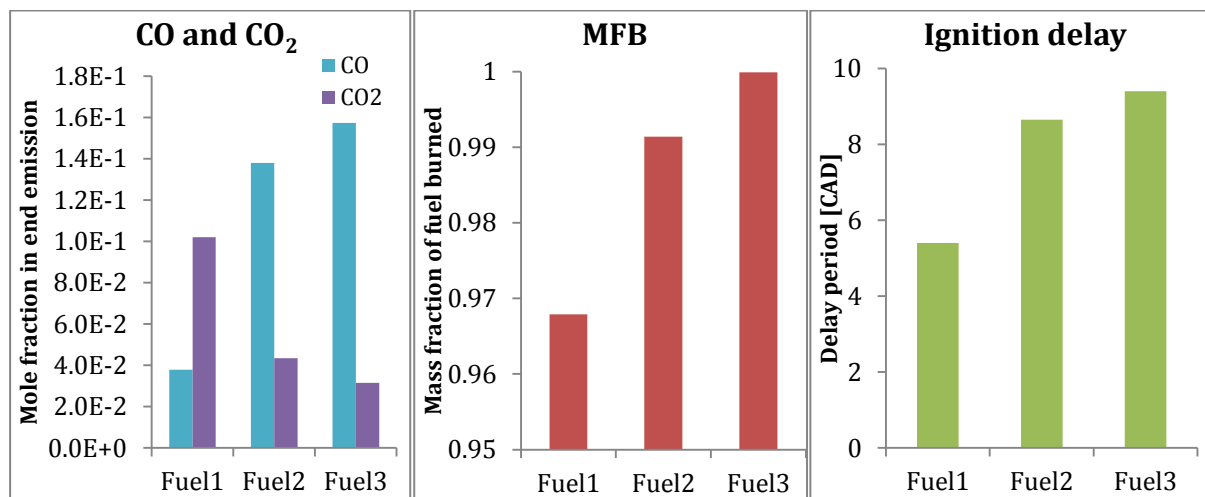


Figure 33: Mole fractions of CO, CO<sub>2</sub> and mass fraction of burned fuel at the end of the cycle, and the ignition delay for Fuel1-3 for FTD operating with different points of injection.

Also the MFB in figure 33 shows the same trends as n-heptane (seen in figure 18, 21 and 23), with a slightly lower fuel conversion for Fuel1 compared to Fuel2 and 3, although still at a relative high mass fraction of 0.967. For Fuel1 and 2 the fractions of converted fuel are slightly lower than for n-heptane, which are the same cases where the alterations in CO and CO<sub>2</sub> levels are lowest when changing the fuel. This may be an effect of less fuel being converted since Fuel3, which has a fuel conversion close to 1, has more evident changes in its emission profiles. However the change in the emissions for Fuel3 is also limited.

When assessing the ignition delays for FTD also presented in figure 33, the same delays as for n-heptane (seen in figure 18, 21 and 23), for Fuel1 and 2 are observed. For Fuel 3 however a decrease in the delay of around 3CAD is detected. This may be an effect of more fuel being injected, yielding a higher visible effect between the characteristics of their ignition quality, where FTD is known to obtain a higher cetane rating than diesel. Due to the later injection for this case and consequently a later point of ignition, the beneficial ignition characteristics of FTD may be of higher importance with the diminishing in-cylinder conditions. However still two of three cases have approximately the same igniton delay, although an expected decrease is present when applying FTD. As mentioned previously the diesel surrogate was originally made up of 0.8 n-heptane and 0.2 iso-octane, which have an octane rating of respectively 0 and 100 [56]. Accordingly the original surrogate fuel for diesel had an octane number of 20, which is a measurement of the activation energy required for ignition. With a higher octane rating a later ignition is expected, so when simplifying the fuel to consist of only n-heptane with an octane rating of zero, one can expect an advancement in the point of ignition when holding the other parameters constant [15]. As a consequence the limited reduction in delay time when applying FTD may originate from n-heptane having superior ignition quality compared to diesel, rather than the FTD surrogate operating with too poor ignition qualities.

### 8.2 NO<sub>x</sub> EMISSIONS

Also for FTD the emissions of NO<sub>2</sub> are present in such low quantities that the level of NO<sub>x</sub> is determined by the level of NO. In figure 34 the levels of NO emissions from FTD with the different settings for Fuel1-3 are given. Here the emissions are highest for Fuel1 and lowest for Fuel3, which is in strong correlation with the temperature profiles in figure 32, as well as the incremental richness as more fuel is added for Fuel2 and 3.

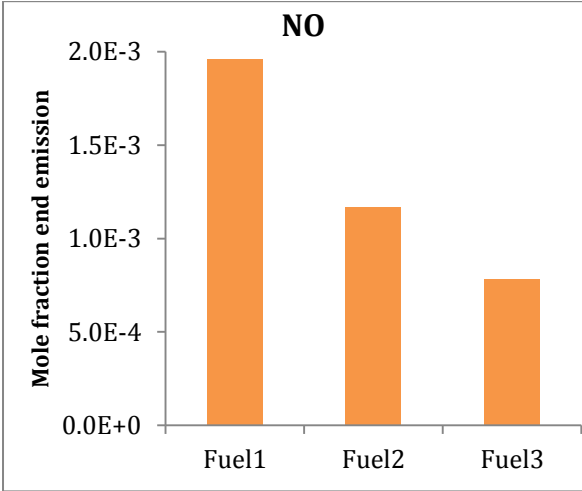


Figure 34: Mole fraction of NO in the end emission when FTD is combusted for Fuel1-3.

When comparing the NO levels to what is obtained for n-heptane in figure 27, a clear increase is detected. This is especially obvious for Fuel2 and 3 where the levels increase from respectively 329ppm and 15.8ppm, to 1170ppm and 783ppm. This high increase is unexpected since the previous results show no or a limited increase in temperature.

### 8.3 EGR

15%EGR has also been applied for FTD where only one EGR cycle has been evaluated, which is labeled Cycle1. This is based on the observations made in chapter 7.5.1., where only a limited additional NO<sub>x</sub> reduction and higher trade-offs with regard to CO and CO<sub>2</sub> levels were present when increasing the number of EGR cycles.

In figure 35 the temperature, pressure and heat release profiles for Fuel1 running with 15% EGR are given, and compared to a base case running without EGR. They show the same tendencies as for n-heptane in figure 28, with decreased maximum values for Cycle1 compared to the base case. Consequently lower NO<sub>x</sub> levels are expected due to a lower temperature peak when applying EGR, at the same time as the lower pressure and heat release profiles reveal a loss with regard to engine efficiency. In the overview of the MFB also found in figure 35, a decrease in converted fuel is observed for the cycle running with EGR, emphasizing deteriorating combustion quality.

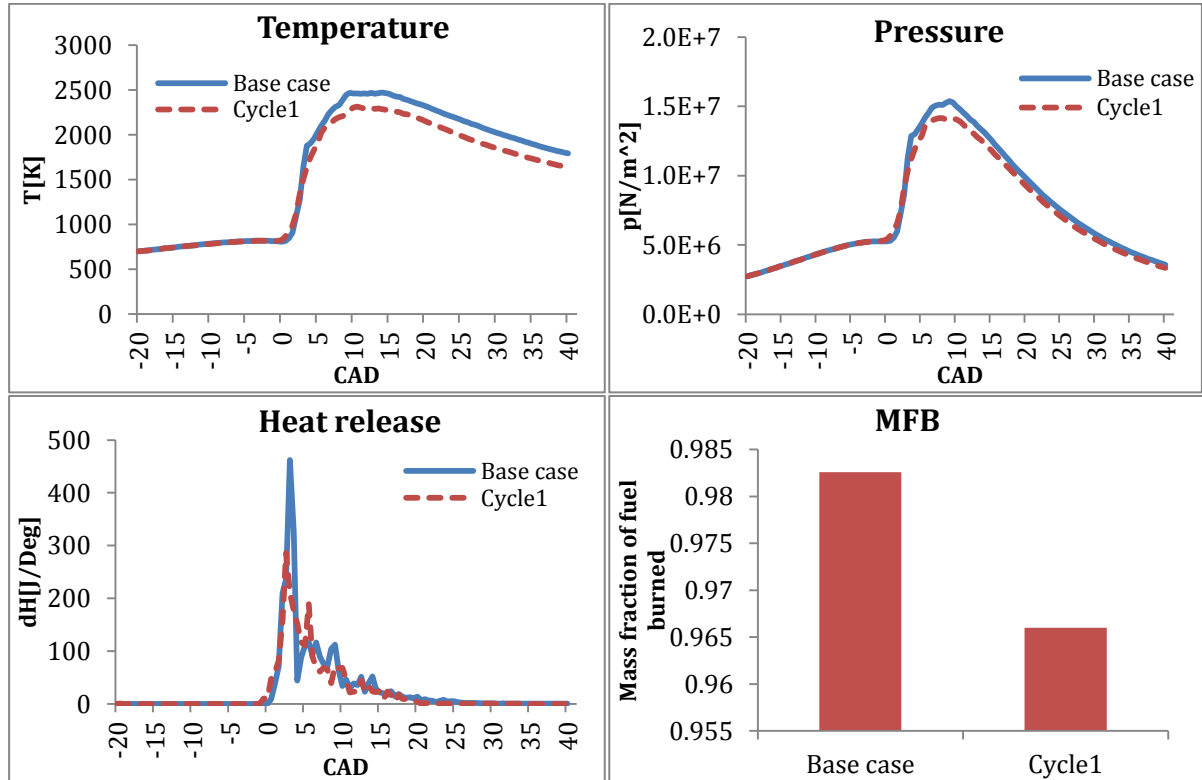


Figure 35: Temperature, pressure and heat release profiles and mass fraction of burned fuel for Fuel1 running with FTD for a base case and a cycle running with 15%EGR.



In figure 36 the mole fractions of CO, CO<sub>2</sub> and NO<sub>x</sub> during the cycles are given. Here a 62% reduction is observed for NO when applying EGR, providing a level of 1360ppm in the end emissions of Cycle1. The level of NO<sub>2</sub> experiences an increase for Cycle1, but its presence in the exhaust is still at such a low level that this is insignificant with regard to the total quantity of NO<sub>x</sub>. The reduction seen here for NO is lower than the effect seen for n-heptane in figure 28, where an 81% reduction is obtained when the same degree of EGR is applied. However due to a higher concentration of NO in the emissions from FTD, the impact from the 62% reduction on the emissions composition is of greater order, than the 81% obtained for n-heptane. Actually the 1360ppm of NO present in the emissions from FTD for Cycle1 is still higher than the NO fraction in the emissions from the base case of n-heptane.

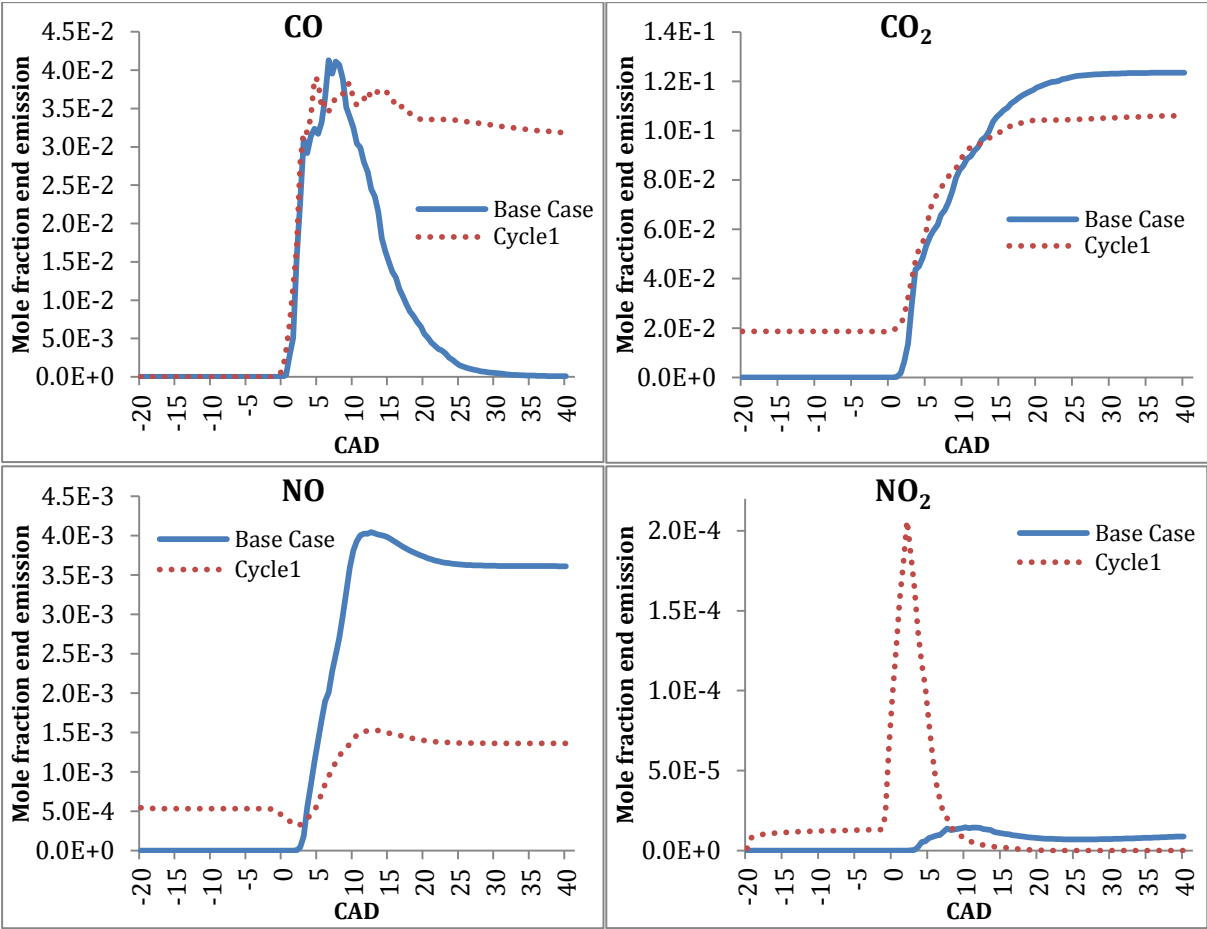


Figure 36: Mole fractions of NO, NO<sub>2</sub>, CO and CO<sub>2</sub> during the combustion cycle of FTD for a base case and a case running with 15%EGR (Cycle1).

As mentioned previously there will almost always exist a trade-off with regard to the parameters indicating a more incomplete combustion. This is represented by the alteration in CO and CO<sub>2</sub> levels. The CO emission after the base case is approaching zero, which is unlikely results. When looking at the CO emission in figure 33, where the same case is ran excluding EGR, its mole fraction of CO in the end emissions is 1.38e-1, i.e. higher than the emissions from the cycle here with EGR. The base cycle and the cycle shown in figure 33 should in theory be identical; however this is not the case neither here, nor when applying

EGR for n-heptane. The reason for this deviation in the base cycles is not further investigated here since the source codes are not available, hence certain affects caused by the EGR remains unexplained. The emission level from figure 33 cannot be used when assessing the effect of EGR, since it is not the cycle the EGR is based on. Consequently a true evaluation of the CO increase is not obtained here, however the decrease in CO<sub>2</sub> indicates that an increase in CO is present.

The CO<sub>2</sub> experiences a decrease of 14%, which is a much lower trade-off than what is seen for n-heptane. This indicates that when running with FTD a higher degree of EGR can be applied compared to n-heptane, without sacrificing too much of the combustion quality. This would also be preferred due to the massive NO<sub>x</sub> fraction in its end emissions, making the NO<sub>x</sub> targets harder to reach.

## 9. QUALITATIV VALIDATION OF MODELS UTILIZED

### 9.1 EVALUATING FUEL2

In order to run the simulations presented in this work, simplified models have been used for both the engine and fuels simulated. To validate the quality of the models applied the emissions of the criteria pollutants CO, CO<sub>2</sub> and NO<sub>x</sub> have been compared to experimental data, where the combustion of both pure diesel and a blend with 30% FTD were tested in a real CI engine. The FTD simulated does not exist as a blend as for 30%FTD, however the vast simplifications in the models for both FTD and the surrogate fuel representing diesel, would diminish the accuracy when simulating such a blend. Therefore more reliable information regarding the characteristics of FTD can be retrieved when simulated as a pure fuel, but can still be compared with the experimental data for 30%FTD. Both fuels modeled are as mentioned strong simplifications of the cases ran in the real engine, and accordingly it is just as important to reveal trends as it is to provide the exact results. Here emissions from the simulations of n-heptane and FTD for Fuel2 are compared to the emissions from the experimental data. As defined in table 5, Fuel2 represents an engine operating at 1500rpm with a load of 40Nm. Fuel1 and Fuel3 have also been looked into, however the findings were inconclusive and need further investigation, and will not be discussed.

From figure 37 a correlation between the simulated cases and the experimental data can to some extent be observed. When evaluating the CO<sub>2</sub> emissions for n-heptane they are found to exist in the same range as diesel, with values lying approximately 0.25% higher. Also the trend of increased levels with advanced injection points are seen for both the simulated and experimental data, indicating good quality in the predicted CO<sub>2</sub> emissions. FTD has only been run with an injection at -1.65CAD, where its CO<sub>2</sub> emission lies slightly above the emissions from n-heptane. For the experimental data at this injection point, the CO<sub>2</sub> emissions from 30%FTD are slightly lower than diesel. However this alters for the cases operating with more advanced injections, and even though the elevated level of CO<sub>2</sub> for FTD compared to n-heptane is not reflected in the experimental values at this point, it is in accordance with the experimental values at advanced injections. Consequently the CO<sub>2</sub> emission level of FTD compared to n-heptane might have correlated with the experimental data if more results were obtained for FTD.

The NO<sub>x</sub> emissions from n-heptane are in the same area as the emissions from diesel when injecting at -1.65CAD. However since the NO<sub>x</sub> level of n-heptane increases as the NO<sub>x</sub> level of diesel decreases with advanced points of injection, the deviation between the simulated and experimental NO<sub>x</sub> level increases by a fraction of 7 from the latest to the earliest point of injection. For FTD the NO<sub>x</sub> emissions for the case injected at -1.65CAD are widely over predicted, and the only trend that matches the experimental data is the advanced level compared to diesel.

The CO levels are over predicted for all injection points of n-heptane and for the case ran for FTD, and they provide poor indication of the emissions from the original fuels.

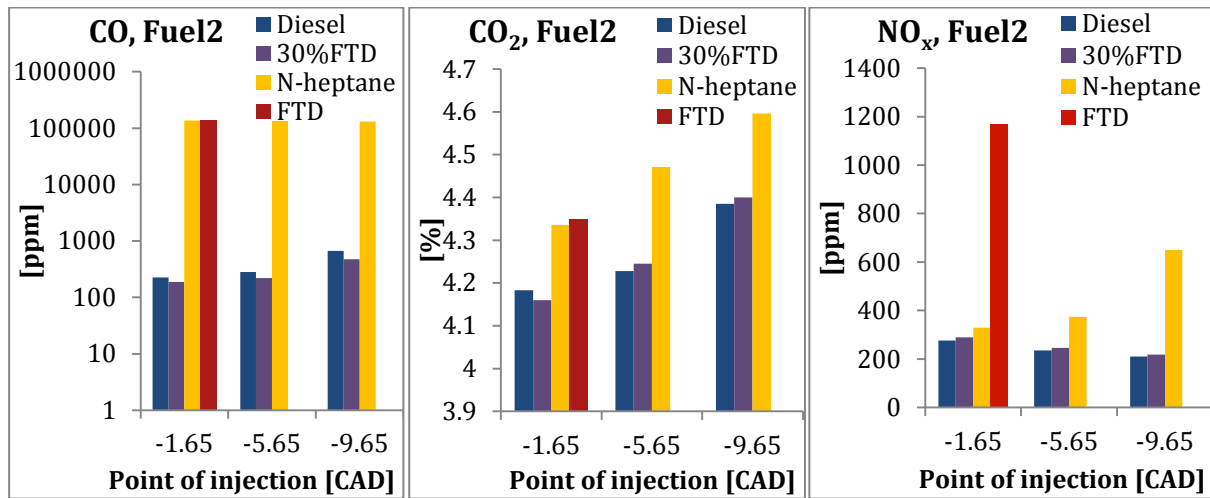


Figure 37: Mole fraction of CO, CO<sub>2</sub> and NO<sub>x</sub> in the end emissions for the simulated cases of n-heptane and FTD for Fuel2 compared to experimental values for diesel and 30%FTD. Notice that the CO emission has a logarithmic scale.

It can be concluded that the simulated cases for Fuel2 at different extent over predicts their emissions. However for n-heptane both CO<sub>2</sub> and NO<sub>x</sub> levels are found in the same area as the experimental data, where also the CO<sub>2</sub> level of FTD seems to coincide. As discussed previously in this work the models applied to represent the fuels are extreme simplifications, which explain the alterations in the quality of the results. Also the load each case represents provides an element of insecurity since this is determined from qualitative guessing, owing to the method of incorporating load in the model. The load is namely represented by the amount of fuel injected which is not predetermined in the experiments, but adjusted automatically by the ECU. Hence the experimental data used for validation might not be the actual engine operation that the simulations aim to recreate.

Another interesting observation from these figures is the characteristics of the real fuels, where the CO and CO<sub>2</sub> levels show beneficial results for 30%FTD compared to diesel. Also the NO<sub>x</sub> emissions behave as expected, with increased levels due to higher oxygen content. This indicates that an engine operating with 30%FTD experiences improved combustion characteristics at the given conditions.

## 9.2 EVALUATING THE IMPACT OF EGR

The same criteria pollutants have been used to evaluate the results withdrawn when EGR is applied, seen in figure 38. Here an increase in CO level is present for all cases when applying EGR, but the increase detected for n-heptane is significantly larger than for diesel. The initial CO level for FTD is as explained earlier probably not tangible, and the huge increase seen for

this case is therefore not evaluated. The diesel experiences an increase of 22%, whereas the n-heptane increases by 98% and 116% when operating with respectively 1 and 5 EGR cycles. This gives an indication of more aggravating combustion characteristics for the simulated n-heptane compared to diesel when EGR is applied, which is further implied by the change in CO<sub>2</sub> levels. Here a slight increase is detected for diesel and 30%FTD, however a larger decrease is observed for the n-heptane and FTD. When applying EGR there will be a fraction of CO<sub>2</sub> already present in the beginning of the combustion cycle due to the recirculated exhaust gas, hence the level of CO<sub>2</sub> produced in the combustion cycle will experience a larger reduction than what is indicated in figure 38.

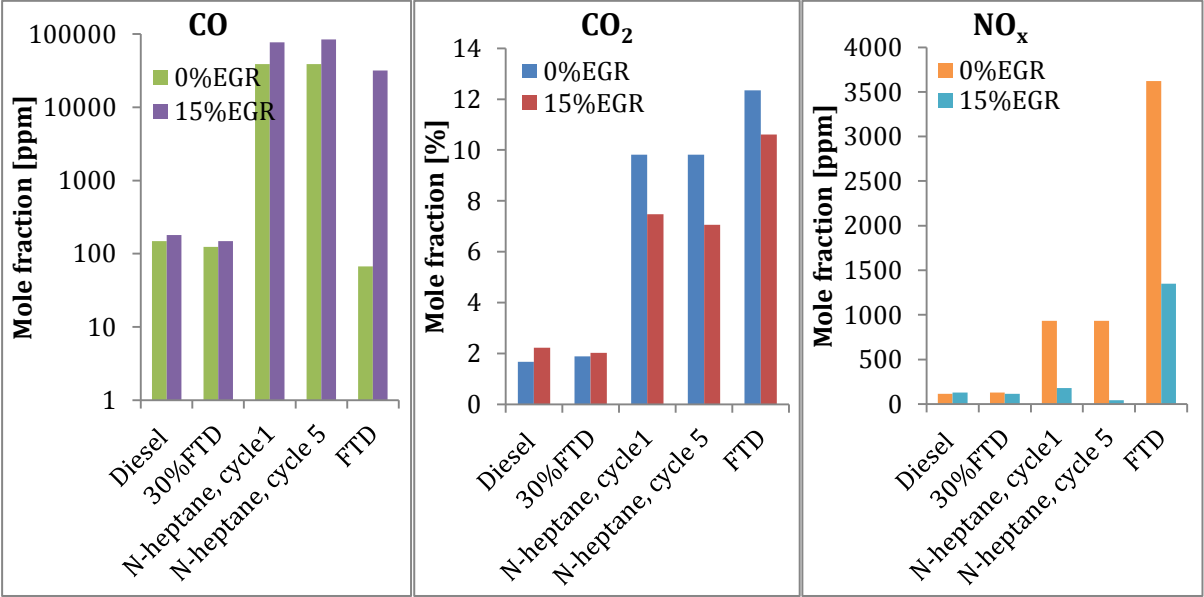


Figure 38: Mole fraction of CO, CO<sub>2</sub> and NO<sub>x</sub> in the end emissions for the simulated cases of n-heptane and FTD, compared to experimental values for diesel and 30%FTD, for a base case and when 15%EGR is applied. Notice that the CO emission has a logarithmic scale.

When studying the NO<sub>x</sub> emissions an increase is actually detected for the combustion of diesel when applying 15% EGR, which is contradictory to the EGRs objective. It is not within the scope of this thesis to further reason for this effect; however it deviates from the results obtained for 30%FTD and what is found in the data sheet for diesel with 30% EGR. For n-heptane the NO<sub>x</sub> level reduces, which is a more expected result when applying EGR, although at a very high rate. The reductions add up to 81% and 96% when applying respectively 1 and 5 EGR cycles. For FTD a slightly lower reduction of 63% is obtained, although still at a high level compared to the 9% reduction for 30%FTD. The high reductions may be an effect of the widely over predicted NO<sub>x</sub> levels in the base cycles. Actually the NO<sub>x</sub> level after the EGR cycles for n-heptane approaches the levels from the experimental testing before use of EGR, whereas the level for FTD is still significantly over predicted even after applying EGR.

## 10. CONCLUSION

When the right feedstock, crop land, cultivation method and conversion technology are applied to produce biofuels, the environmental savings can be substantial. One such prominent fuel is the second generation biofuel FTD, which when substituting diesel obtains an 84% reduction in GHG emissions and a 88% reduction in fossil fuel consumption, as demonstrated in the LCA discussed in this thesis. It is also a desirable fuel with regard to engine efficiency and emission reduction with its high cetane rating, low sulfur and toxic content and relatively high presence of oxygen. Another important aspect is its easy introduction to already existing infrastructure, and consequently avoiding one of the main barriers for utilizing alternative fuels like hydrogen and electric power. The FTD can actually be applied both as a blend with diesel and as pure FTD in the current diesel engines, without requiring modifications.

FTD is a novel fuel and currently not commercial available due to the complex structure of its lignocellulosic feedstock, requiring a more advanced and expensive conversion technology. However incentives are present to encourage more research and development of both FTD and other second generation and advanced biofuels, such as rewarding them double credit in REDs 10% renewable energy share by 2020. In order to increase the use of these novel fuels it is not only the barrier with conversion technology that needs to be overcome, there are also uncertainties regarding the combustion characteristics and their end use emissions, which have to be fully explored. As a powerful supplement in this work, computational simulation has arisen as an important tool, saving both time and cost. This can be particularly interesting when assessing novel fuels, where experimental data might not be available yet. Here the simulations of their chemical mechanisms can provide important information regarding expected combustion characteristics as engine performance and emission profiles.

In this thesis surrogate fuels for diesel and FTD have been tested in the simulation software DARS. Due to limited computational power available, along with errors in DARS prolonging the time required to run the simulations, only a selection of cases were ran for the FTD surrogate. However important information could be withdrawn for the available cases for both fuels. From the results obtained for n-heptane representing diesel, the combustion characteristics alters significantly when changing the operational parameters such as engine speed, load and injection profile. When advancing the point of fuel injection a general increase in the temperature and pressure peaks are observed. This can be caused by the combustion occurring in the compression stroke and/or earlier in the expansion stroke, avoiding losses due to volume expansion. The highest temperature, pressure and heat release peaks are obtained for Fuel1, representing the lowest engine speed and load. Both these latter operational settings are beneficial with regard to mixing, yielding shorter ignition delay as well as high quality combustion. This is also evident from its relatively low CO emissions and high fraction of CO<sub>2</sub> compared to the other cases.

Fuel2 and 3 ran at 1500rpm with incremental fuel injection, operated with poorer combustion characteristics compared to Fuel1. An alteration is also detected between these two cases

operating with a fixed engine speed, where the leanest case, i.e. Fuel2, obtains more beneficial combustion characteristics. This change is not as significant as the alteration between Fuel1 and 2, and underlines that both engine speed and load will affect the combustion quality. From the results obtained for 2500rpm it appears that this engine speed exceeds the limits in DARS for the area of interest in this thesis, and viable information could not be obtained.

When comparing the results for the different surrogate fuels, only small alterations are detected in the combustion cycle with regard to temperature, pressure and heat release profiles. Due to higher oxygen content in the original FTD, higher temperature peaks are expected here as a consequence of the higher local flame temperatures. However a decrease is actually detected for all cases except for Fuel2, where a small increase of 70K is present. Also the levels of CO and CO<sub>2</sub> are in the same area as n-heptane, although expected to improve with regard to a more complete combustion due to the higher oxygen content. The conflicting results with regard to the characteristics of the original fuel reflect the simplification of the model, where the higher oxygen content most likely is omitted.

For the leaner operations a general increase is observed in the NO<sub>x</sub> levels, due to a higher maximum temperature and oxygen concentration. These are key factors in NO<sub>x</sub> formation. Accordingly case Fuel1 for both fuels, operating with the lowest amount of fuel being injected and hence the highest oxygen concentration, produces the highest levels of NO<sub>x</sub>. This is unfortunate with an increasing urban traffic operating at generally lower loads, hence emitting more NO<sub>x</sub>. The NO<sub>x</sub> level for FTD experiences a huge increase compared to n-heptane.

There are great challenges associated with the reduction of NO<sub>x</sub> since new technology employed to improve engine performance intensify the NO<sub>x</sub> emissions. EGR is one of the most efficient mean to reduce NO<sub>x</sub> emissions, and here huge trade-offs with regard to parameters for incomplete combustion were observed. When running n-heptane with 15%EGR for Fuel1, an 81% reduction is obtained for NO<sub>x</sub>, but also a 24% reduction in CO<sub>2</sub> concentration. For the same level of EGR applied for FTD, the NO<sub>x</sub> concentration reduces by 62%, whereas the CO<sub>2</sub> level decreases by 14%. Consequently it appears that FTD can withstand a higher degree of EGR compared to n-heptane, which is also required due to its high NO<sub>x</sub> levels.

For further work with this problem additional effort should be put into approaching the conditions in a real engine with regard to the amount of fuel injected, to truly represent the engine load. Also more reliable models should be used for modelling both diesel and FTD in such a manner that their difference in quality becomes more evident, and with less factors adding to the insecurity of the results.

## 11. REFERENCES

1. B. Metz, O.R.D., P.R. Bosch, R. Dave & L.A. Meyer (eds), *Contribution of Working Group III to the Fourth Assessment Report of the Intergovernmental Panel on Climate Change*. 2007, Intergovernmental Panel on Climate Change.
2. *Utslipp av klimagasser, 2011, foreløpige tall*. 2012; Available from: <http://www.ssb.no/natur-og-miljo/statistikker/klimagassn/aar-forelopige/2012-05-08?fane=om#content>.
3. Fulton, L., Howes, T. & Hardy, J. *Biofuels for transport: an international perspective*. in *GEFSTAP Liquid Biofuels Workshop, August*. 2005.
4. Liebe, L., Halsør, T., Hojem, J.F., Opdal, O. & Andreassen, G.L., *Bærekraftig biodrivstoff - Et avgjørende klimatiltak*. 2010, ZERO.
5. Tunér, M., *Stochastic reactor models for engine simulations*. 2008: Division of Combustion Physics.
6. Larsen, O.M., Valderhaug, V., Selvig, E., Hjelde, F., Langtvvet, E., Pettersen, M.V.H., Gislerud, A., Fjærbu, R.J., Espenes, L.C., Figenbaum, E., Kleven, O., Kjerkreit, A. & Kirkeby, W. *Sektoranalyse for transport. Klimakur 2020- tiltak og virkemidler for å nå norske klimamål mot 2020*. 2010; Available from: [www.vegvesen.no/attachment/180268/binary/345422](http://www.vegvesen.no/attachment/180268/binary/345422).
7. Guomin Xiao, L.G., *First Generation Biodiesel*, in *Biofuel Production-Recent Developments and Prospects*, D.M.A.D.S. Bernardes, Editor. 2011, InTech.
8. Brunvoll, F., Monsrud, J. & Wethal, A.W. *En utfordring å minske miljøpåvirkningene fra transport*. 2008; Available from: <http://www.ssb.no/natur-og-miljo/artikler-og-publikasjoner/en-utfordring-aa-minske-miljopaavirkningene-fra-transport>.
9. *Biodrivstoff*. [cited 2013 02.22.]; Available from: <http://energilink.tu.no/leksikon/biodrivstoff.aspx>.
10. Eisentraut, A., Brown, A. & Fulton, L., *Technology Roadmap. Biofuels for Transport*. 2011, OECD/IEA.
11. Vessia, Ø., *Biofuels from lignocellulosic material*. 2005, NTNU: Trondheim.
12. Sims, R., Taylor, M., Saddler, J. & Mabee, W., *From 1st- to 2nd-generation biofuel technologies. An overview of current industry and R&D activities*. 2008, International Energy Agency Secretary and the Implementing Agreement on Bionenergy.
13. Holmengen, N., *Biodrivstoff - et omstridt miljøtiltak*. *Samfunnspeilet* 2008, 2008. **22**(4): p. 53-56.
14. Naik, S.N., Goud, V. V., Rout, P. K., & Dalai, A. K., *Production of first and second generation biofuels: A comprehensive review*. *Renewable and Sustainable Energy Reviews*, 2010. **14**(2): p. 578-597.
15. Smallbone, A.J., Coble, A.R., Bhave, A.N., Mosbach, S., Kraft, M., Morgan, N. & Kalghatgi, G., *Simulating PM emissions and combustion stability in gasoline/diesel fuelled engines*. SAE Paper 2011-01, 2011. **1184**.
16. Kerschgens, B., Lackmann, T., Pitsch, H., Janssen, A., Jakob, M & Pischinger, S., *Tailored surrogate fuels for the simulation of diesel engine combustion of novel biofuels*, in *Institute for Combustion Technology and Institute for Combustion Engines*. 2012, RWTH Aachen University.
17. Poonawala, Y.M., *Effect of EGR, injection pressure and swirl ratio on engine-out emissions for a HSDI diesel engine at low load and medium speed condition*. 2007: ProQuest.
18. Dangar, H. and G.P. Rathod, *Combine Effect of Exhaust Gas Recirculation (EGR) and Varying Inlet Air Pressure on Performance and Emission of Diesel Engine*. *Journal of Mechanical and Civil Engineering*, 2013. **6**(5): p. 26-33.
19. Diez, A., Løvås, T. & Crookes, R. J., *An experimental and modelling approach to the determination of auto-ignition of diesel fuel, dodecane and hexadecane sprays at high pressure*.



20. Quirin, M., Gartner, S.O., Pehnt M. & Reinhardt A.G., *CO<sub>2</sub> Mitigation through Biofuels in the Transport Sector, Status and Perspectives*, in *Institute for Energy and Environmental Research*. 2004, Heidelberg University.
21. Hossain, A.B.M.S. and M.A. Mazen, *Effects of catalyst types and concentrations on biodiesel production from waste soybean oil biomass as renewable energy and environmental recycling process*. Australian Journal of Crop Science, 2010. **4**(7): p. 550-555.
22. Adlam, E., *LCA of Transportation Biofuels*, in *Department of Energy and Process Engineering*. 2007, NTNU.
23. Taherzadeh, M.J. and K. Karimi, *Enzymatic-based hydrolysis processes for Ethanol*. BioResources, 2007. **2**(4): p. 707-738.
24. Sun, Y. and J. Cheng, *Hydrolysis of lignocellulosic materials for ethanol production: a review*. Bioresource technology, 2002. **83**(1): p. 1-11.
25. Hamelinck, C.N., G.v. Hooijdonk, and A.P. Faaij, *Ethanol from lignocellulosic biomass: techno-economic performance in short-, middle-and long-term*. Biomass and bioenergy, 2005. **28**(4): p. 384-410.
26. Bridgwater, A., *Renewable fuels and chemicals by thermal processing of biomass*. Chemical Engineering Journal, 2003. **91**(2): p. 87-102.
27. Antonakou, E.V., Dimitropoulos V. S. & Lappas, A. A., *Production and characterization of bio-oil from catalytic biomass pyrolysis*. Thermal Science, 2006. **10**(3): p. 151-160.
28. Opdal, O.A., *Production of synthetic biodiesel via Fischer-Tropsch synthesis*, in *Department of Energy & Process engineering*. 2006, NTNU.
29. Van Thuijl, E., C. Roos, and L. Beurskens, *An overview of biofuel technologies, markets and policies in Europe*. Energy research Centre of the Netherlands. ECN Policy Studies Report No. ECN-C--03-008, 2003.
30. *Microalgae or Macroalgae?* 2011 [cited 2013 04.09]; Available from: <http://www.oilgae.com/blog/2011/08/microalgae-or-macroalgae.html>.
31. Dragone, G., Fernandes, B. D., Vicente, A. A. & Teixeira, J. A., *Third generation biofuels from microalgae*, in *Current Research, Technology and Education Topics in Applied Microbiology and Microbial Biotechnology*, A. Méndez-Vilas, Editor. 2010. p. 1355-1366.
32. Riis, T., Hagen, E.F., Sandrock, G., Vie, P.J.S. & Ulleberg, Ø., *Hydrogen Production and Storage. R&D Priorities and Gaps*. 2006, OECD/IEA.
33. Carere, C.R., Sparling, R., Cicek, N. & Levin, D.B., *Third generation biofuels via direct cellulose fermentation*. International journal of molecular sciences, 2008. **9**(7): p. 1342-1360.
34. Lynd, L.R., Zyl, W.H.V, McBRIDE, J. E. & Laser, M., *Consolidated bioprocessing of cellulosic biomass: an update*. Current Opinion in Biotechnology, 2005. **16**(5): p. 577.
35. Heywood, J.B., *Internal combustion engine fundamentals*. Vol. 930. 1988: McGraw-Hill New York.
36. Taylor, C.F., *The Internal-combustion Engine in Theory and Practice: Combustion, fuels, materials, design*. Vol. 2. 1985: MIT press.
37. Moran, M.J. and H.N. Shapiro, *Principles of Engineering Thermodynamics, 5th Edition (SI Units)*. 2008: John Wiley & Sons, Inc.
38. Zheng, M., G.T. Reader, and J.G. Hawley, *Diesel engine exhaust gas recirculation—a review on advanced and novel concepts*. Energy Conversion and Management, 2004. **45**(6): p. 883-900.
39. Crua, C., *Combustion processes in a diesel engine*. 2002, University of Brighton.
40. Abd-Alla, G., *Using exhaust gas recirculation in internal combustion engines: a review*. Energy Conversion and Management, 2002. **43**(8): p. 1027-1042.
41. Maiboom, A., Tauzia, X. & Hétet, J.-F., *Experimental study of various effects of exhaust gas recirculation (EGR) on combustion and emissions of an automotive direct injection diesel engine*. Energy, 2008. **33**(1): p. 22-34.
42. Kowalewicz, A. and M. Wojtyniak, *Synthetic fuels and their application to internal combustion engines*. Silniki Spalinowe, 2007. **46**.

43. Malik, A., Schramm, J., Nielsen, C. & Lovas, T. *Development of Surrogate for Fischer-Tropsch Biofuel and Reduced Mechanism for Combustion in Diesel Engine*. 2013 [cited 2014 02/27]; Available from: <http://papers.sae.org/2013-01-2599/>.
44. *New Commission proposal to minimise the climate impacts of biofuel production*. 2012 [cited 2013 15.04]; Available from: [http://europa.eu/rapid/press-release\\_IP-12-1112\\_en.htm](http://europa.eu/rapid/press-release_IP-12-1112_en.htm).
45. Holtsmark, B., *Virkningene på klimagassutslipp ved økt bruk av biodrivstoff*. En litteraturgjennomgang. 2010, Statistisk Sentralbyrå: ssb.no. p. 29.
46. Berneds, G., Bird, N. & Cowie, A., *Bioenergy, land use change and climate change mitigation*. 2011, IEA Bioenergy.
47. Menichetti, E. and M. Otto, *Energy balance and greenhouse gas emissions of biofuels from a life-cycle perspective*. Biofuels: environmental consequences and interactions with changing land use, Proceedings of the Scientific Committee on Problems of the Environment (SCOPE) International Biofuels Project Rapid Assessment, 2008: p. 22-25.
48. Wu, M., Y. Wu, and M. Wang, *Energy and Emission Benefits of Alternative Transportation Liquid Fuels Derived from Switchgrass: A Fuel Life Cycle Assessment*. Biotechnology Progress, 2006. **22**(4): p. 1012-1024.
49. Muhammad Shukri, R., *Performance and emission characteristics of a diesel engine operating with biodiesel*. 2010, Universiti Malaysia Pahang.
50. Scarlat, N. and J.-F. Dallemand, *Recent developments of biofuels/bioenergy sustainability certification: A global overview*. Energy Policy, 2011. **39**(3): p. 1630-1646.
51. Warnatz, J., Maas, U. and Dibble, R.W., *Combustion: physical and chemical fundamentals, modeling and simulation, experiments, pollutant formation*. 2006: Springer. 73-81.
52. Peters, N. and B. Rogg, *Reduced kinetic mechanisms for applications in combustion systems*. 1993: Springer. 1-26.
53. Ra, Y. and R.D. Reitz, *A reduced chemical kinetic model for IC engine combustion simulations with primary reference fuels*. Combustion and Flame, 2008. **155**(4): p. 713-738.
54. Wang, H. and M. Frenklach, *Detailed reduction of reaction mechanisms for flame modeling*. Combustion and Flame, 1991. **87**(3): p. 365-370.
55. DARS, *Manual Book 5: Mechanism Reduction*. 2012.
56. Arvidsson, A., *Development of an Automatic Reduction Tool for Chemical Mechanisms and an Optimized Sparse Matrix Solver for Systems of Differential and Algebraic Equations*. 2010, Lund University.
57. Rabitz, H., M. Kramer, and D. Dacol, *Sensitivity analysis in chemical kinetics*. Annual review of physical chemistry, 1983. **34**(1): p. 419-461.
58. Beebe, K.W., *Premixing dry low nox emissions combustor with lean direct injection of gas fule*. 2001, U.S. Patent No. 6,192,688. Washington, DC: U.S. Patent and Trademark Office.
59. *Nitrogenoksid (NOx)*. 2013 [cited 2013 11.07]; Available from: <http://www.miljostatus.no/Tema/Luftforurensning/Sur-nedbor/Nitrogenoksid-NOx/>.
60. DARS, *Manual Book 3: Engien In-Cylinder Reactor Models*. 2011.
61. DARS, *Manual Book 2: Homogeneous Reactor Models*. 2011.
62. DARS, *Tutorial: Stochastic Reactor Models - HCCI, SI and DICI engines*. 2012.
63. Woschni, G., *A universally applicable equation for the instantaneous heat transfer coefficient in the internal combustion engine*. Significance, 1967. **2012**: p. 12-11.
64. Miyano, H., Suzaki, Y., Takahashi, F. & Ogasawara, K.-I., *Control unit of an internal combustion engine control unit utilizing a neural network to reduce deviations between exhaust gas constituents and predetermined values*. 1993, Google Patents.
65. Andersson, M., *Fast NOx predictions in Diesel Engines*, in Department of Energy Science. 2006, Lund University.